MANCHESTER
1824

The University of Manchester

2D materials and van der Waals heterostructures

Roman Gorbachev

All Natural Materials Are 3D

Peierls and Landau:
No long-range crystalline order in 1D and 2D,
but a melting transition in 3D.

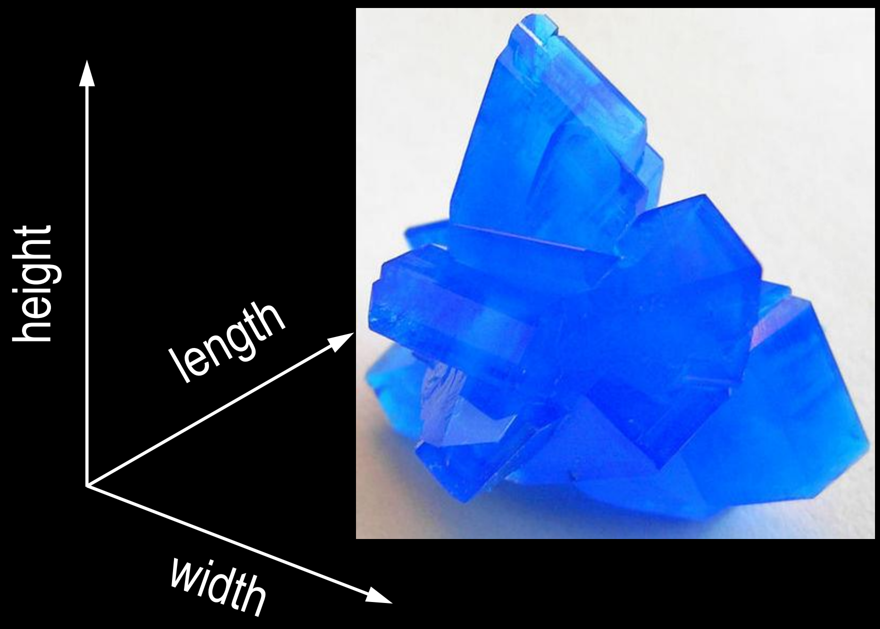

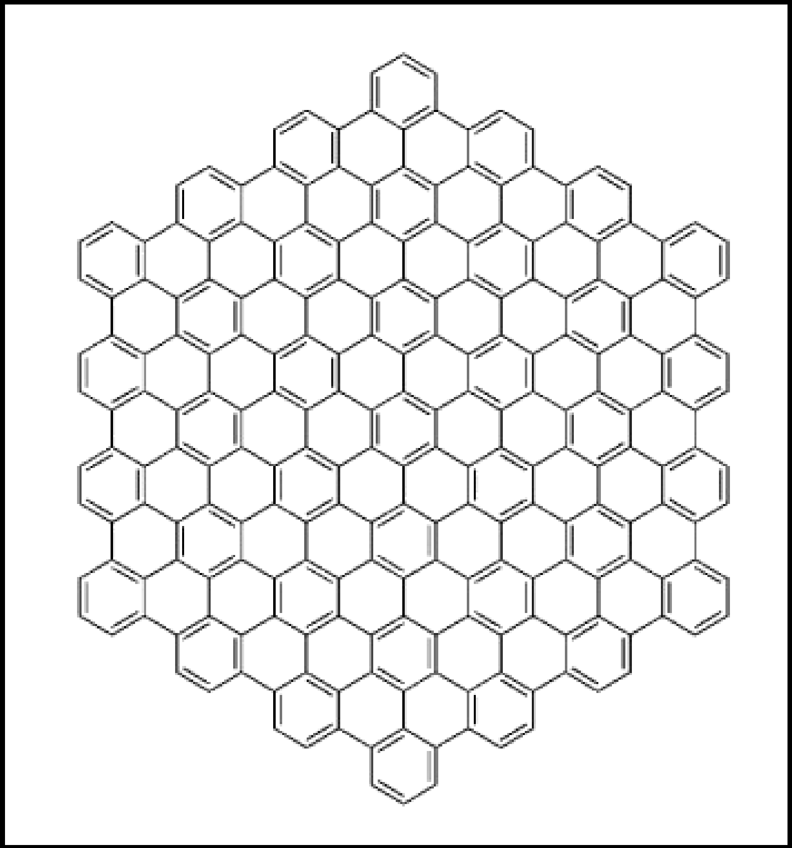

largest known
flat hydrocarbon:
222 atoms or 37 benzene rings
(K. Müllen 2002)

Graphene

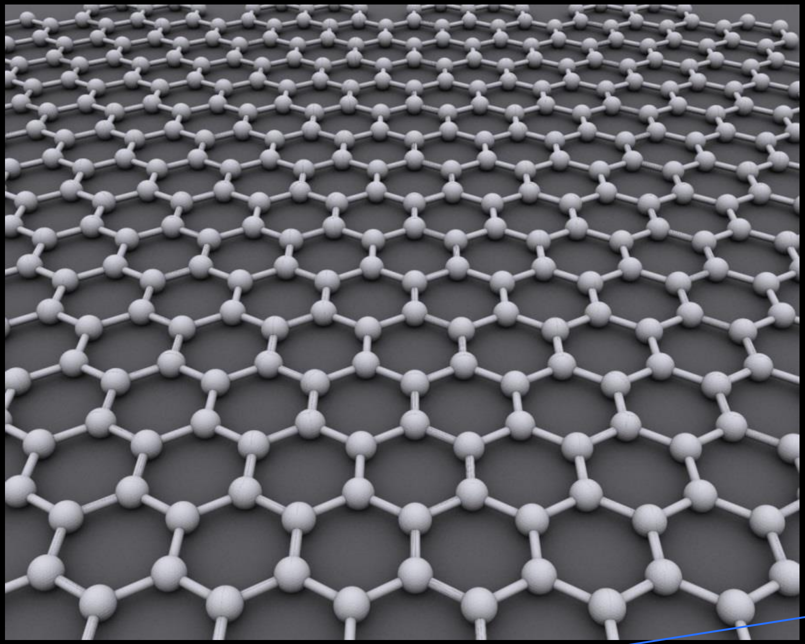

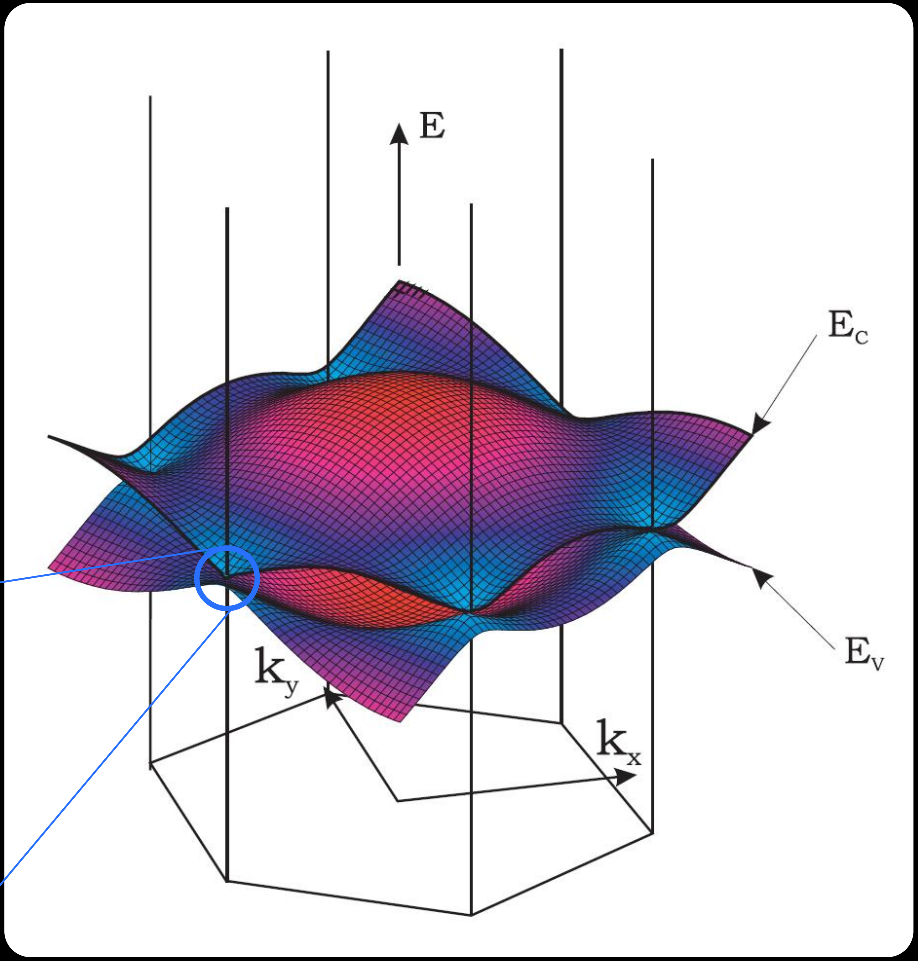

$$\hat{H} = v_F \vec{\sigma} \cdot \hat{p}$$

2 equivalent sublattices ➡ pseudospin index

Graphene + Graphene

“Schrödinger fermions”

Electron metal

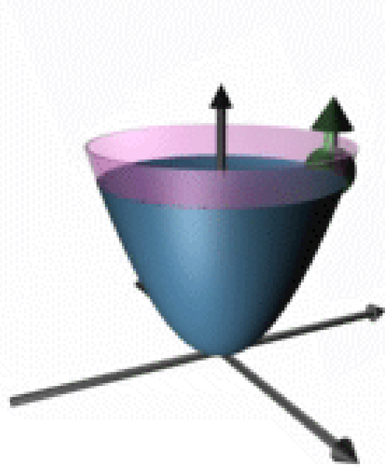

Hole metal

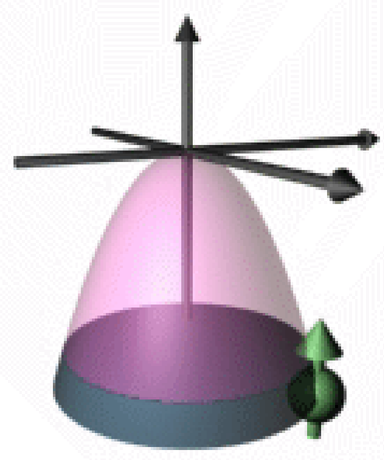

$$\hat{H} = \hat{p}^2 / 2m^*$$

massless
Dirac fermions

Semenoff
1984

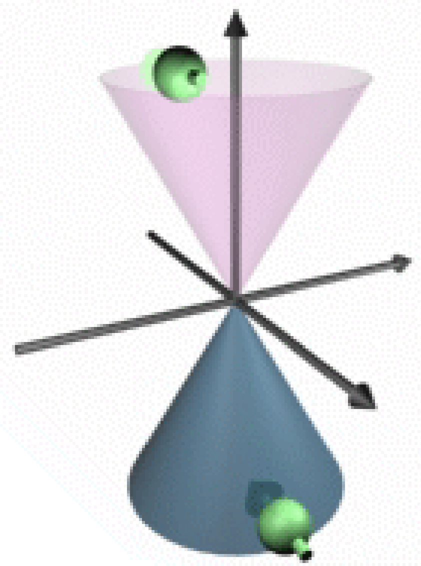

$$\hat{H} = v_F \vec{\sigma} \cdot \hat{p}$$

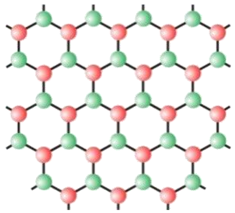

monolayer graphene

massive
chiral fermions

Falko
2006

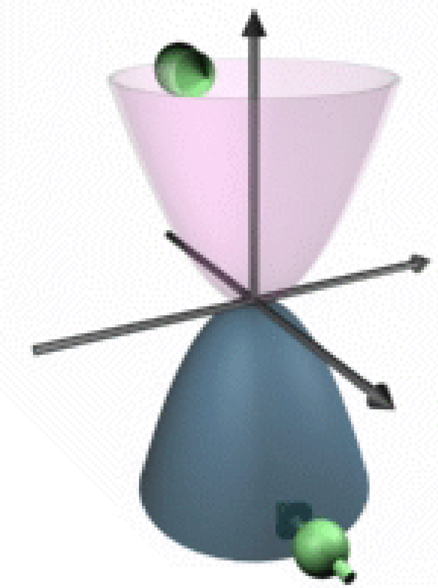

$$\hat{H} = \vec{\sigma} \cdot \hat{p}^2 / 2m^*$$

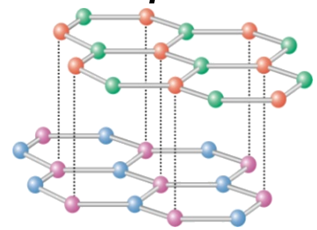

bilayer graphene

Human endeavours
in abstract thinking vs 2D material research

Evolutionists

Creationists

Exfoliationists

Growers

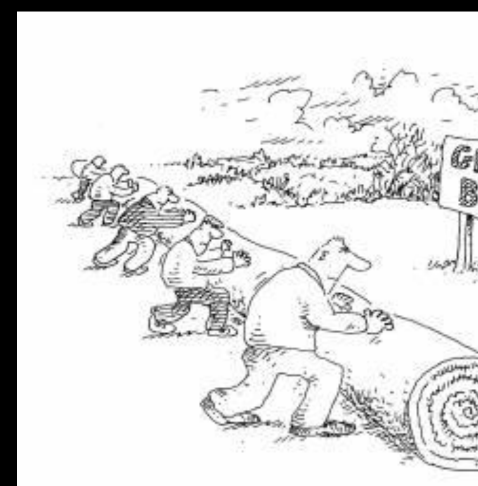

Mass Production

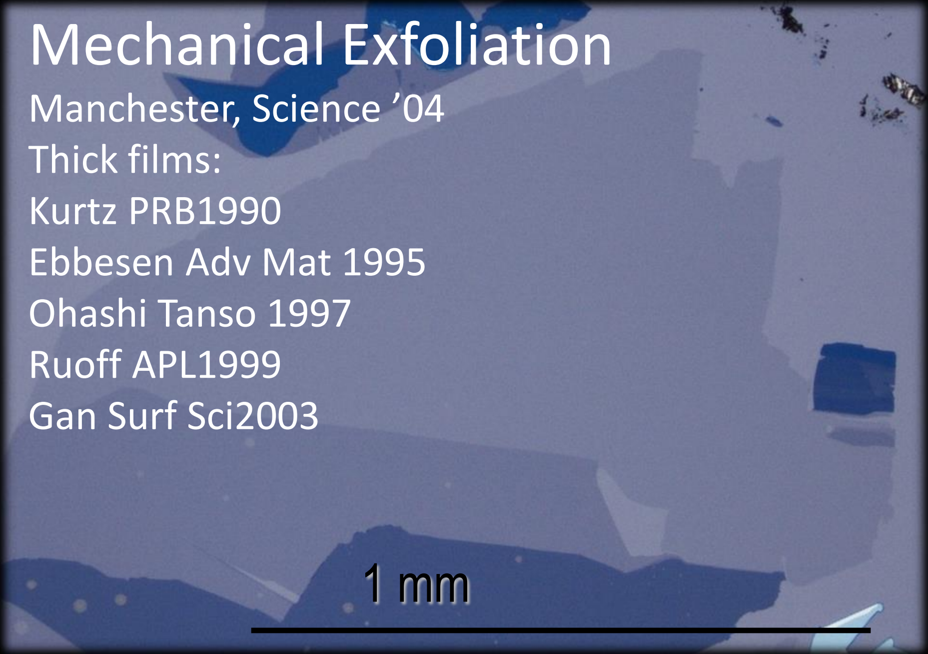

Mechanical Exfoliation

Manchester, Science '04
Thick films:
Kurtz PRB1990
Ebbesen Adv Mat 1995
Ohashi Tanso 1997
Ruoff APL1999
Gan Surf Sci2003

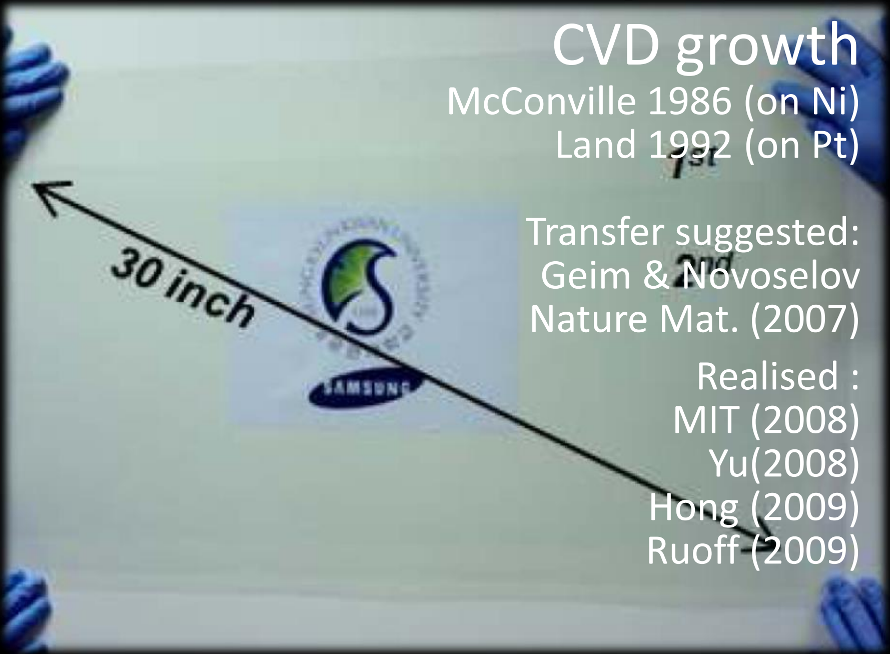

CVD growth

McConville 1986 (on Ni)
Land 1992 (on Pt)

Transfer suggested:
Geim & Novoselov
Nature Mat. (2007)

Realised :
MIT (2008)
Yu(2008)
Hong (2009)
Ruoff (2009)

Epitaxial Growth on SiC

Bommel 1975
Nagashima 1993
Forbeaux 1998
de Heer 2004
HRL 2009
IBM 2009

Chemical Exfoliation

Benjamin Brodie
Phil Trans.1859
Ruess & Vogt 1948
Boehm & Hofmann 1962
Ruoff 2007
Coleman 2008
Manchester 2008

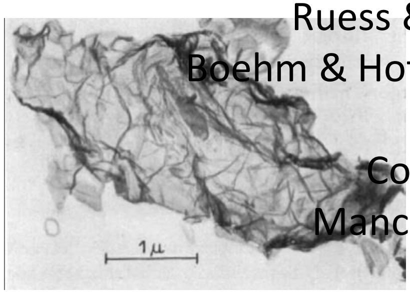

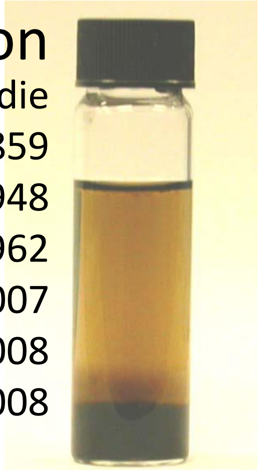

Can We Cheat Nature?

Slice down to one atomic plane

Strongly anisotropic material

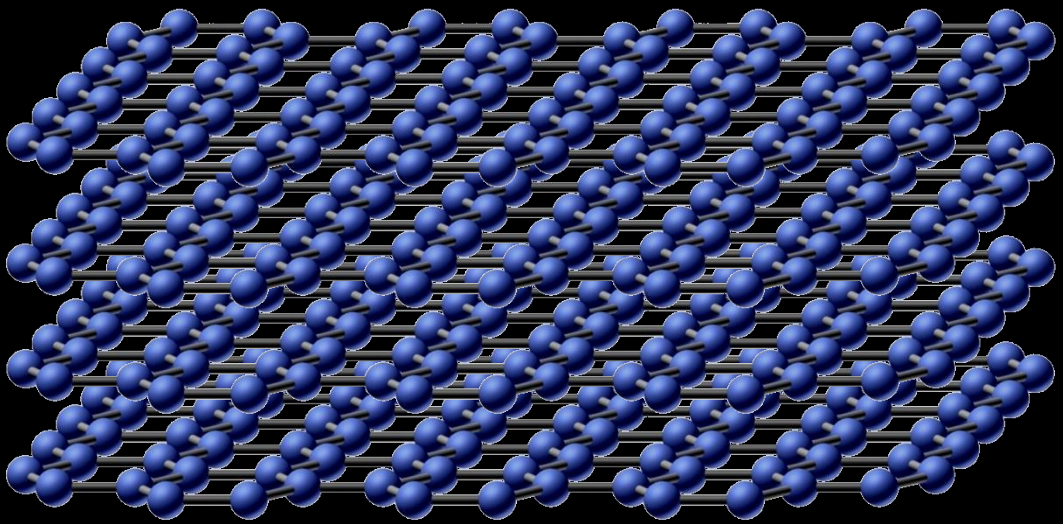

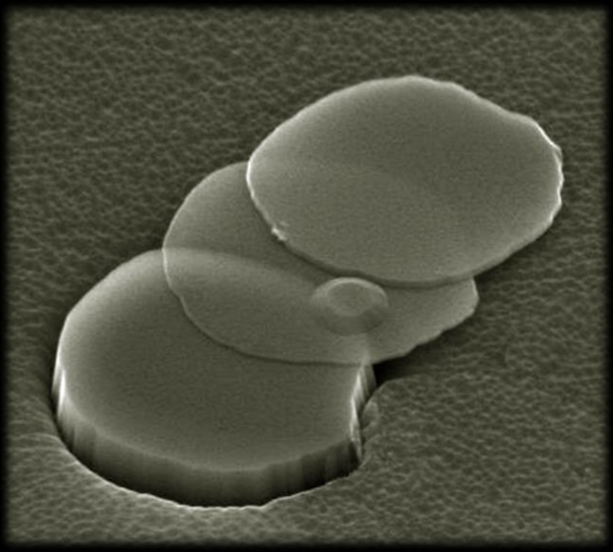

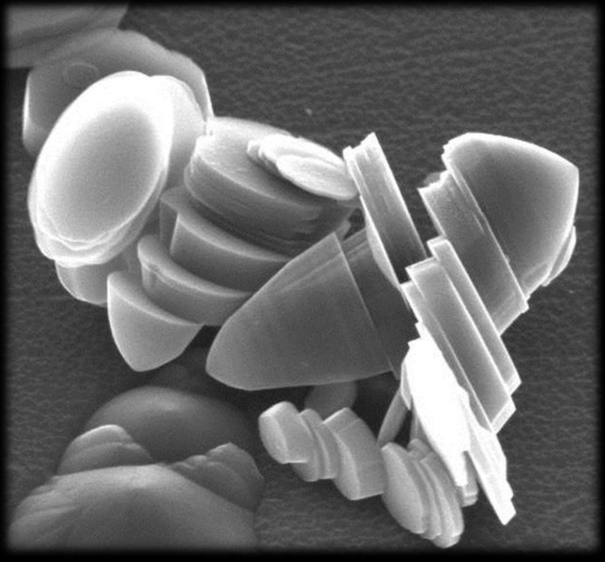

Graphite trace on oxidized Si wafer

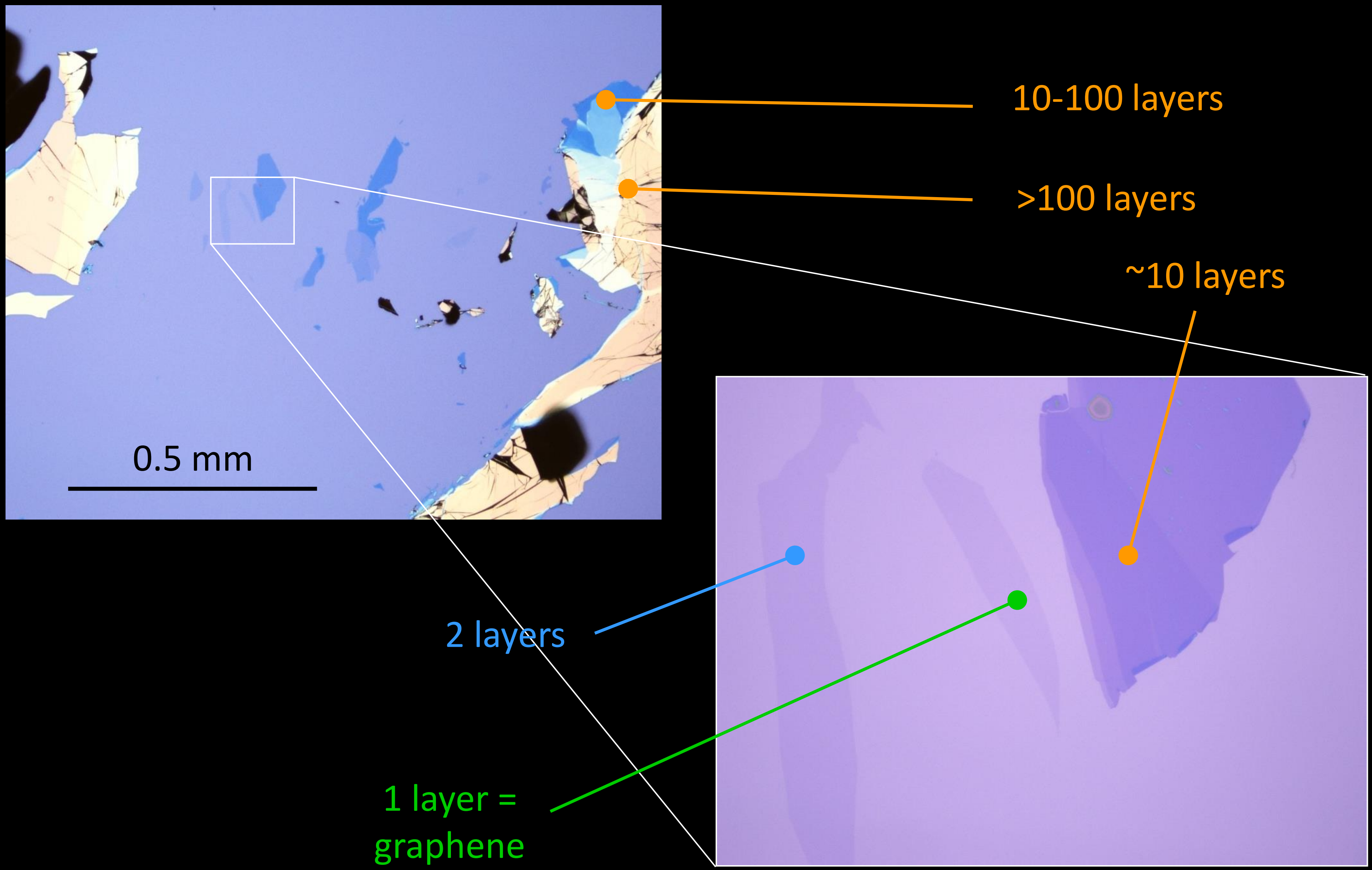

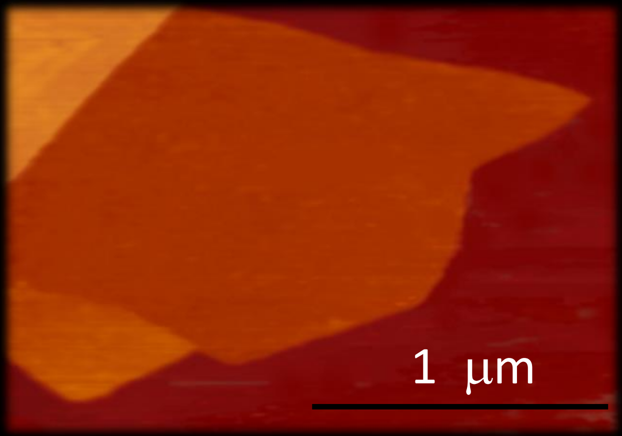

first 2D material demonstrated
- Manchester, Science ‘04

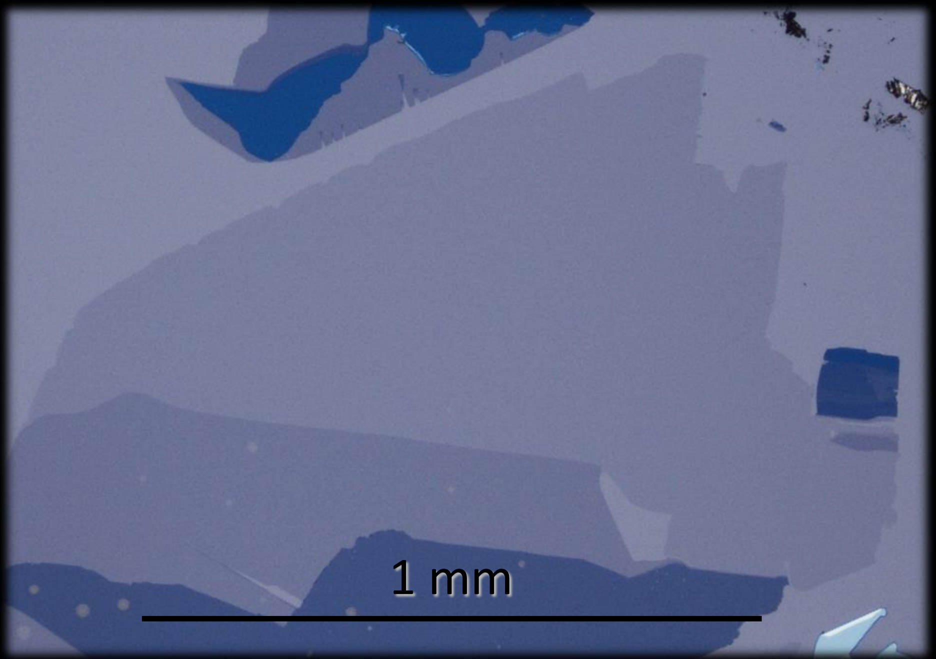

graphite trace
on oxidized Si wafer

First Graphene Electronic Devices

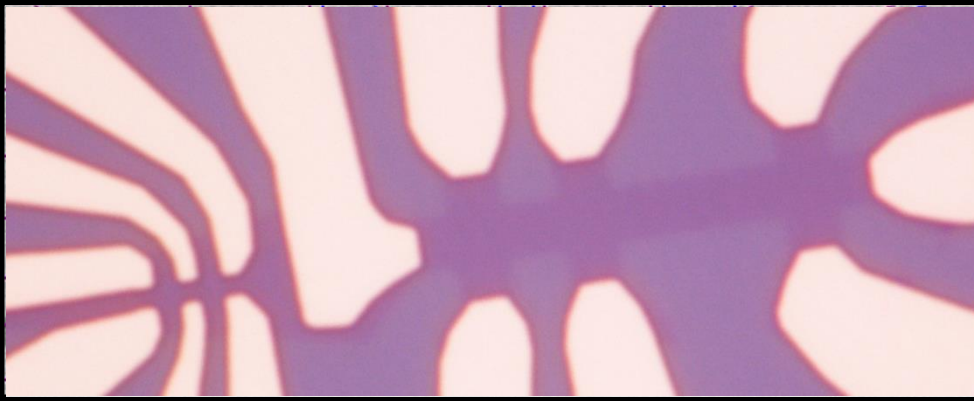

Science 2004 PNAS 2005

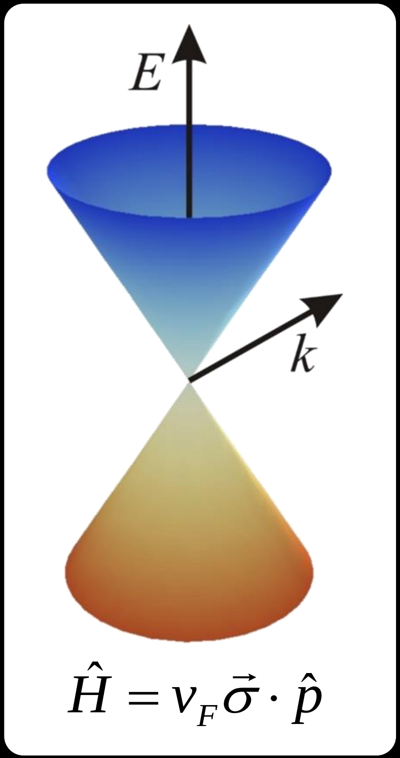

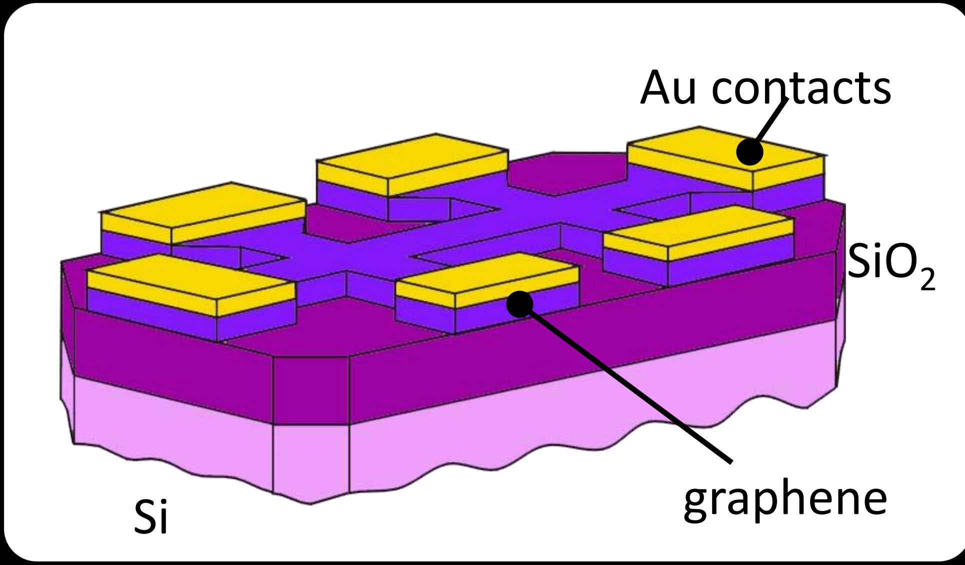

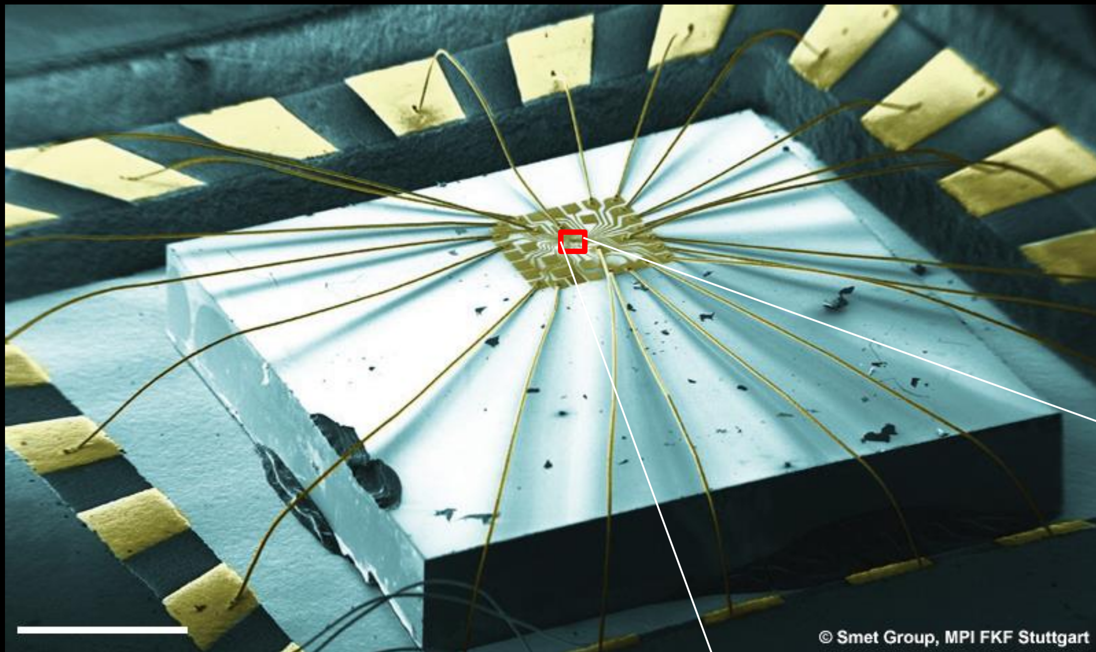
© Smet Group, MPI FKF Stuttgart

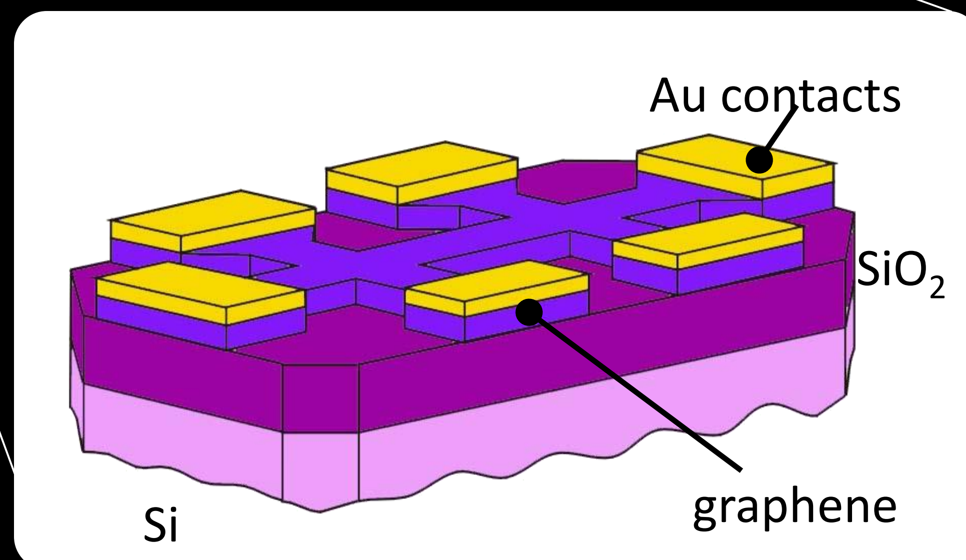
Au contacts
SiO_2
graphene
Si

Electronic transport

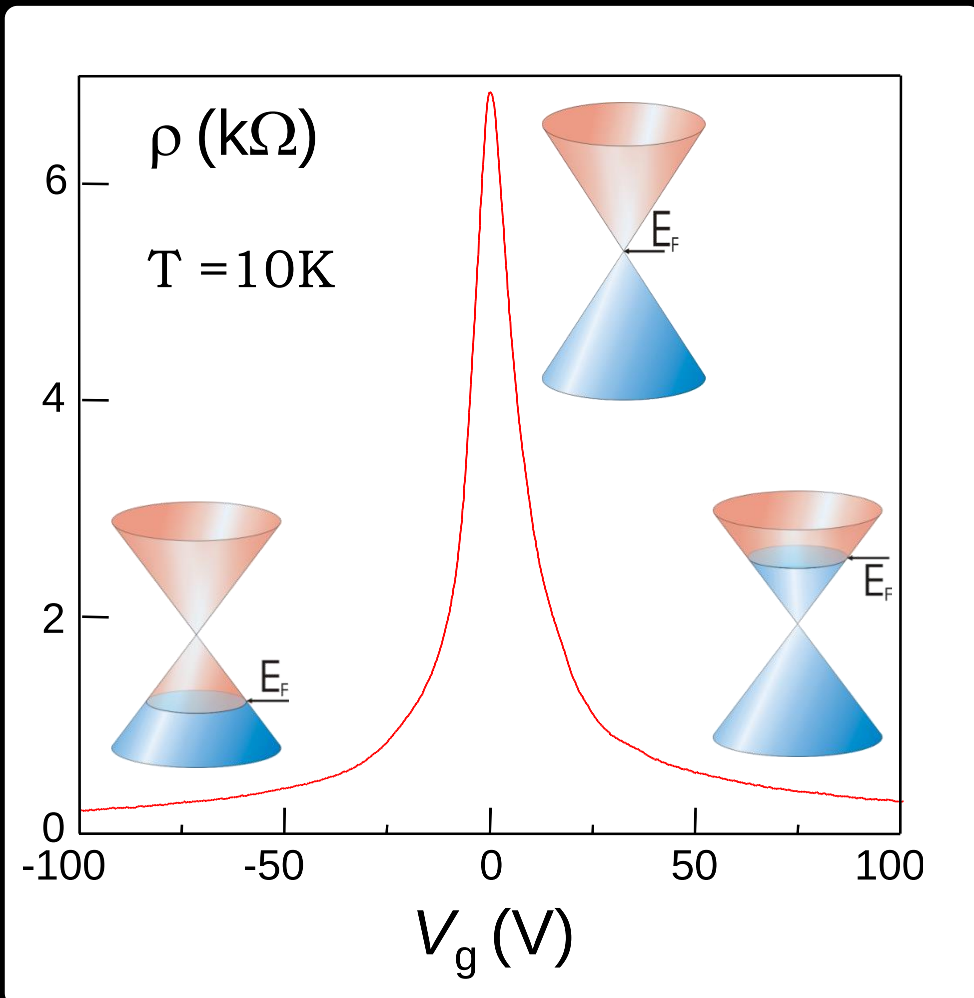

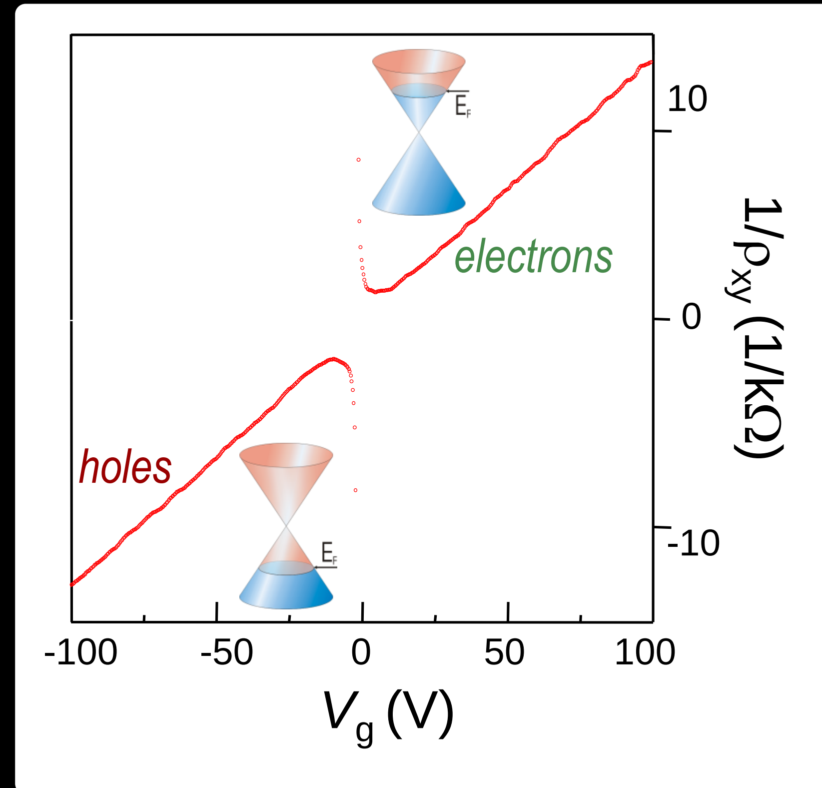

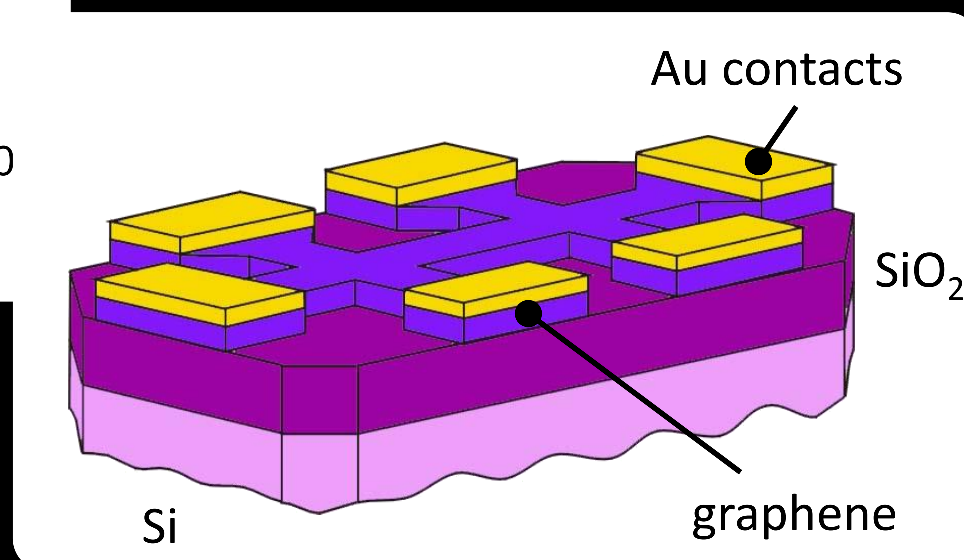

Ambipolar Field Effect

Electro-neutrality point

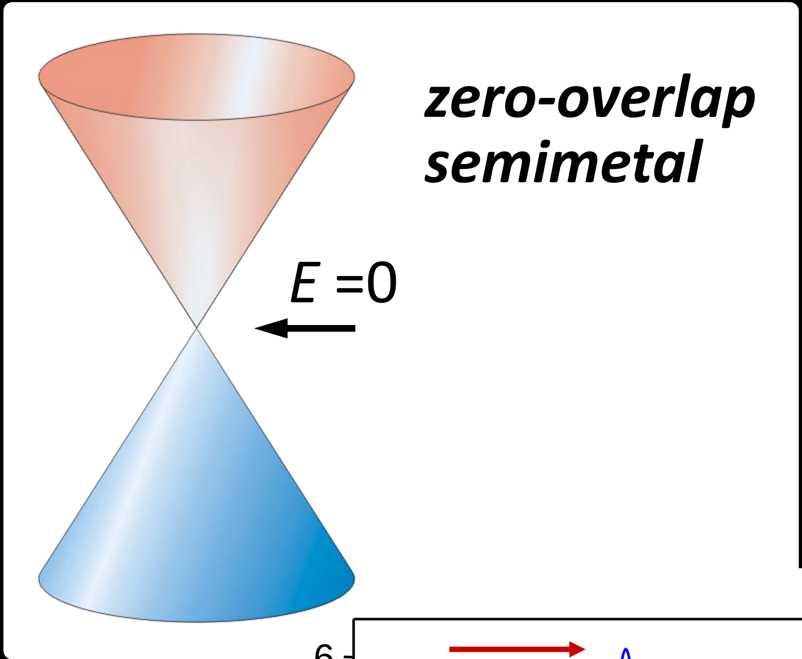

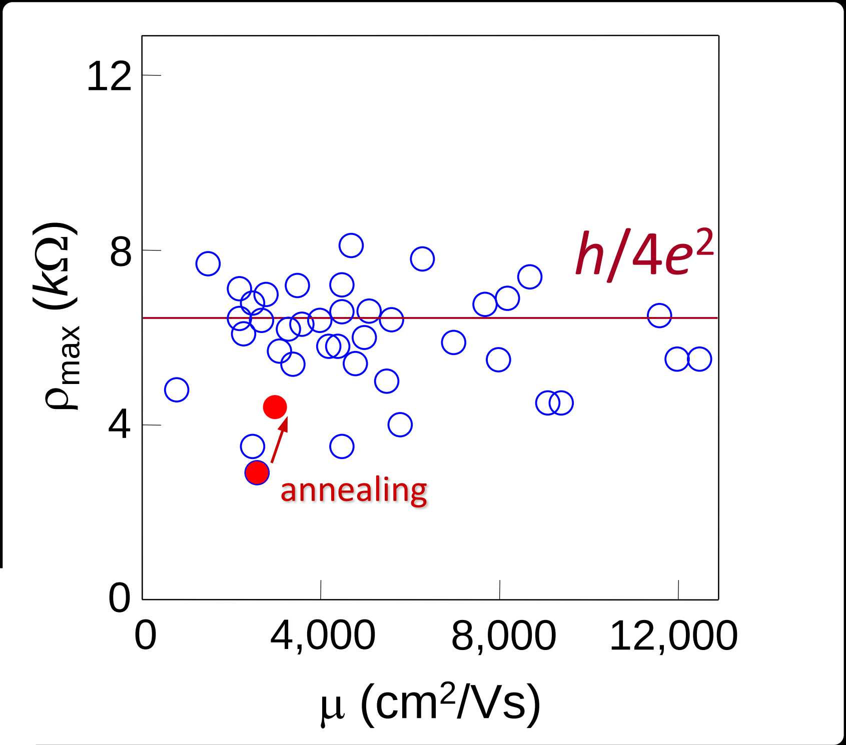

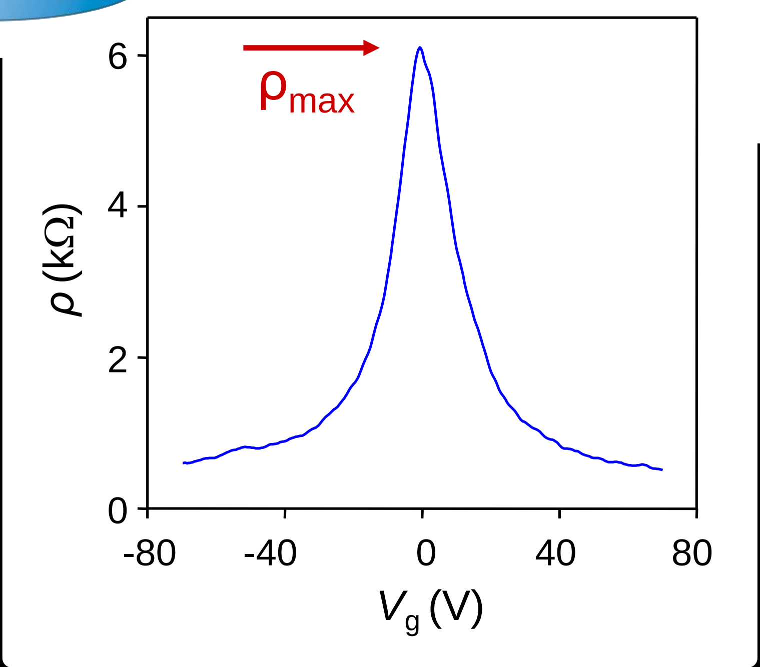

CONDUCTIVITY
WITHOUT
CHARGE CARRIERS?

Scanning Single-Electron Transistor Microscopy

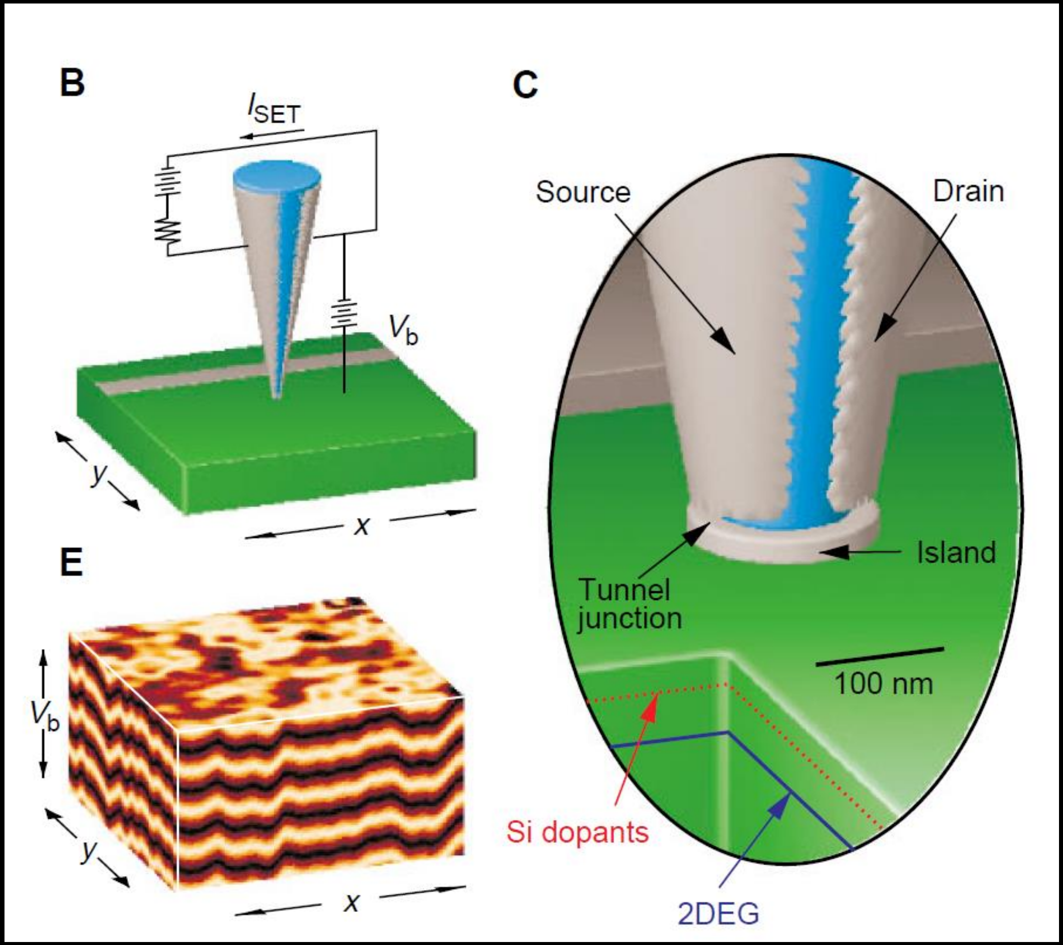

Single electron transistor at the end of scanning probe!

Electronic transport

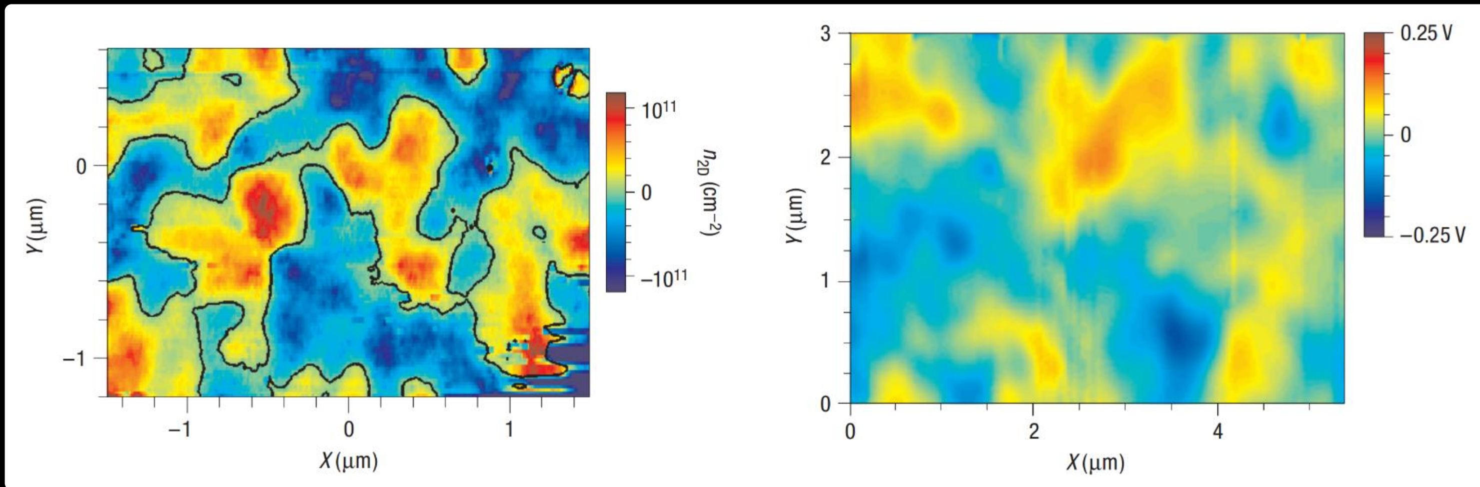

Nature Physics **4**, 144 - 148 (2008)

Near the electroneutrality point the system is dominated by the network of electron-hole puddles

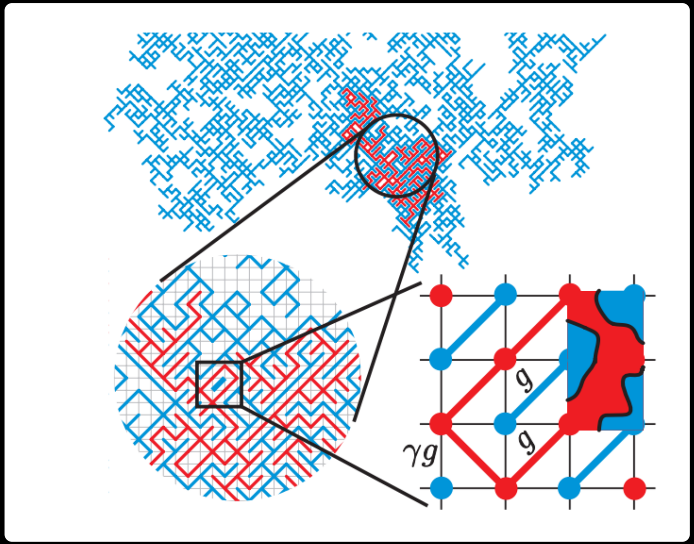

Phys. Rev. Lett. 99, 176801 (2007)

Absence of Localization (Klein paradox)

Massive particles in 2D:

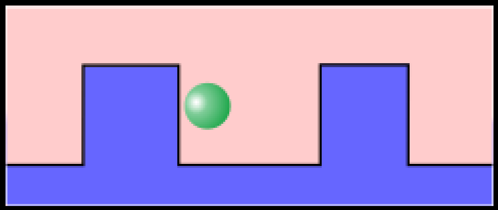

can be localized

Massless particles in 2D:

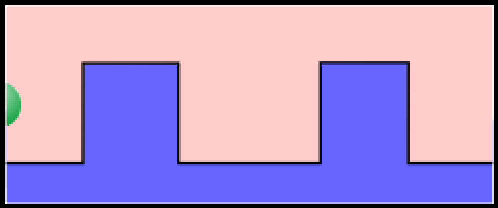

never localized

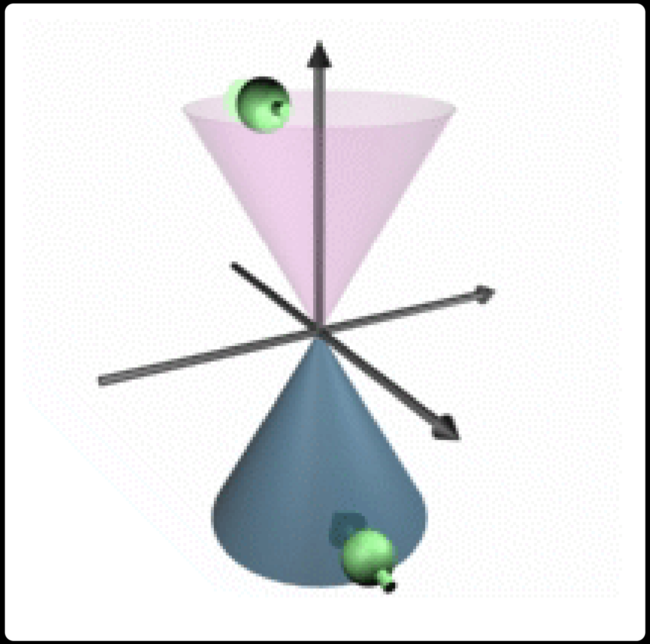

Klein paradox

(propagation of relativistic particles through a barrier)

O. Klein, Z. Phys 53,157 (1929); 41, 407 (1927)

Consequence of pseudo-spin conservation

M.I.Katsnelson et al
Nature Physics 2006

How to confine electrons?

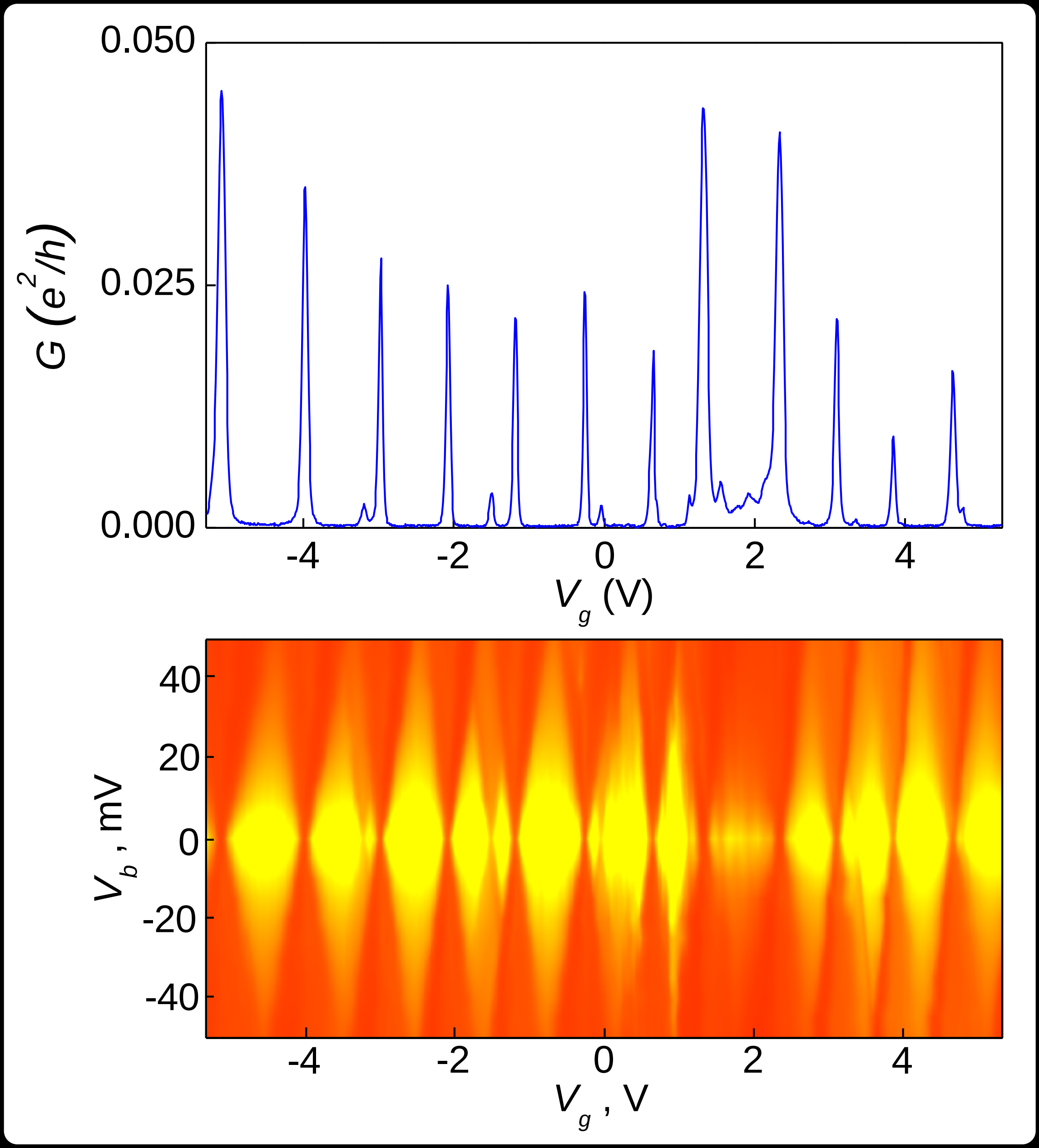

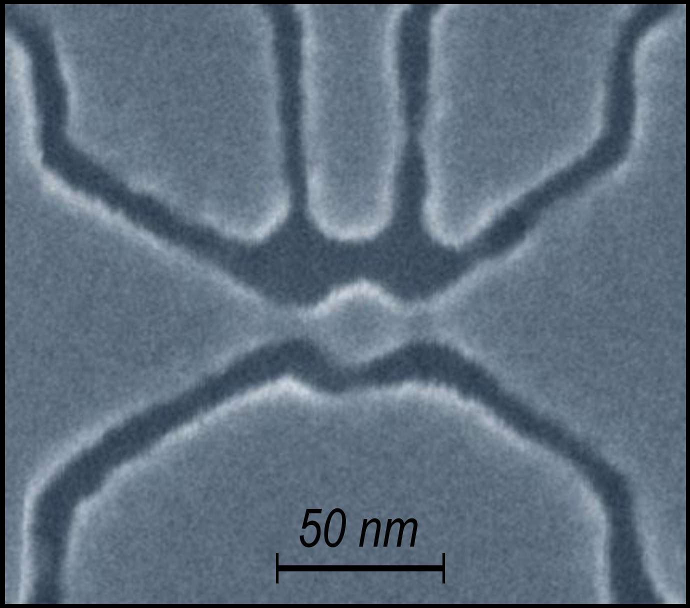

Large distance between
the peaks in V_g
(strong screening by side gates)

Ponomarenko *et al*
Science 2008

Smallest Quantum Dots

Gap: 0.5eV

Size: ~1nm

- Only few benzene rings
- Remarkably stable
- Sustains large currents

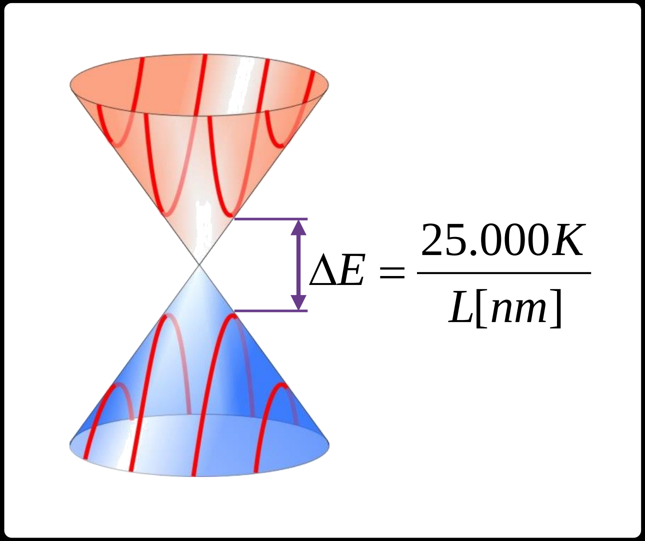

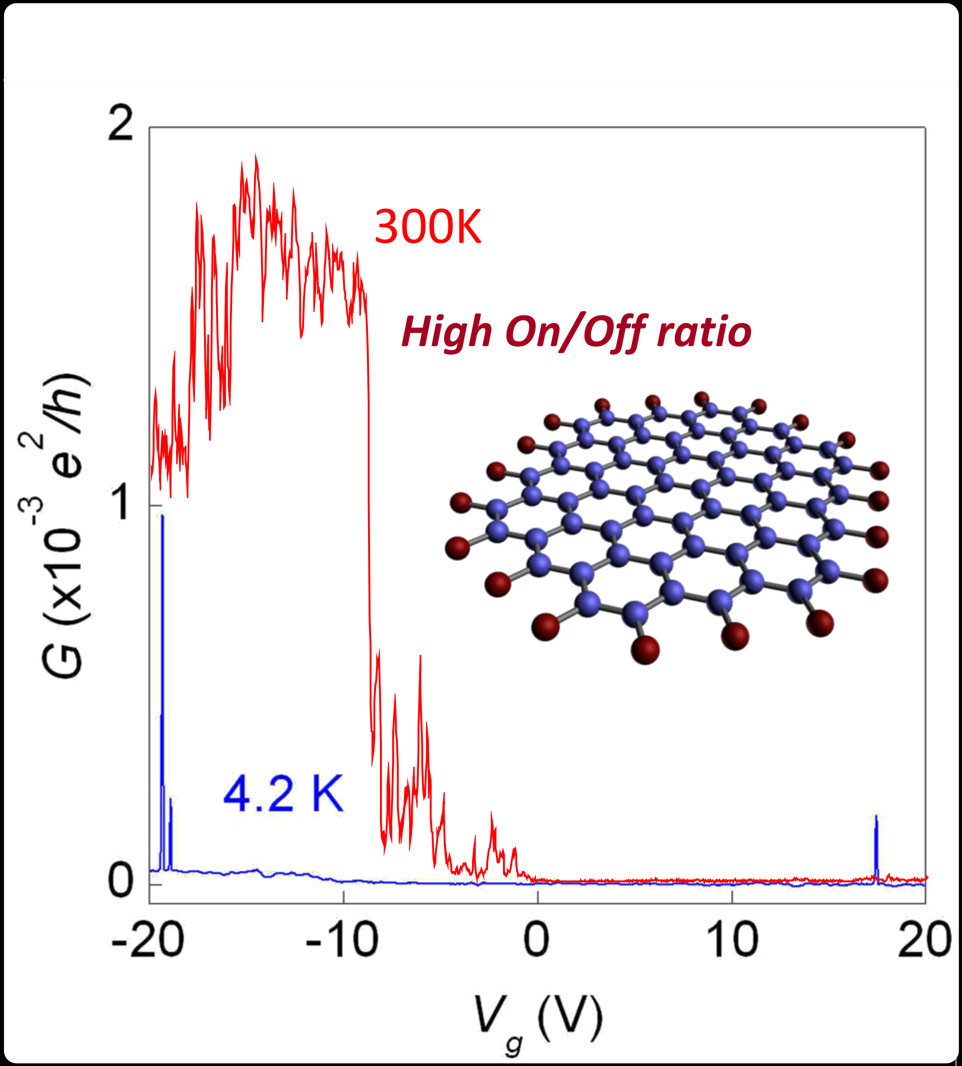

Controlling QD size with nm precision

Previously: Nanoribbons

Ozyilmaz, et al. APL (2007); Han, et al. PRL (2007); Avouris, et al. Nat. Nanotech. (2007).

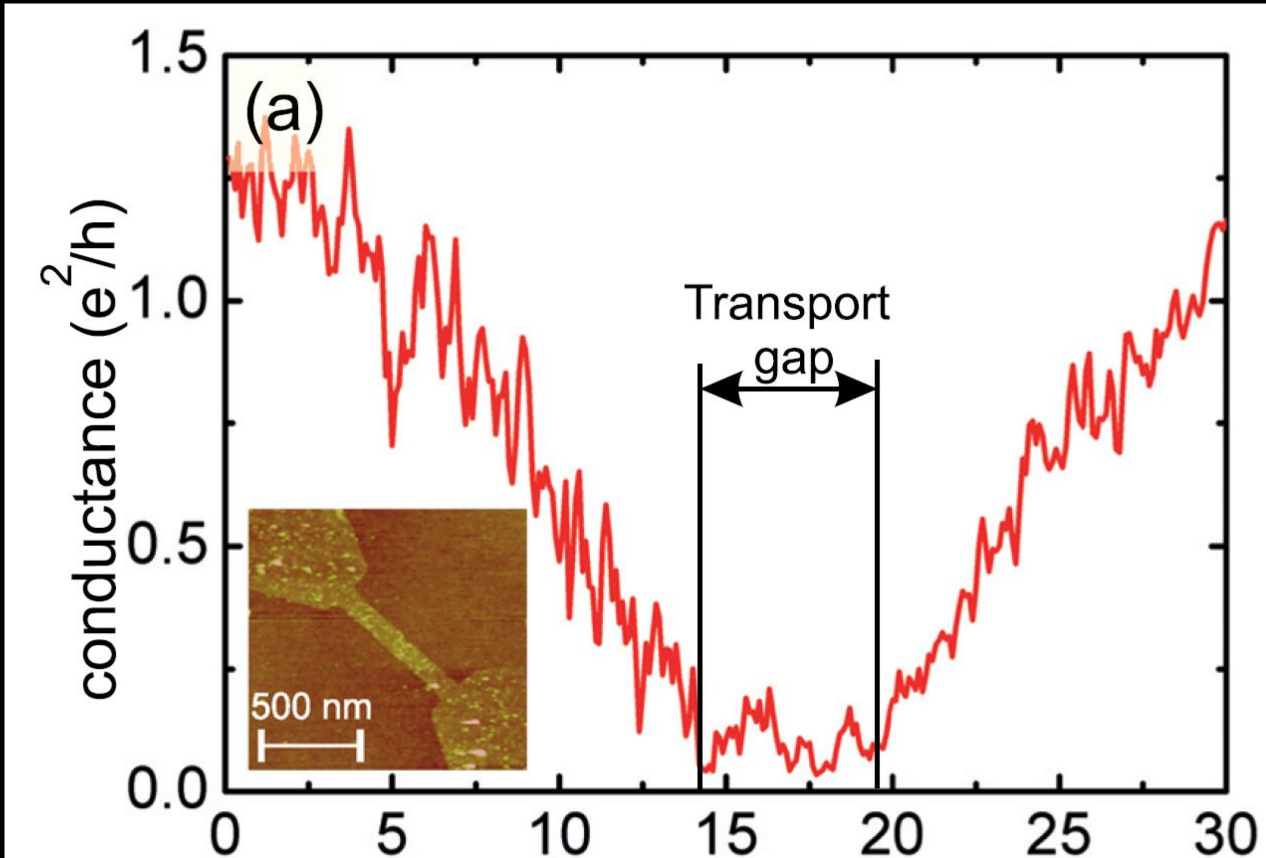

Etched graphene nanoribbons – edges destroy 1D channel, turning it into s series of 0D quantum dots

In the nanoribbon which is examined here, we find that transport must be dominated by two rather small quantum dots, which is consistent with previous transport experiments.

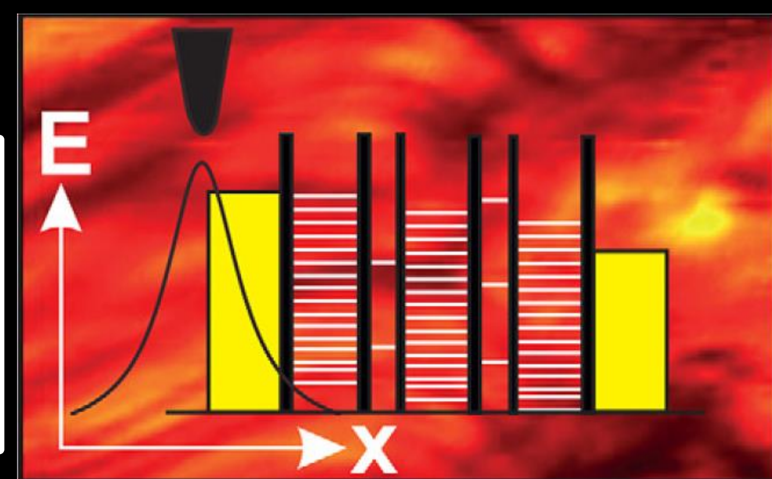

Rep. Prog. Phys. **75** (2012) 126502 (24pp) doi:10.1088/0034-4885/

Transport through graphene quantum dots

J Güttinger[1], F Molitor, C Stampfer[2], S Schnez, A Jacobsen, S Dröscher, T Ihn and K Ensslin

Solid State Physics Laboratory, ETH Zurich, 8092 Zurich, Switzerland

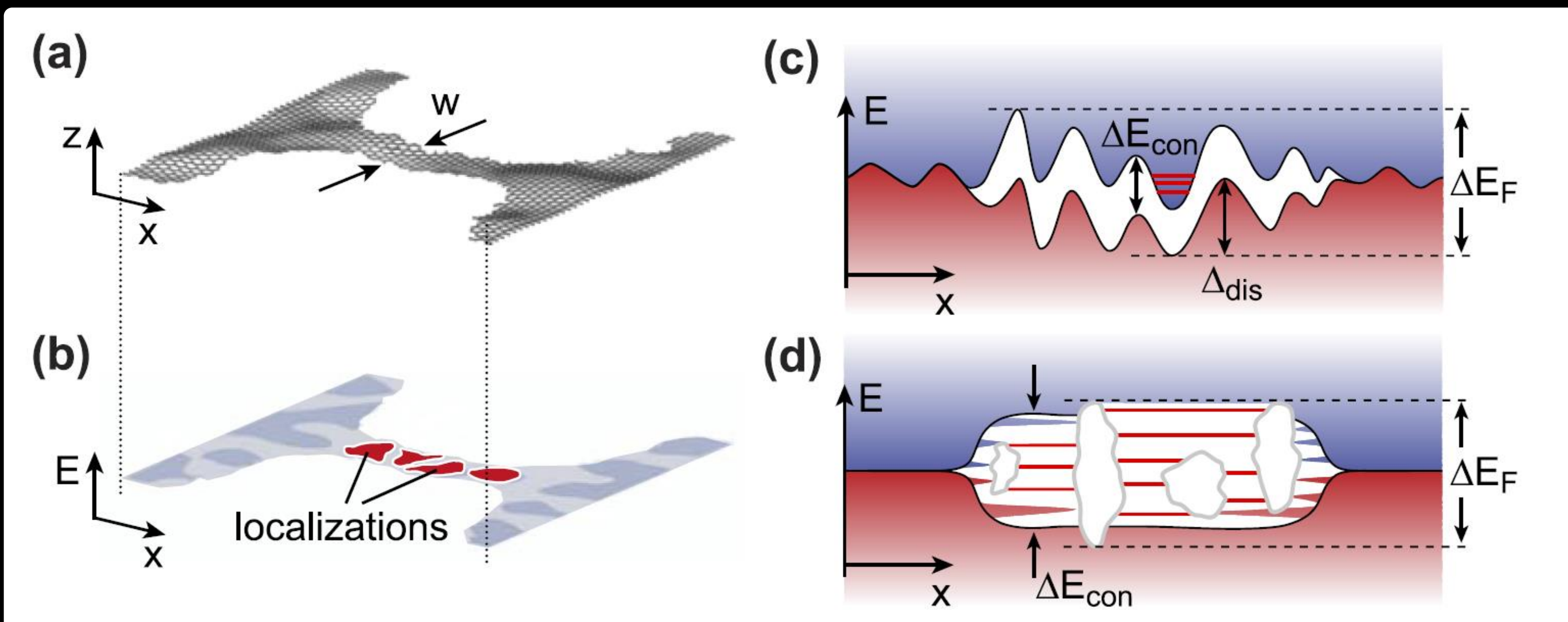

Etching always create disordered edges

Chemical modification

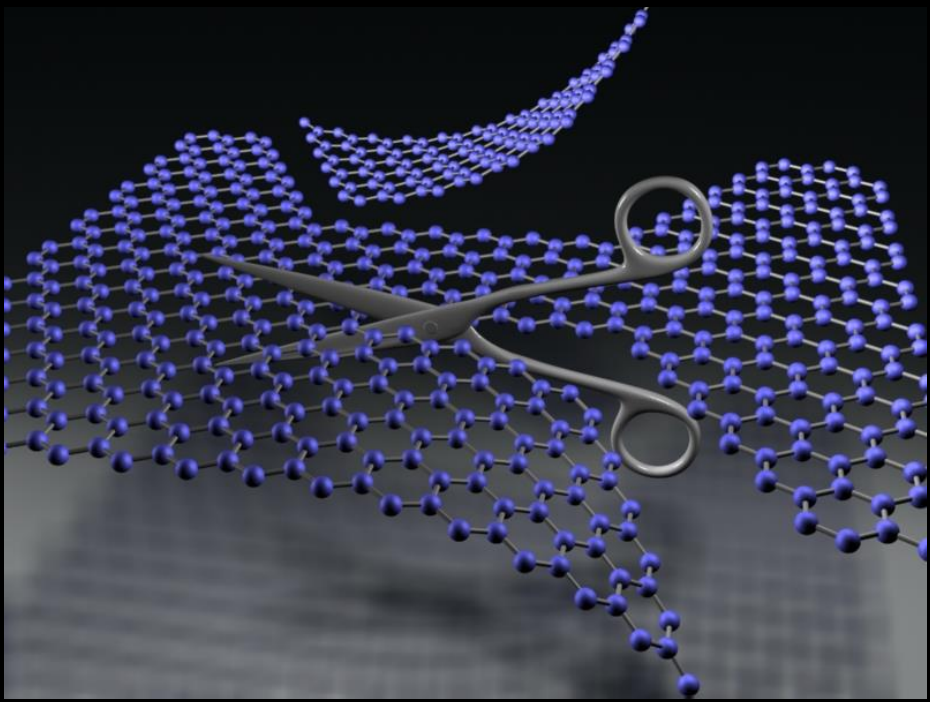

Reactive Plasma Etching

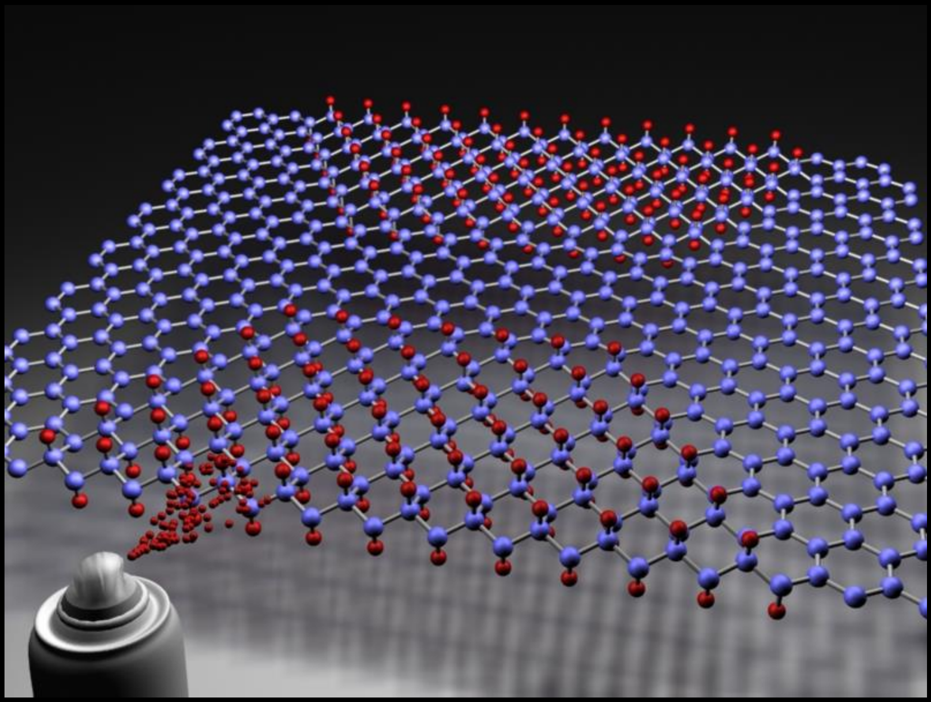

Hydrogenation

Suspended devices

G on SiO_2 device

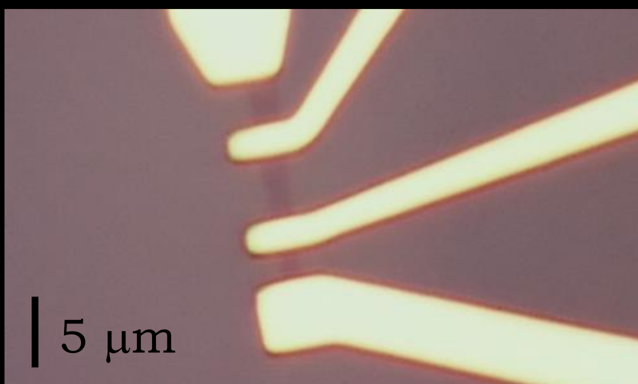

BHF etch

Yield ~100%

suspended

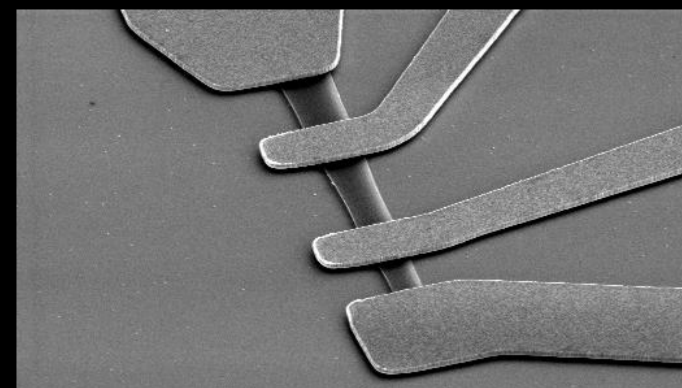

Current annealing

Yield ~ 10% - 20%

first transport measurements:
Phys. Rev. Lett. **101**, 096802, 2008

Graphene devices

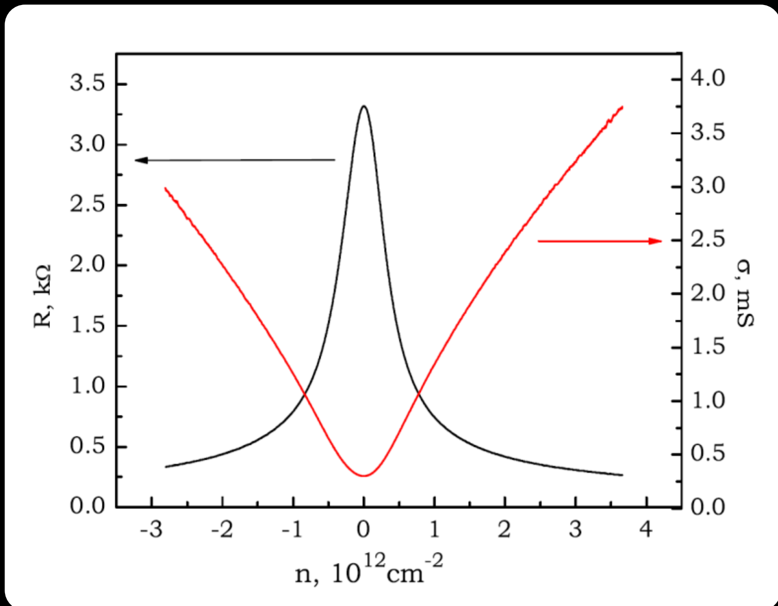

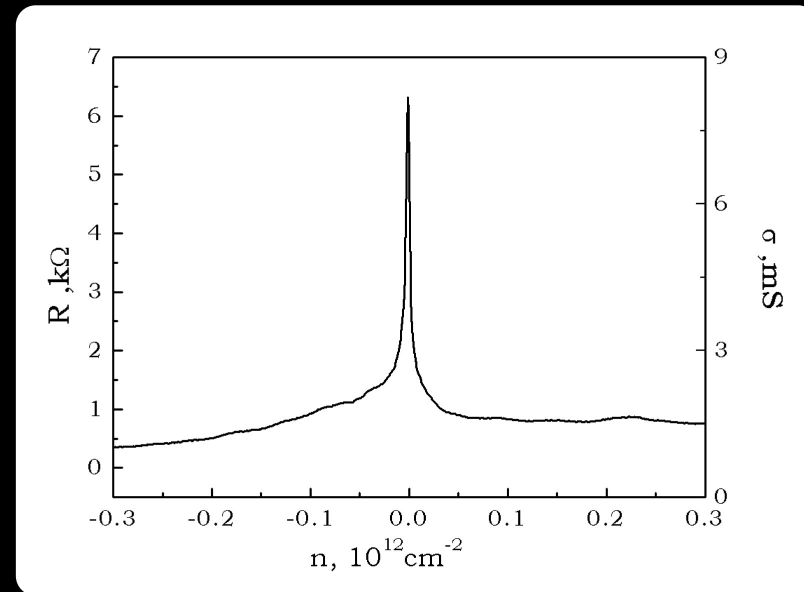

$GSiO_2$

5 000 to
20 000 cm^2/Vs

Suspended

100 000 to
1 000 000 cm^2/Vs

available carrier densities:

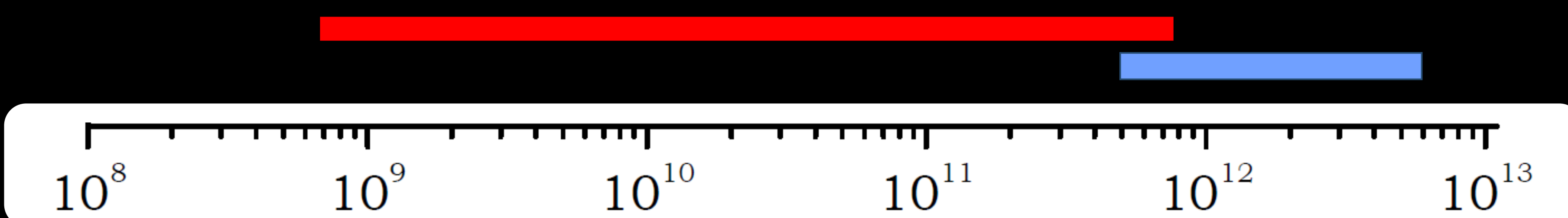

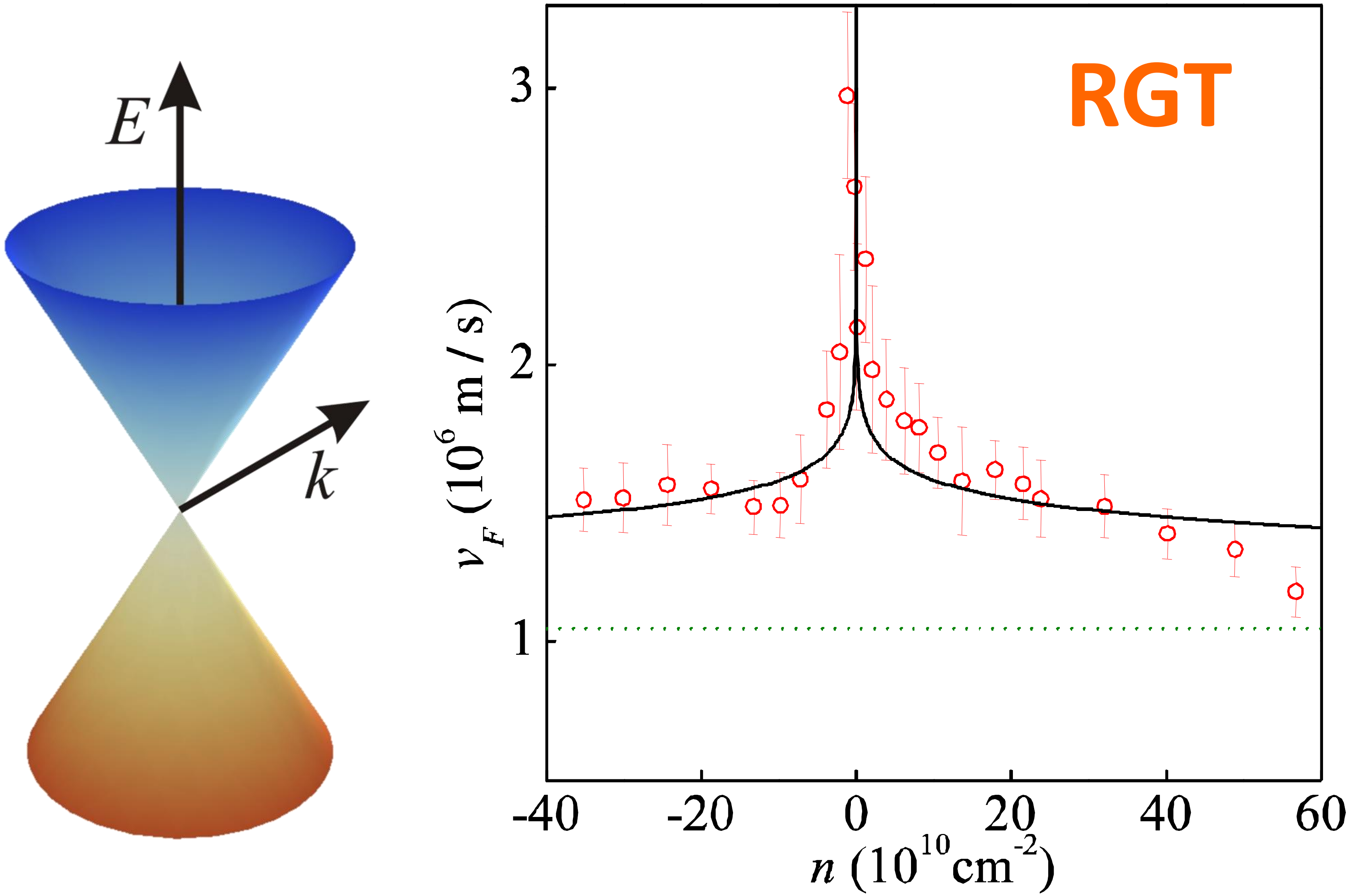

Nature Phys. 7, 701-704 (2011)

Suspended devices have issues:

- Extremely fragile
- Two terminal (if homogeneous)

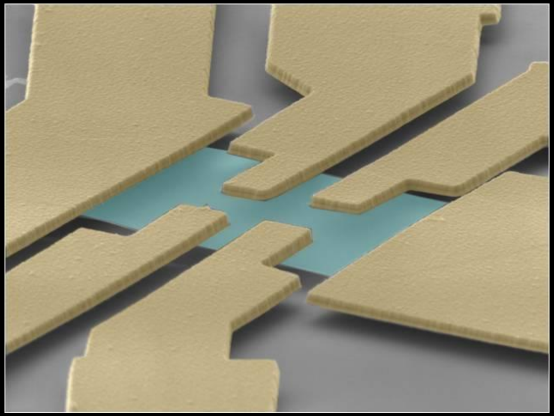

Graphene on hBN
(and beginning of vdW heterostructures)

BN - substrate for Graphene

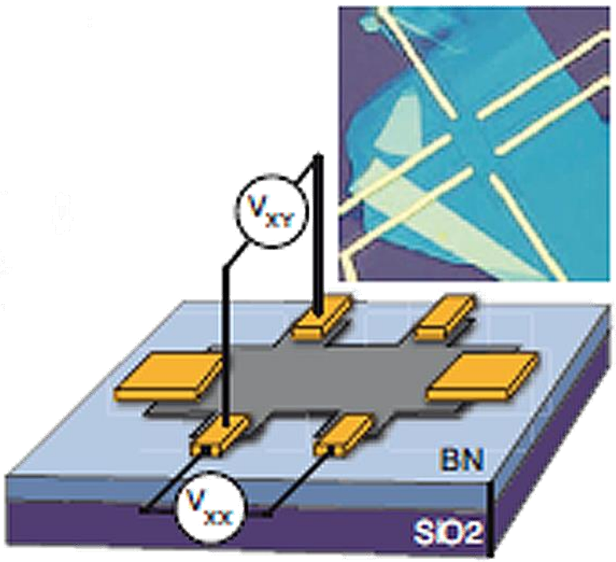

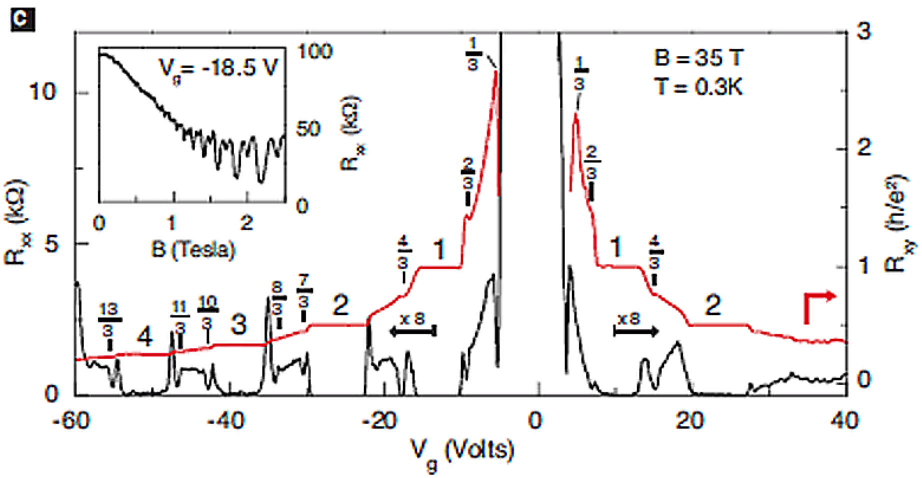

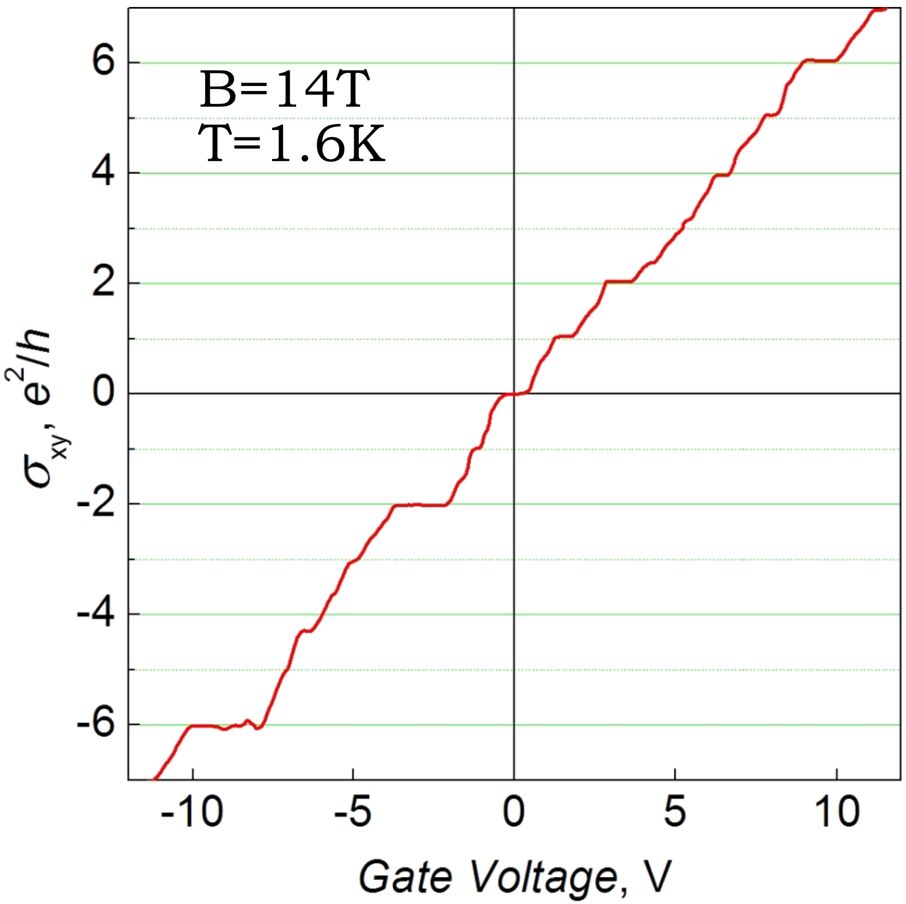

C.R. Dean et al., Nature Nanotechnology 5, 722-726 (2010)

Ballistic Transport at Room Temperature

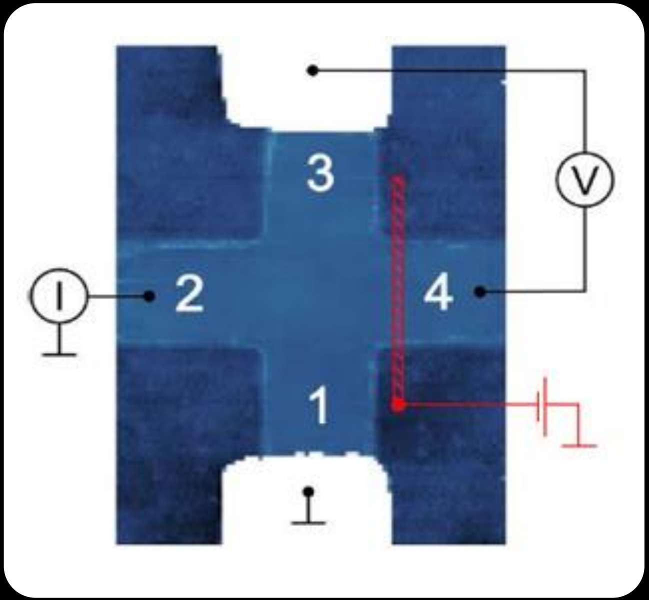

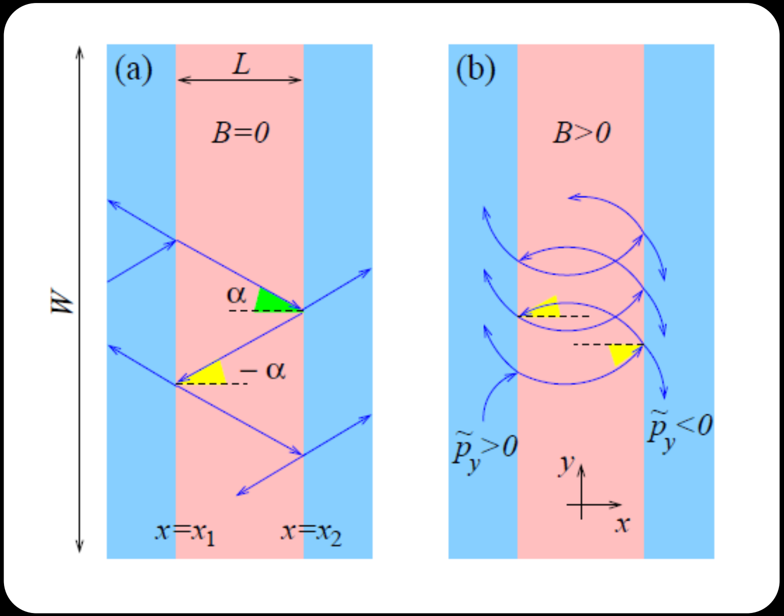

Fabry–Pérot interference in top gate controlled p-n-p structure

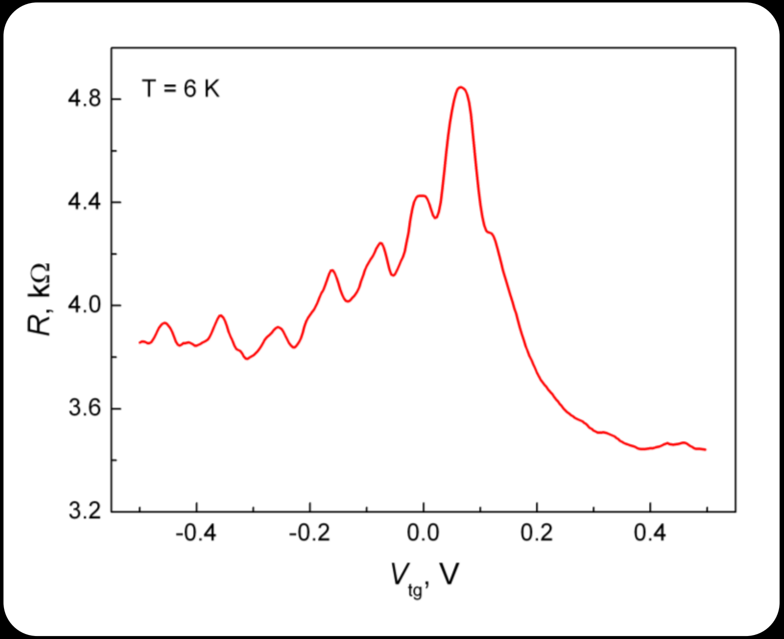

A. V. Shytov, M. S. Rudner, L. S. Levitov PRL 101, 156804 (2008)

A.F. Young, Philip Kim, Nature Physics 5, 222 - 226 (2009)

Hexagonal Boron Nitride

Hexagonal BN

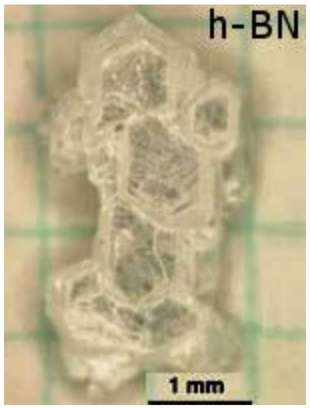

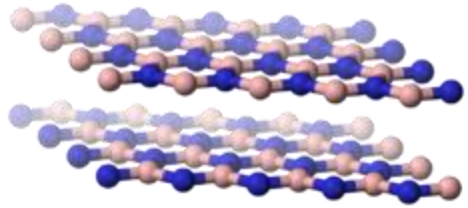

$$C = \frac{I_{BN} - I_0}{I_0}$$

tape cleavage

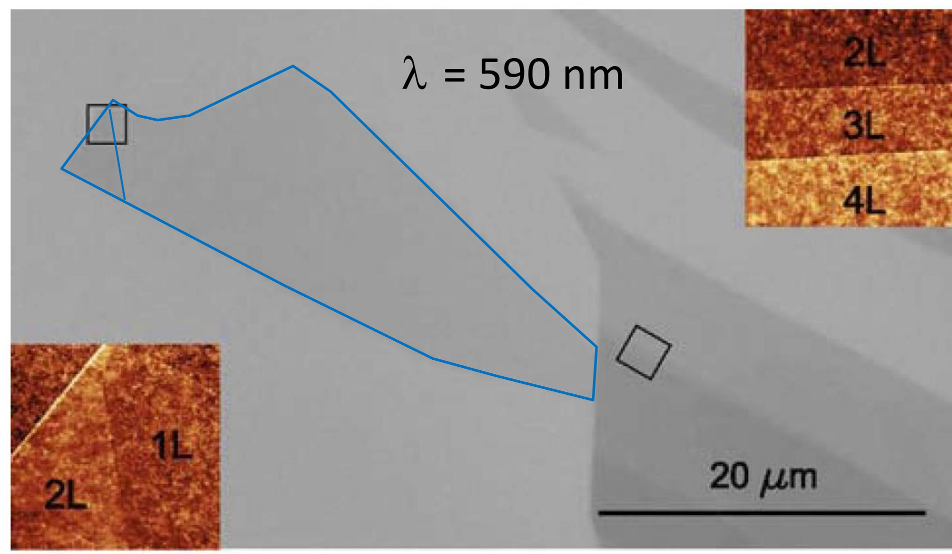

*contrast digitally enhanced by 2

BN is provided by
Kenji Watanabe &
Takashi Taniguchi

Optical contrast 5 times less compared to graphene

Extremely difficult to locate an hBN monolayer

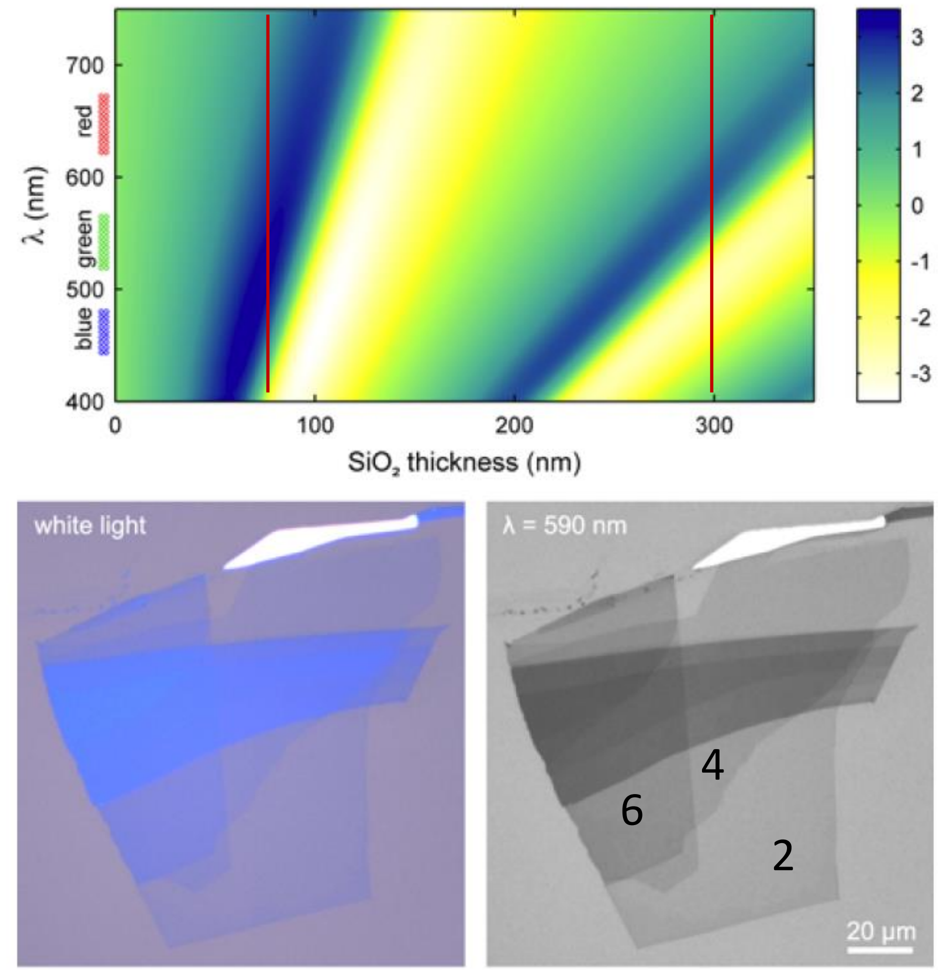

Small 7, 4, 465, 2011

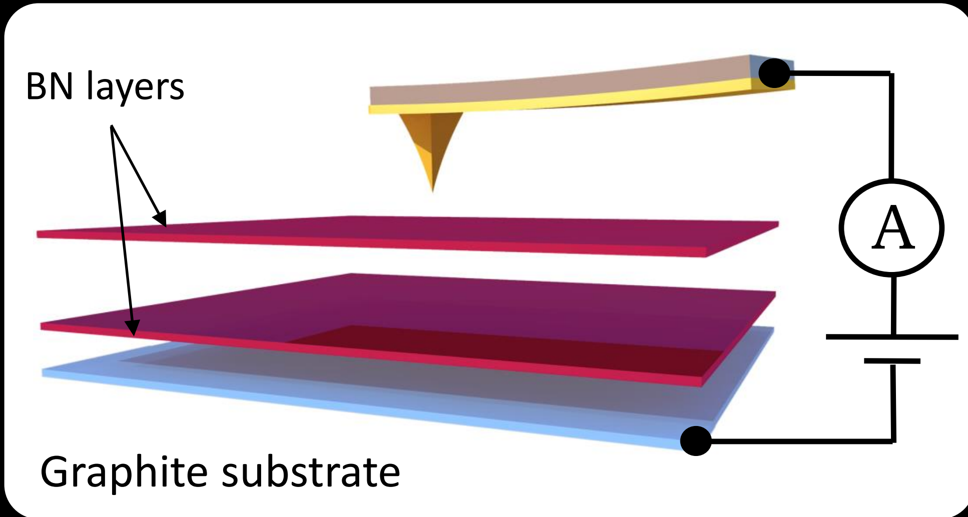

Conductive AFM

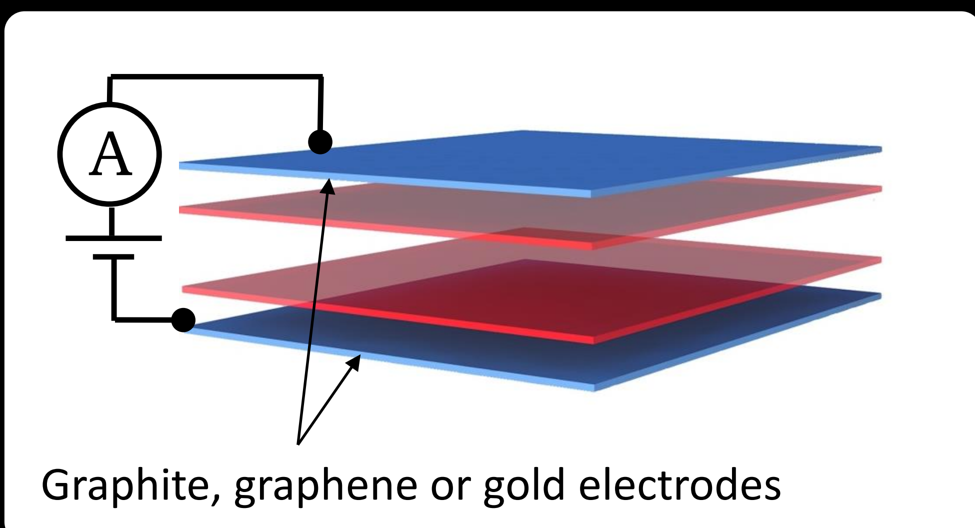

Tunnelling devices

Conductive AFM

Resistance mapping

Topography

Tunnelling resistance

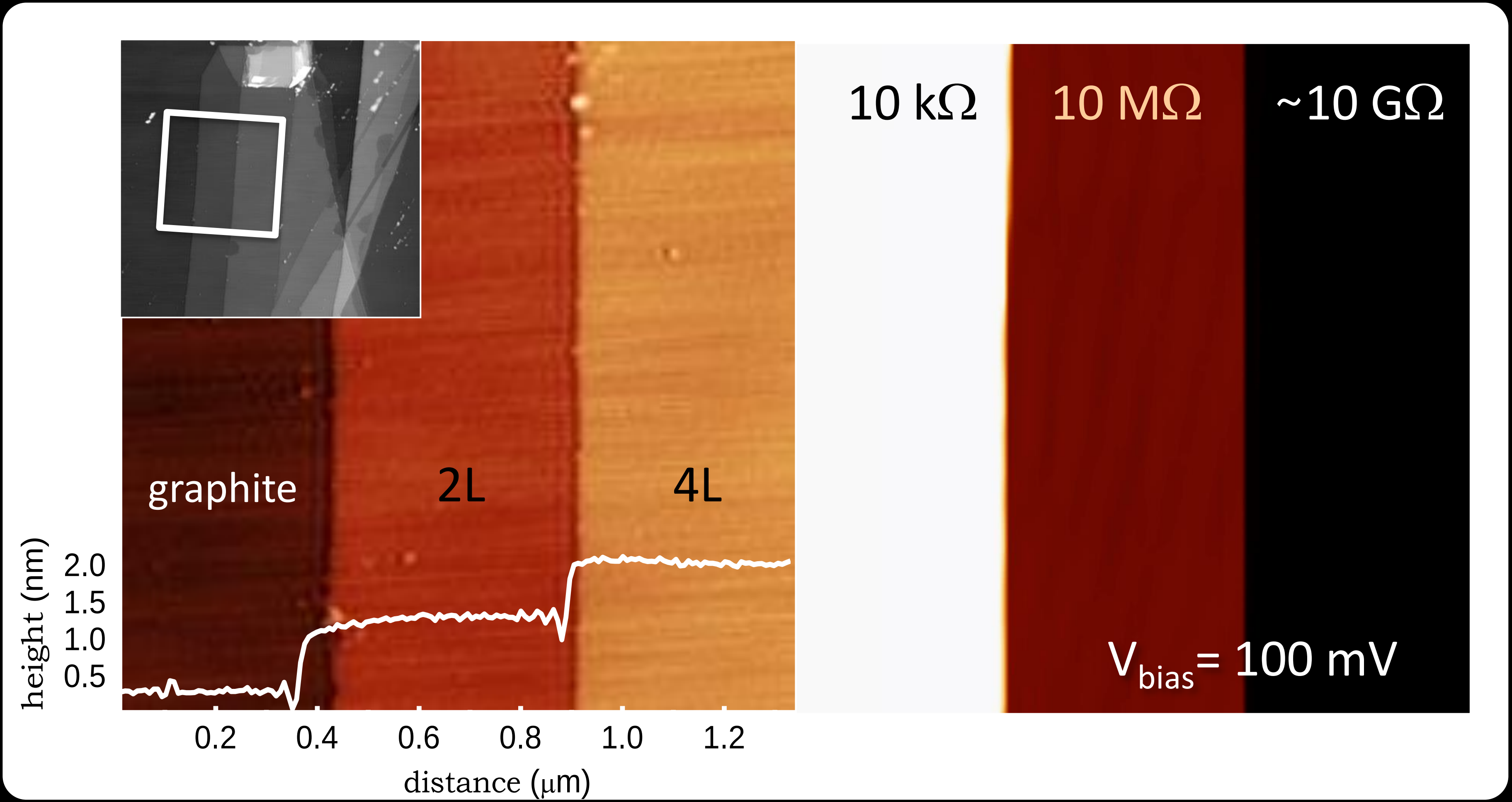

Conductive AFM

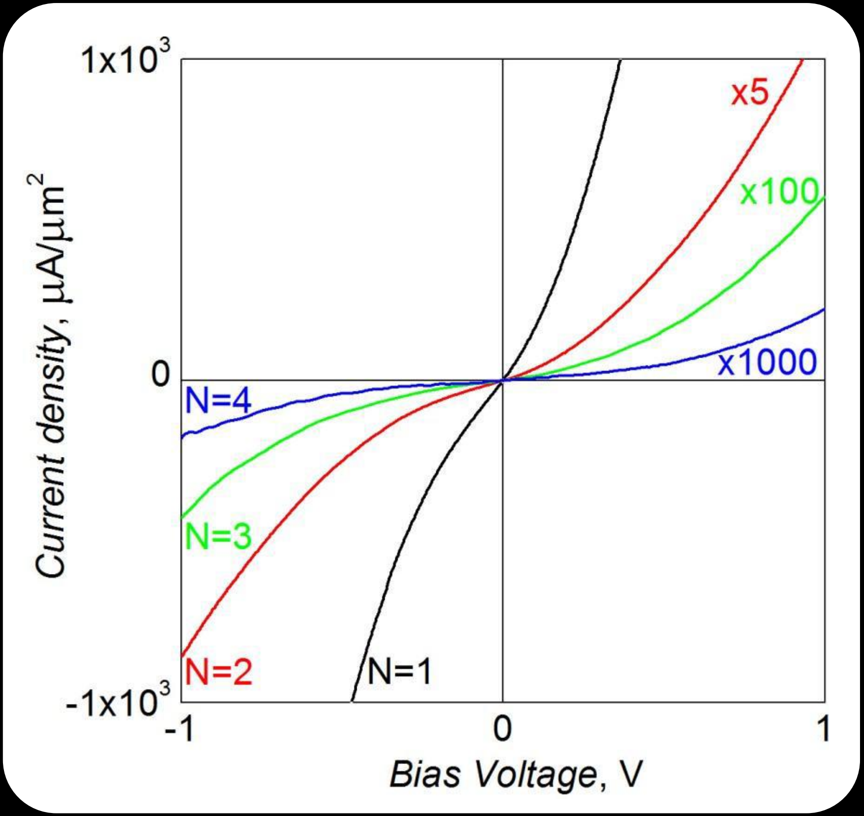

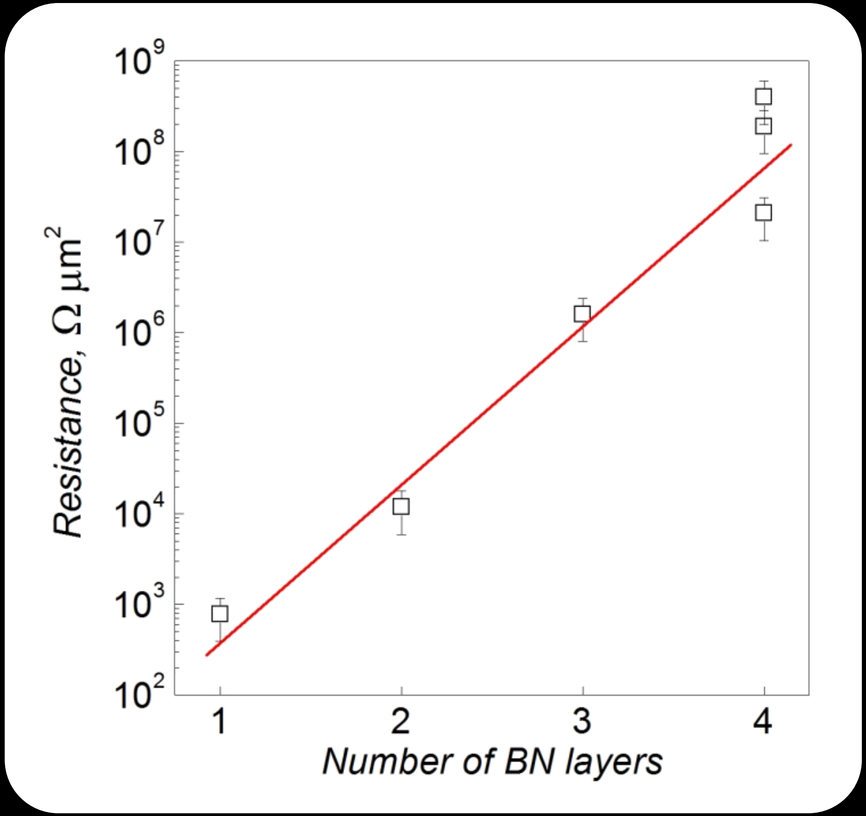

No pinholes
or defects

Transfer

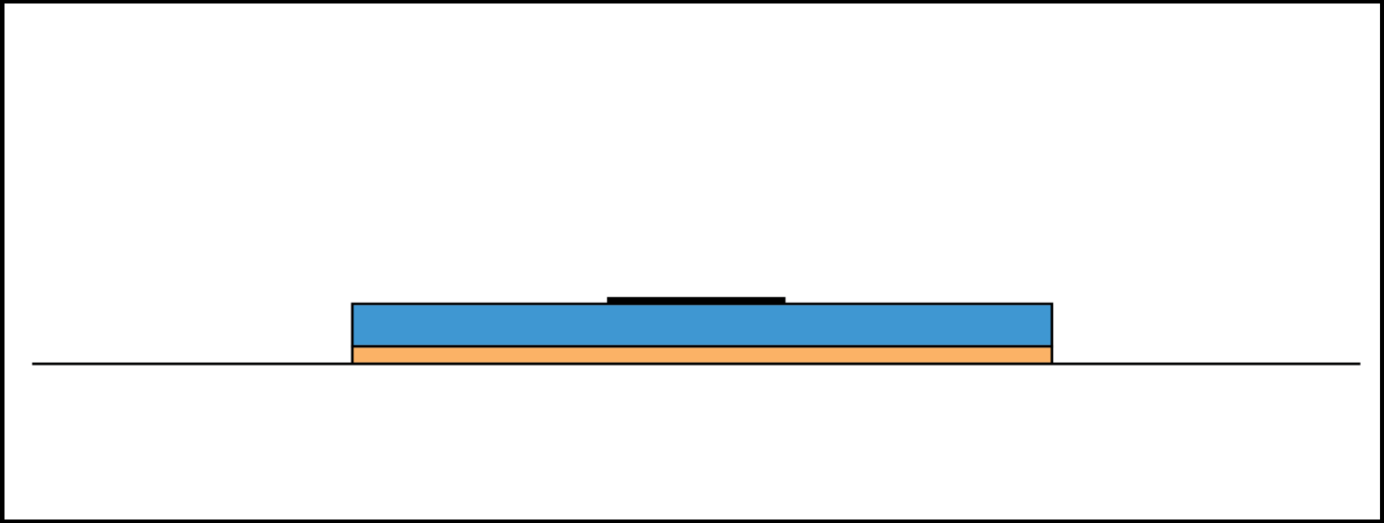

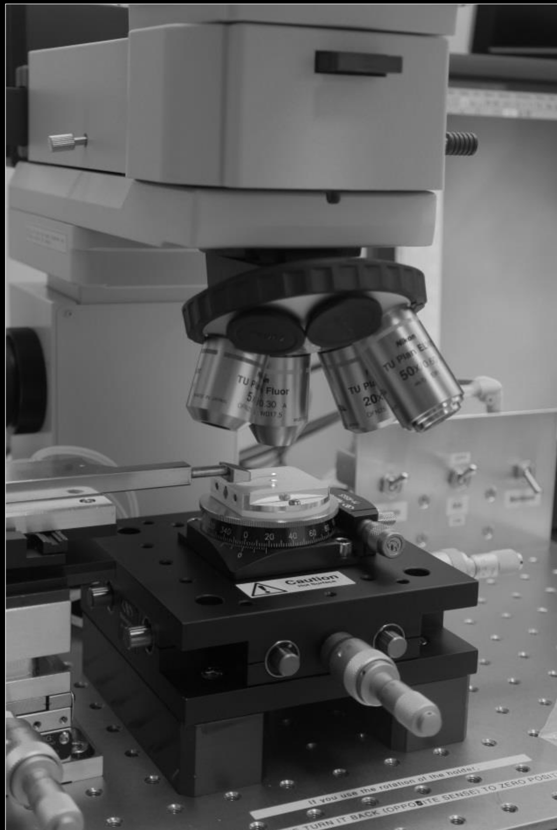

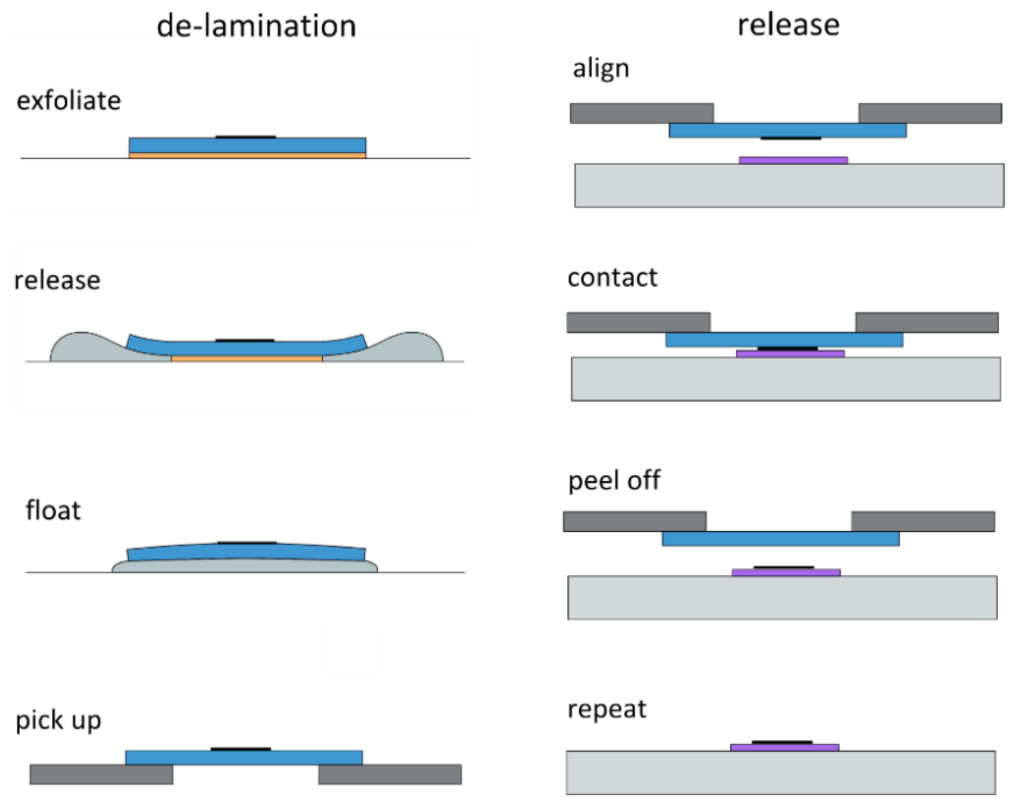

Nano Lett., 14 (6), 3270, 2014

Science 342(6158), 2013

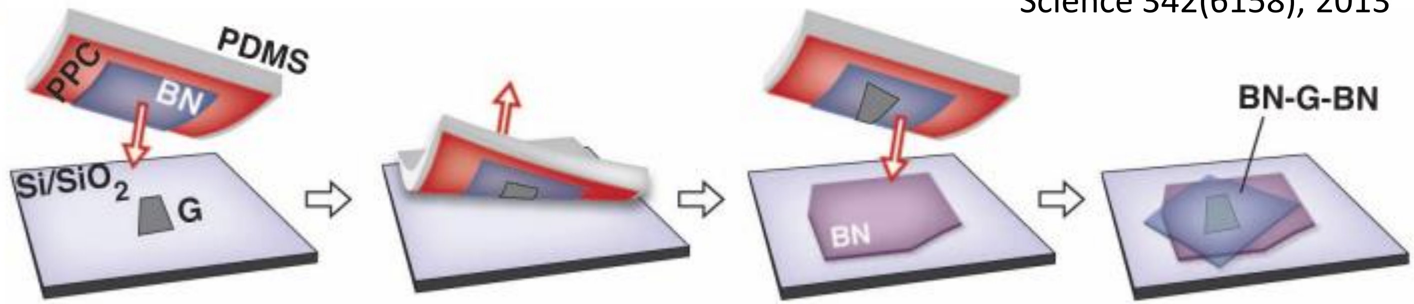

Air contamination and the surface

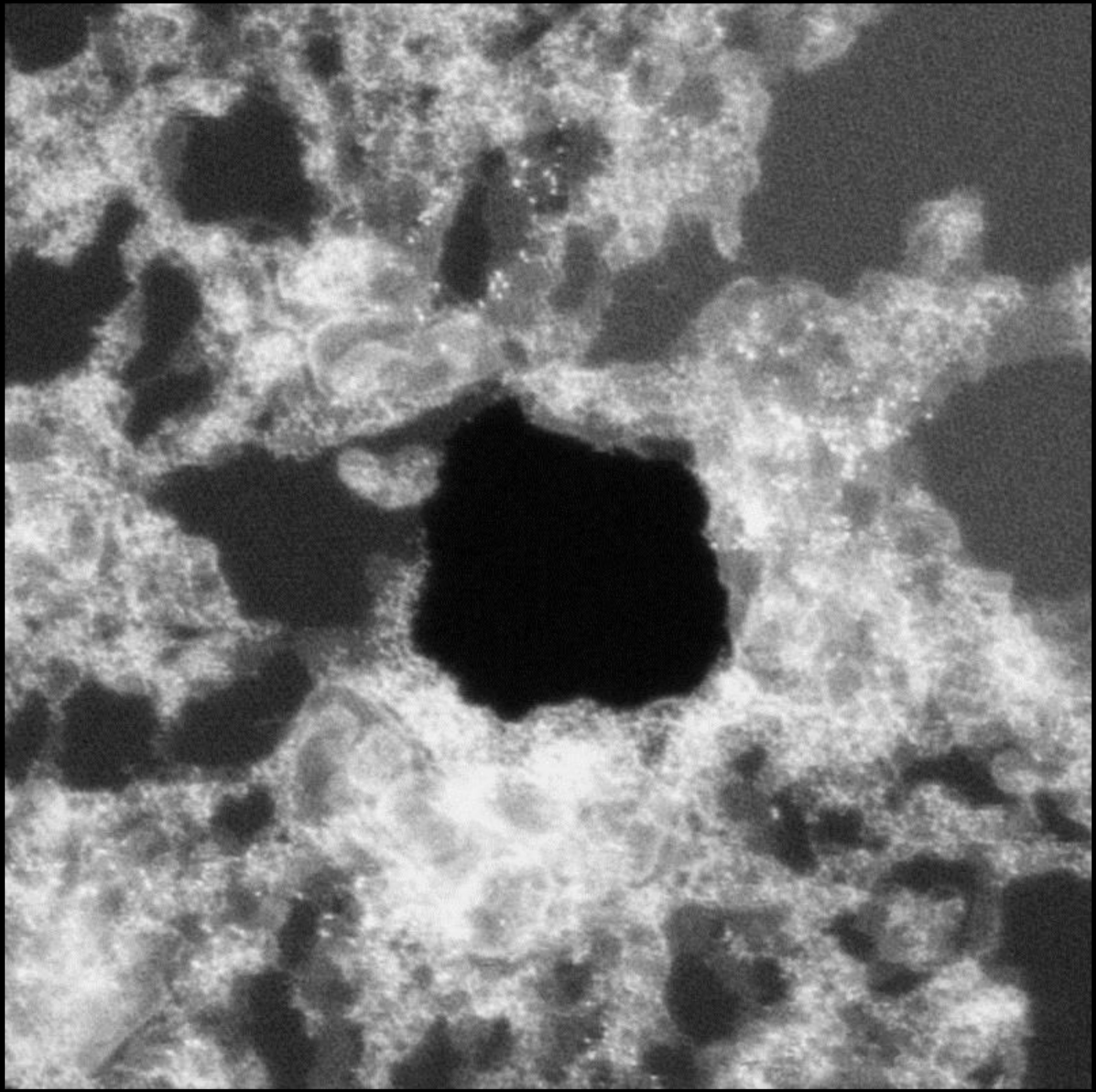

Image courtesy of Juan-Carlos Idrobo

5 year progress »

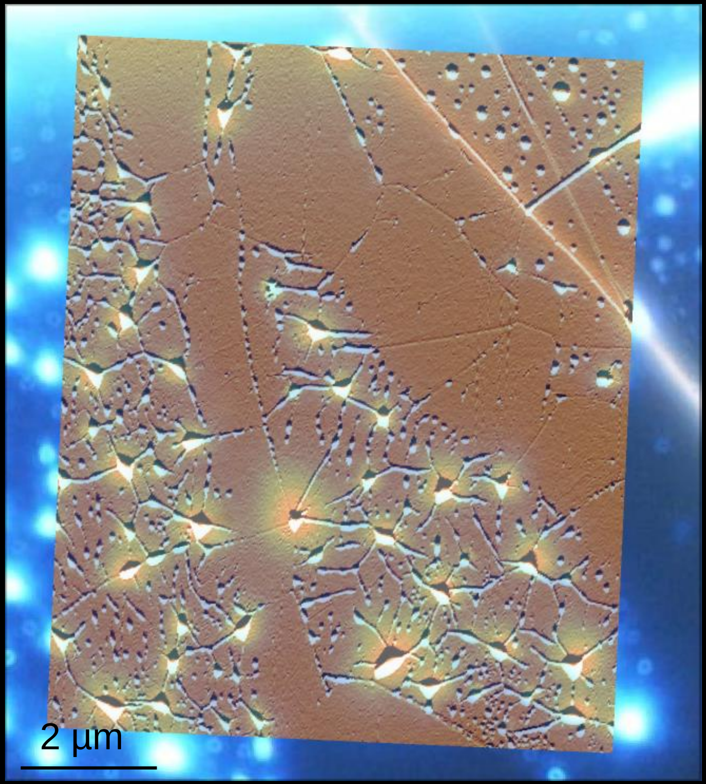

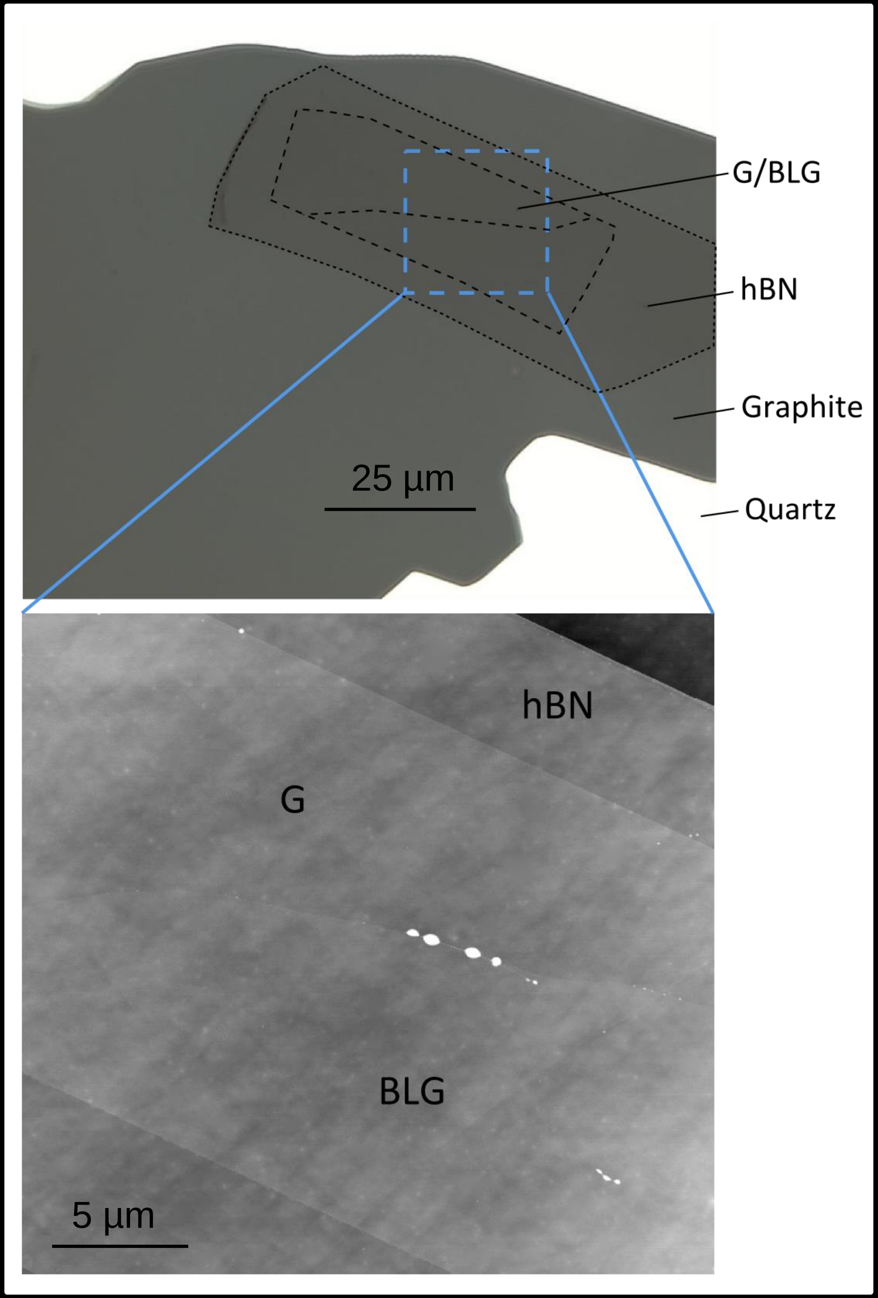

Cross-sectional TEM imaging

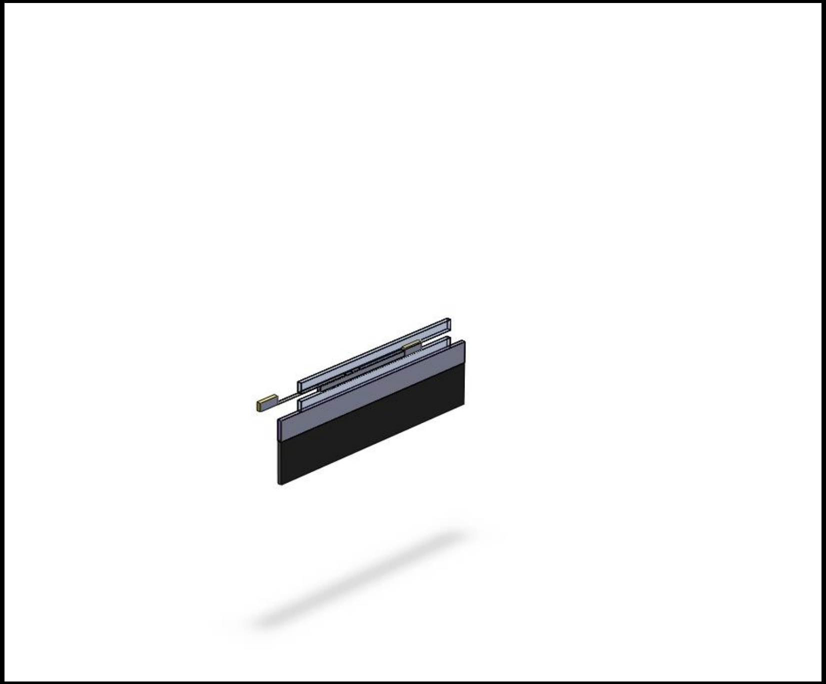

Cross-sectional TEM imaging

Nature Materials **11**, 764, 2012

How do we look inside a buried interface?

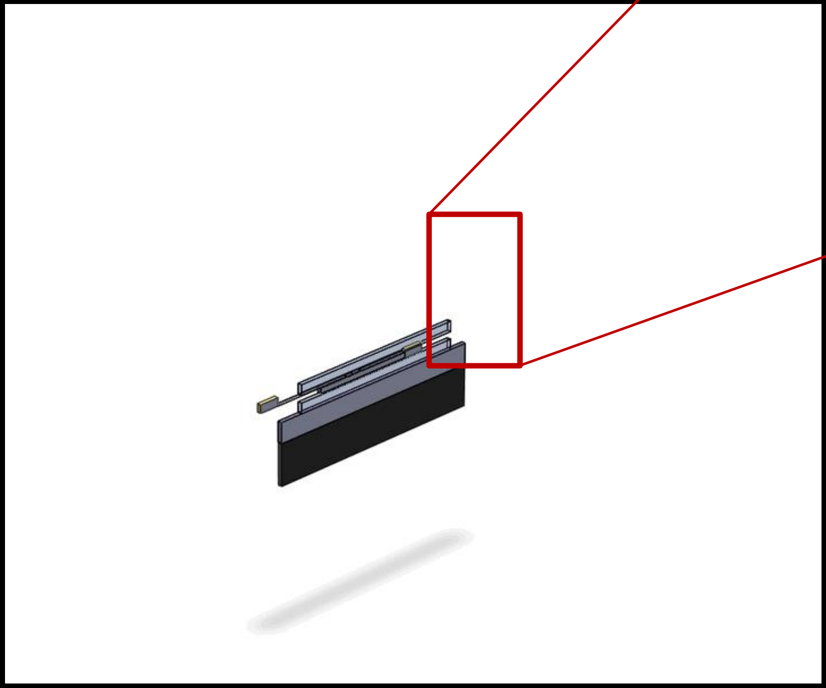

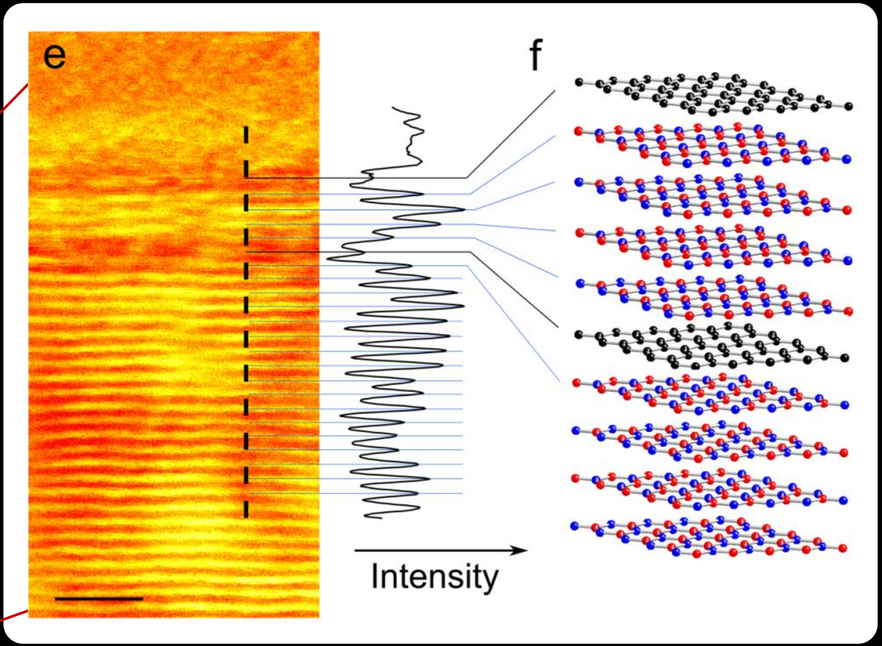

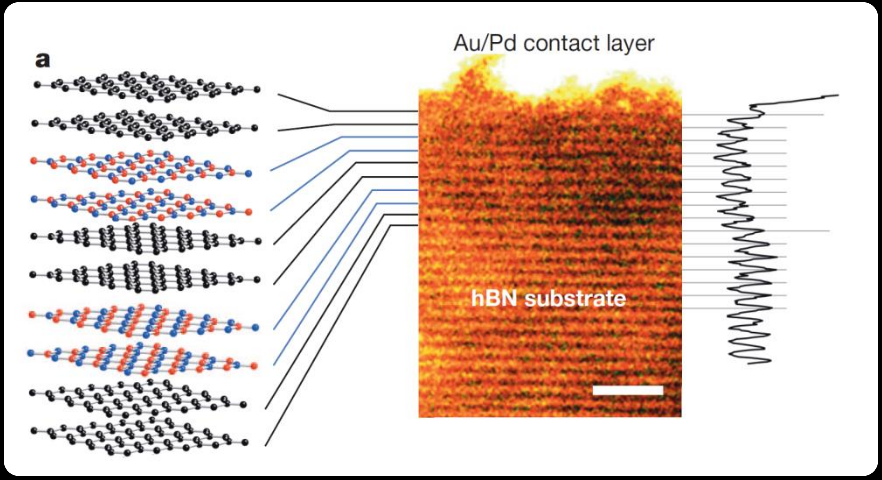

TEM sample prep

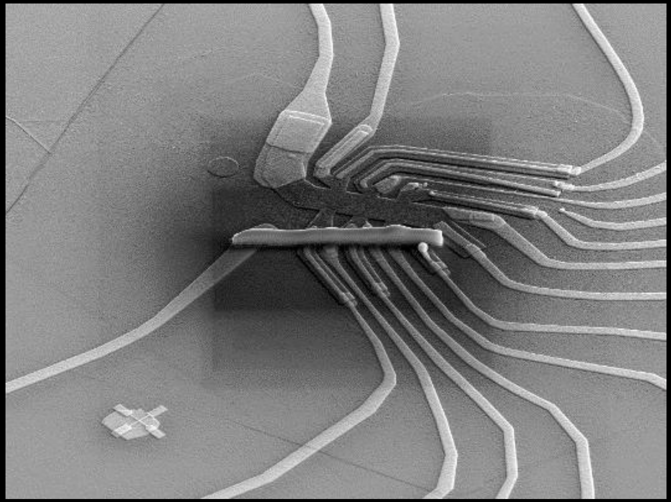

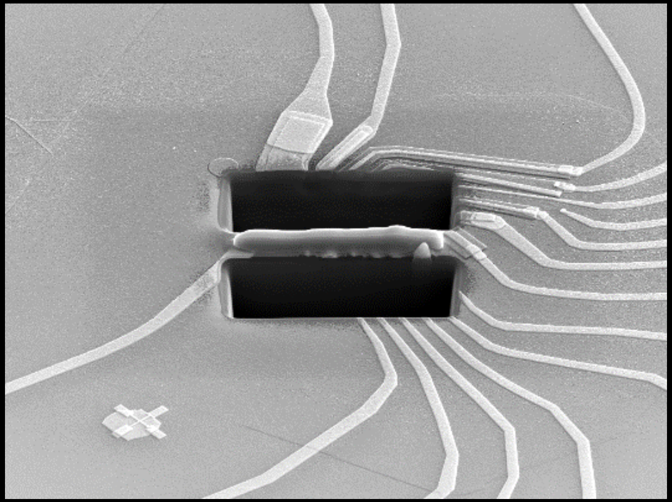

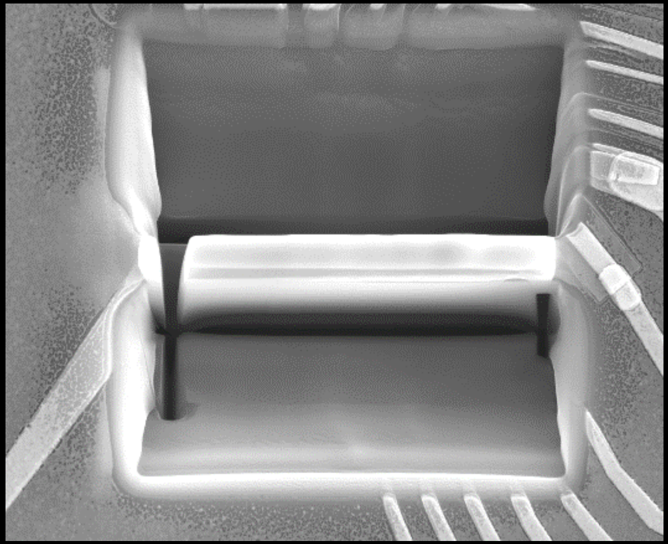

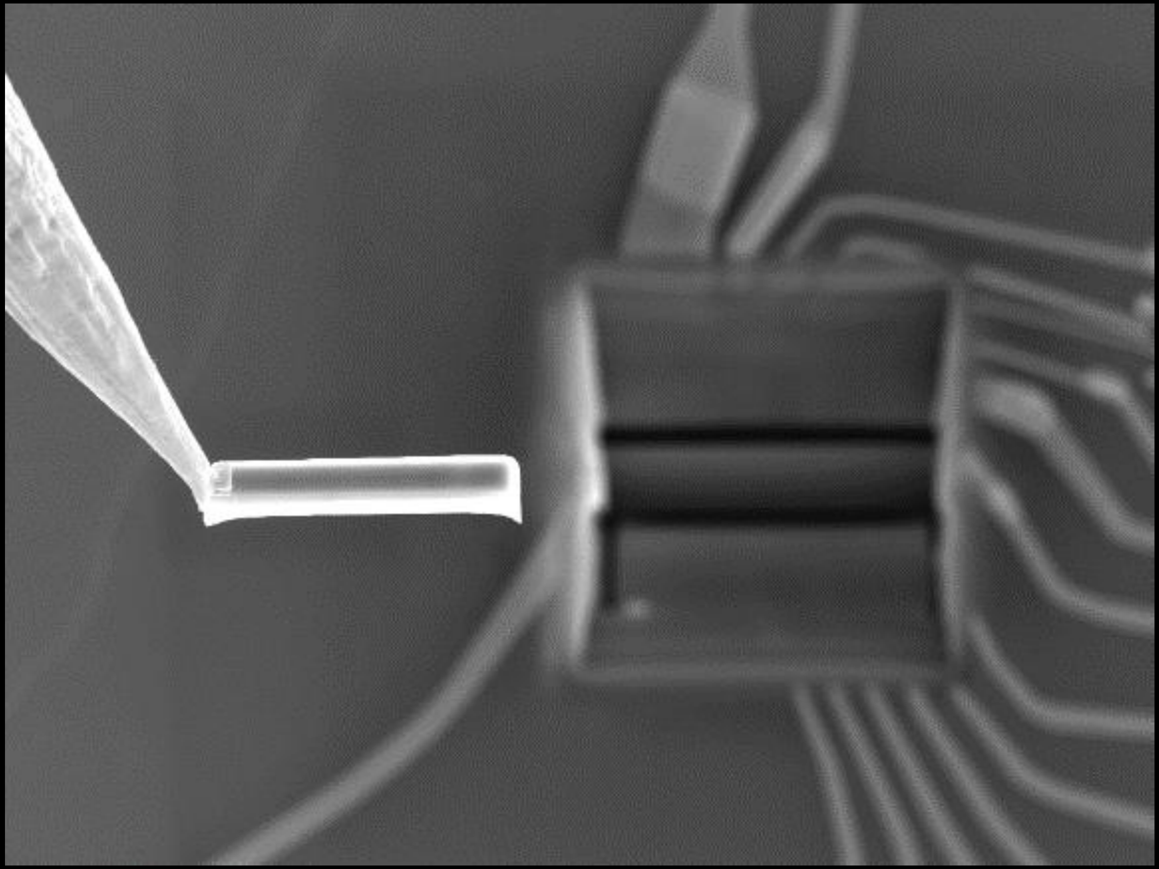

Typical TEM sample prep

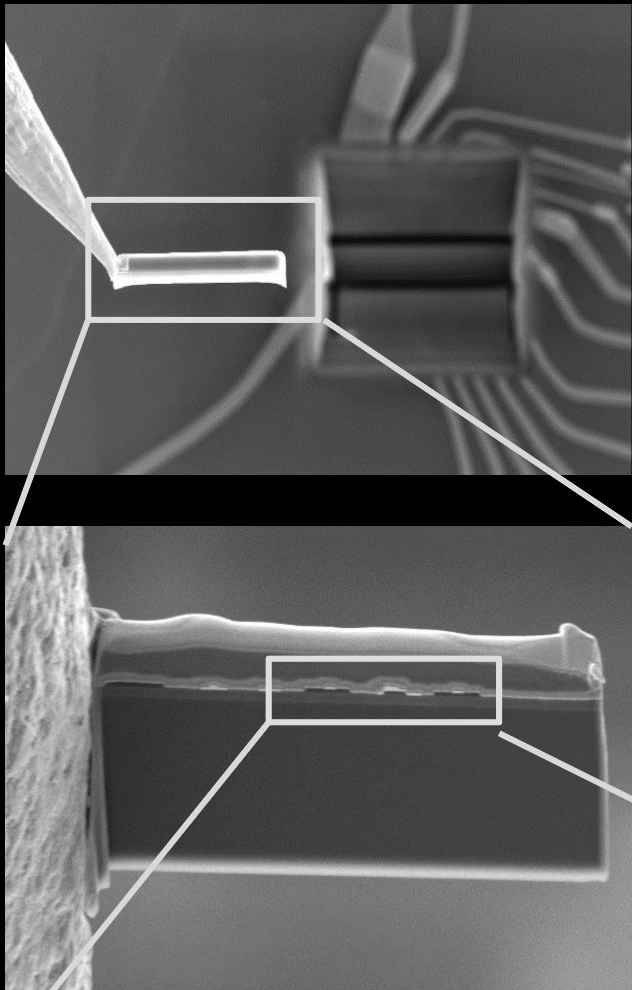

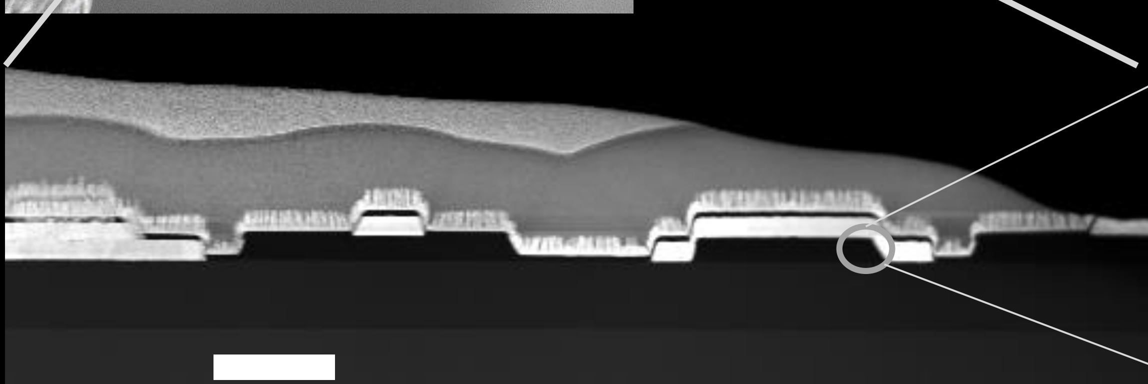

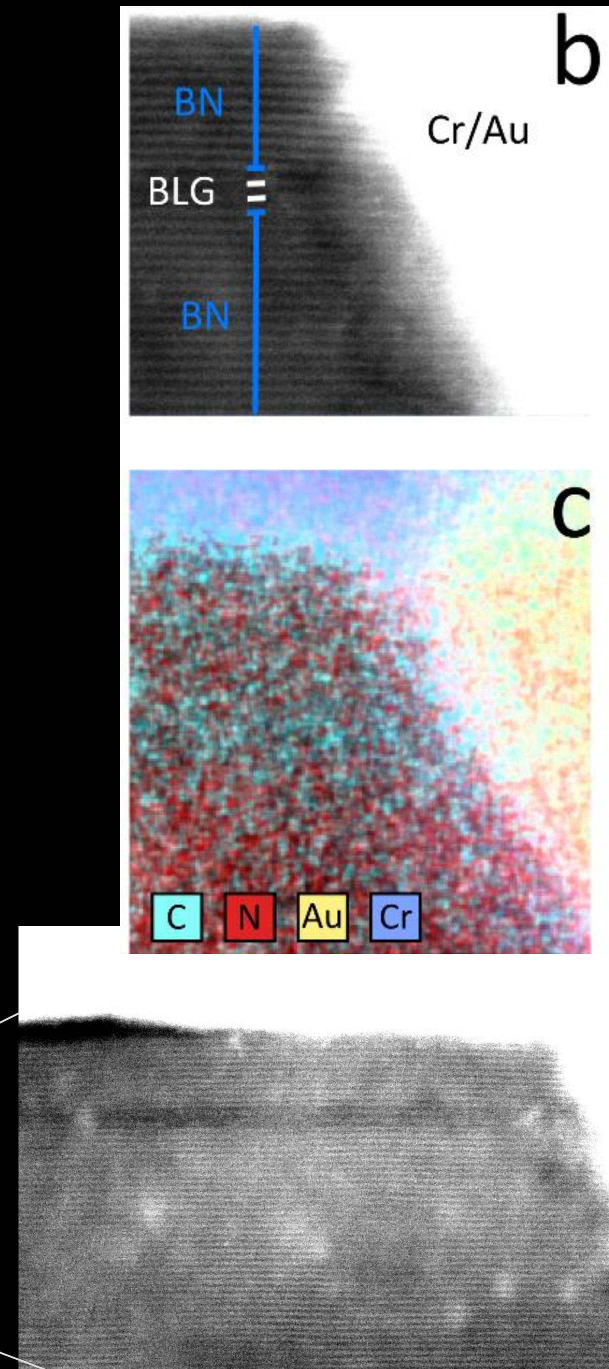

One dimensional contacts

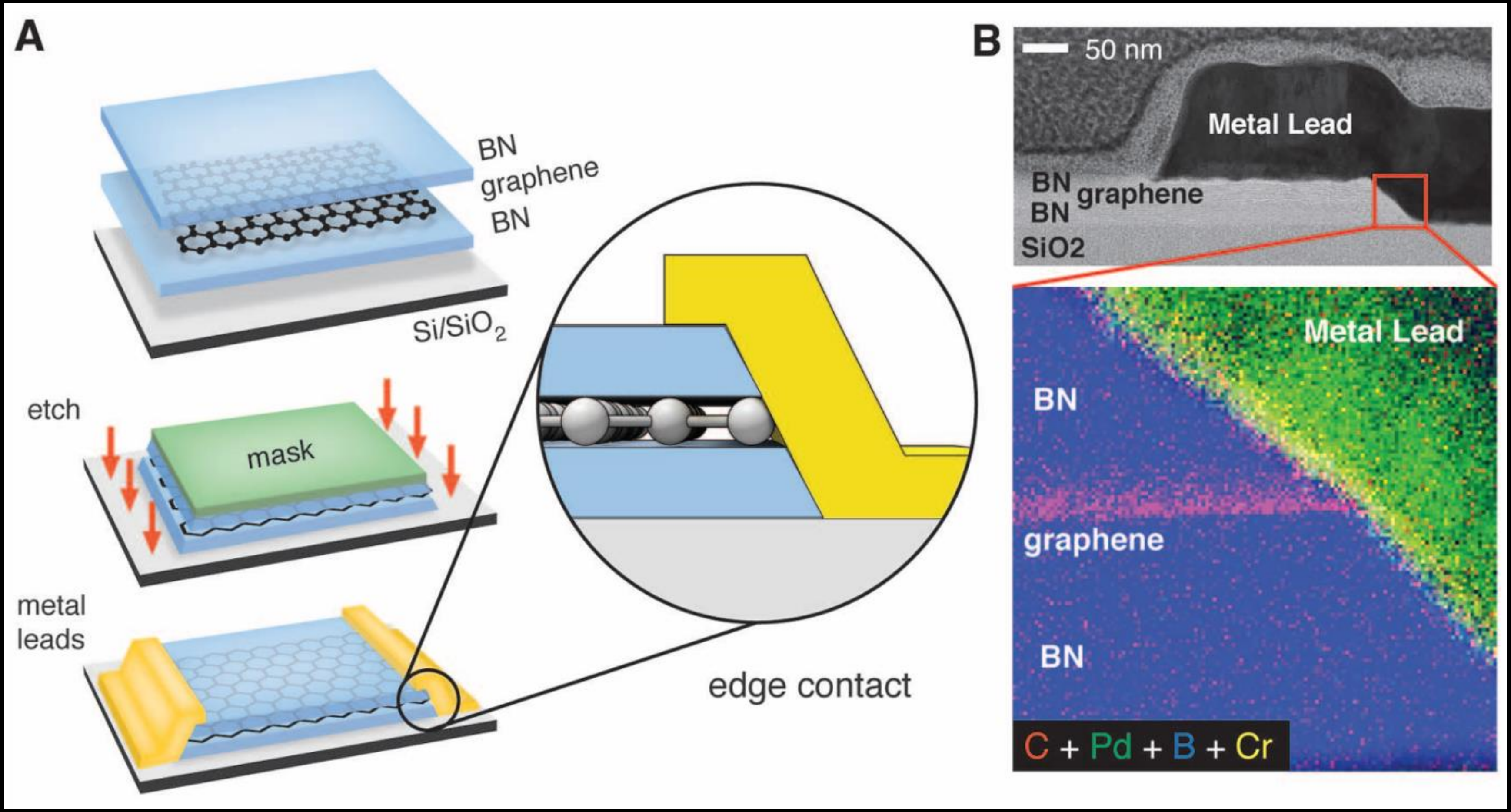

L. Wang et al, Science 342(6158), 2013

One dimensional contacts

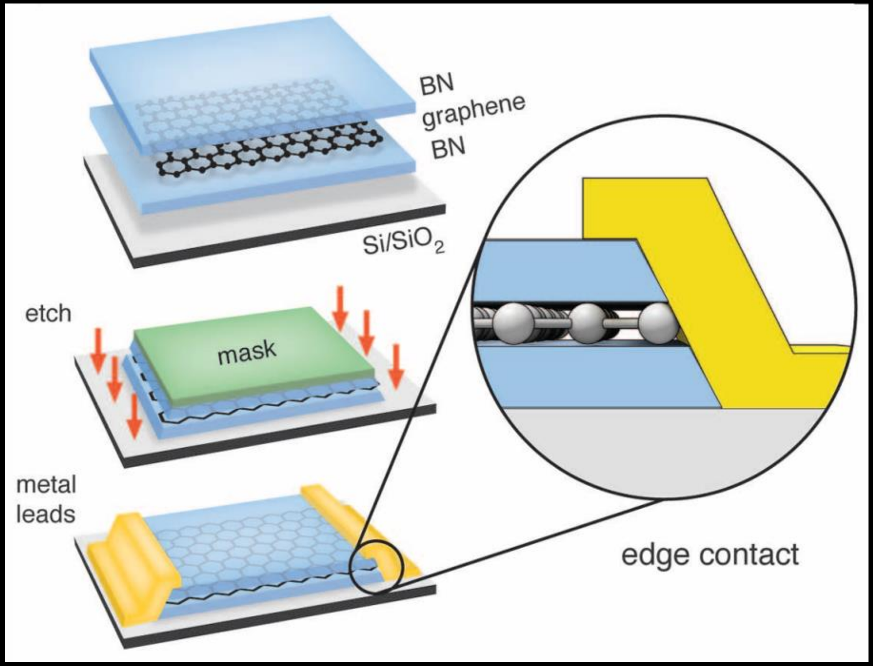

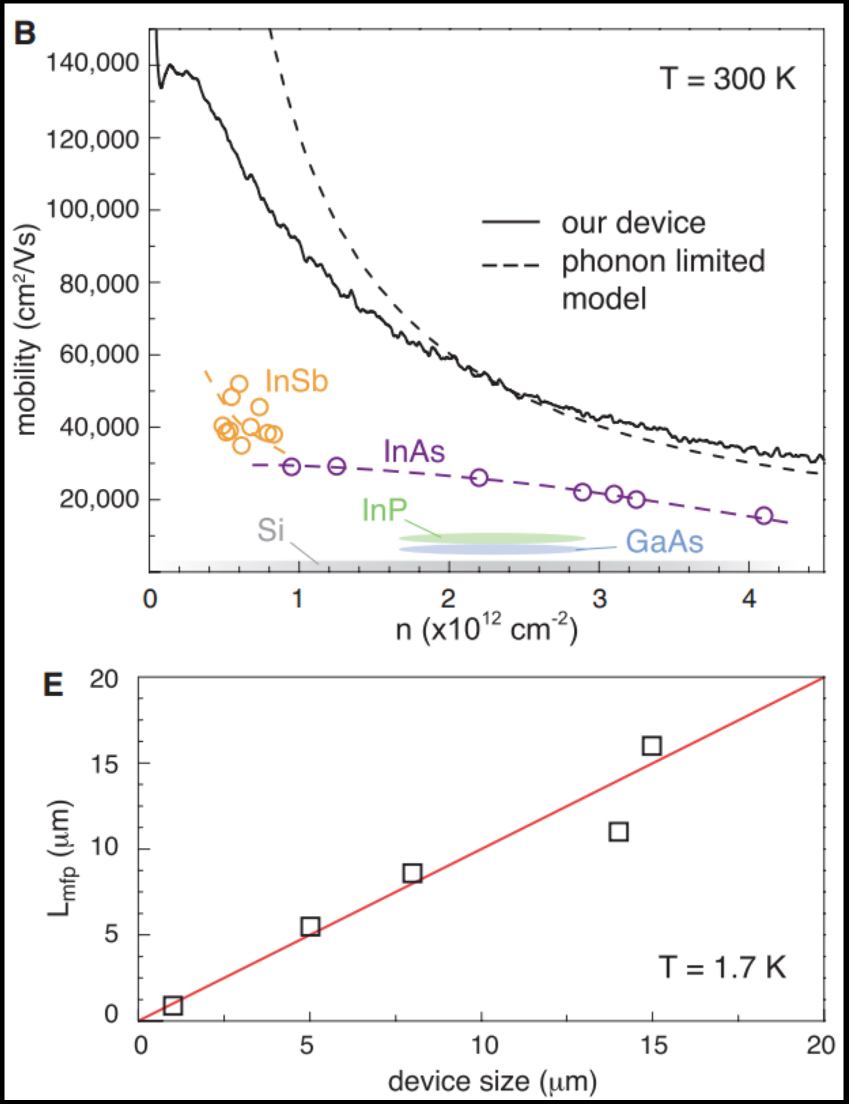

Science, **2013,** 342(6158)

High mobility in CVD graphene

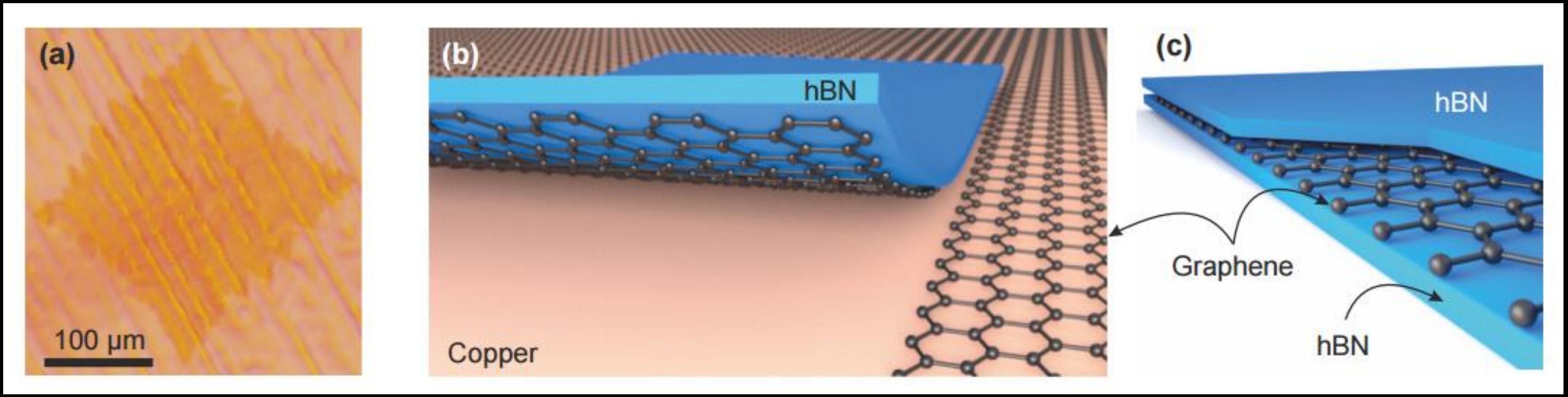

We report on ballistic transport over more than 28 μm in graphene grown by chemical vapor deposition (CVD) that is fully encapsulated in hexagonal boron nitride. The structures are fabricated by an advanced dry van-der-Waals transfer method and exhibit carrier mobilities of up to three million $cm^2/(Vs)$.

Nano Lett., **2016**, *16* (2), pp 1387–1391

Graphene on hBN

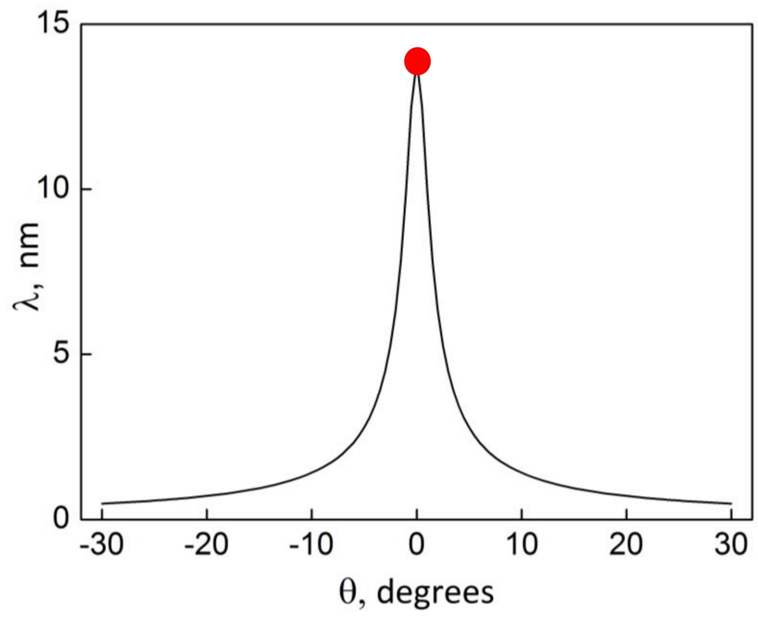

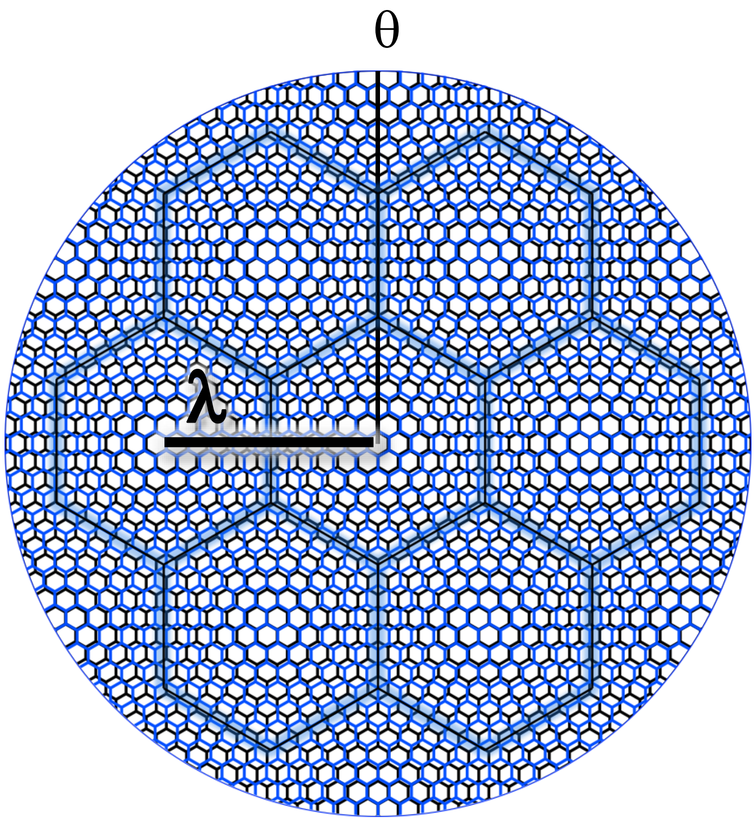

1.8 % lattice mismatch determines

Maximum moiré size is 14 nm

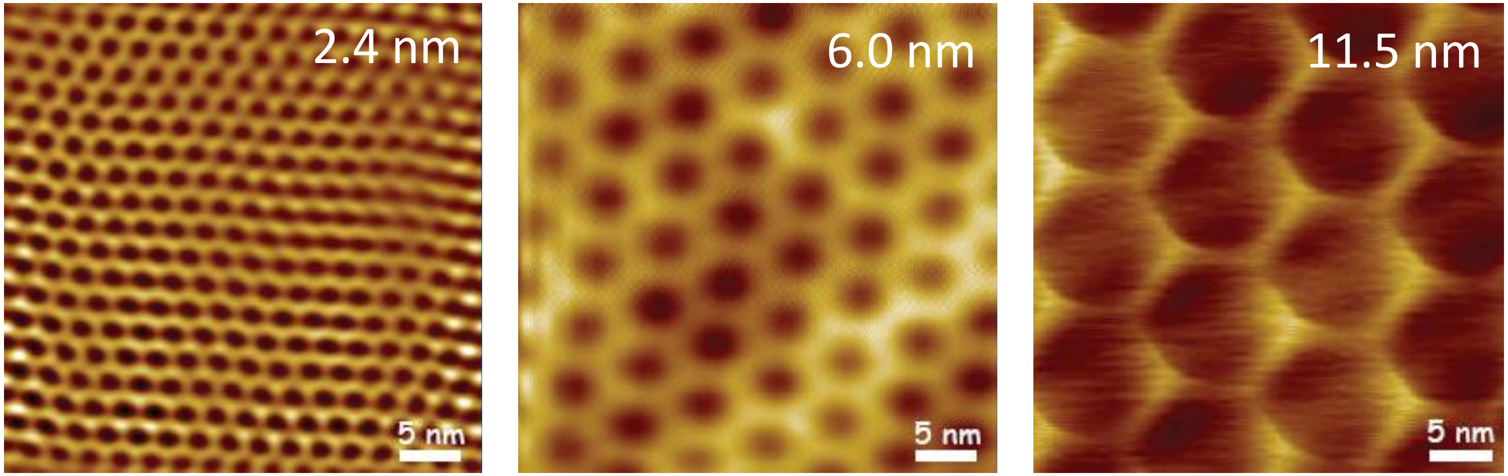

STM, Nature Phys. 8, 382-386 (2012)

Commensurate-incommensurate transition

1 dimensional situation: Frenkel-Kontorova model

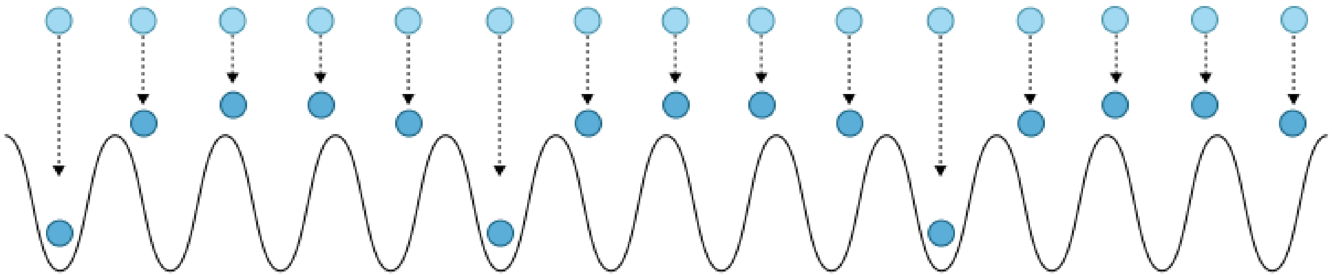

Incommensurate

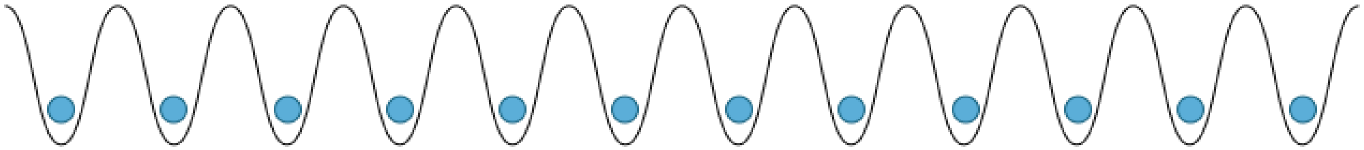

Commensurate

Commensurate-incommensurate transition

What do we do with the spare atoms?

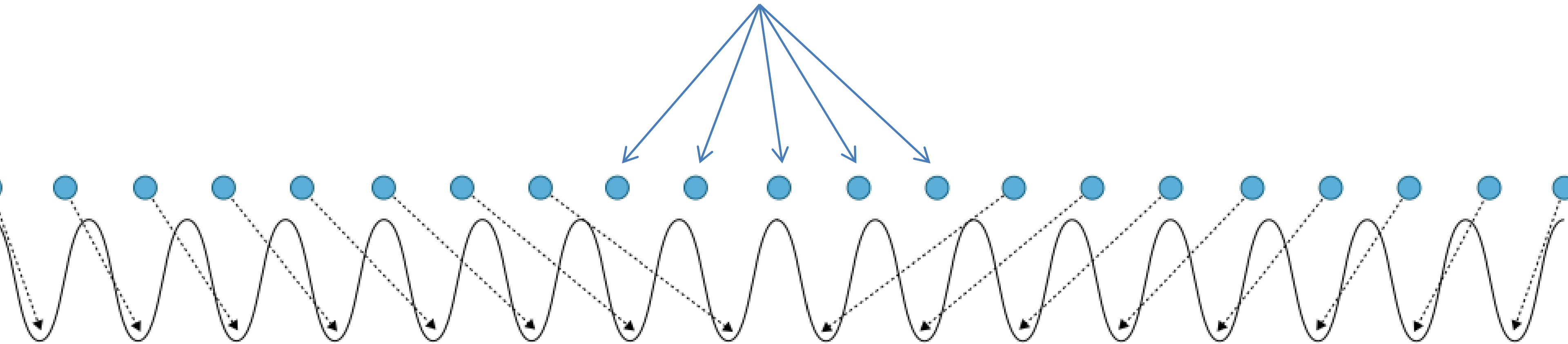

Commensurate-incommensurate transition

Soliton: Increased strain region

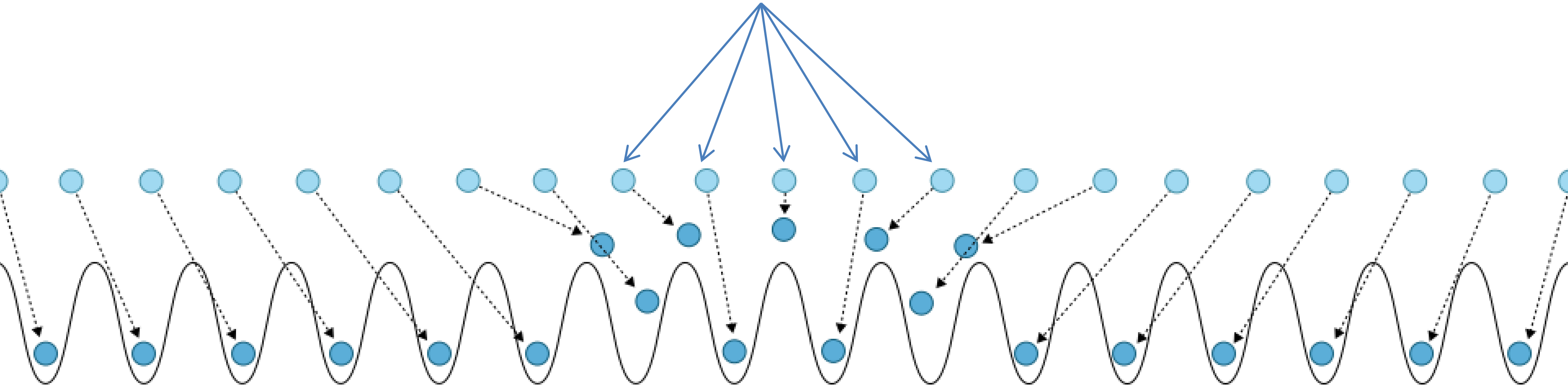

Incommensurate

Commensurate

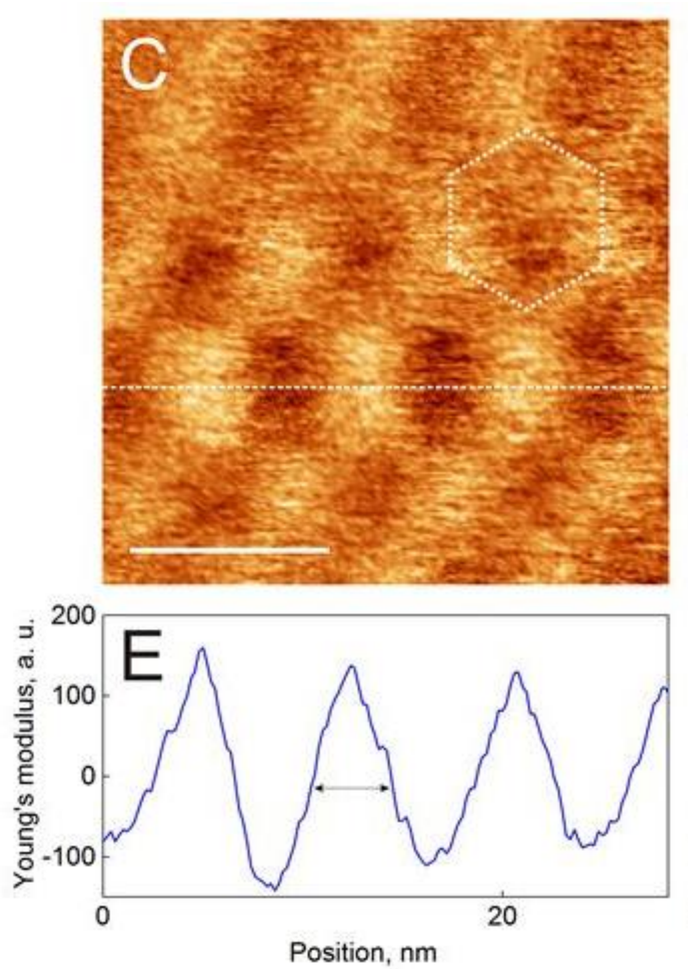

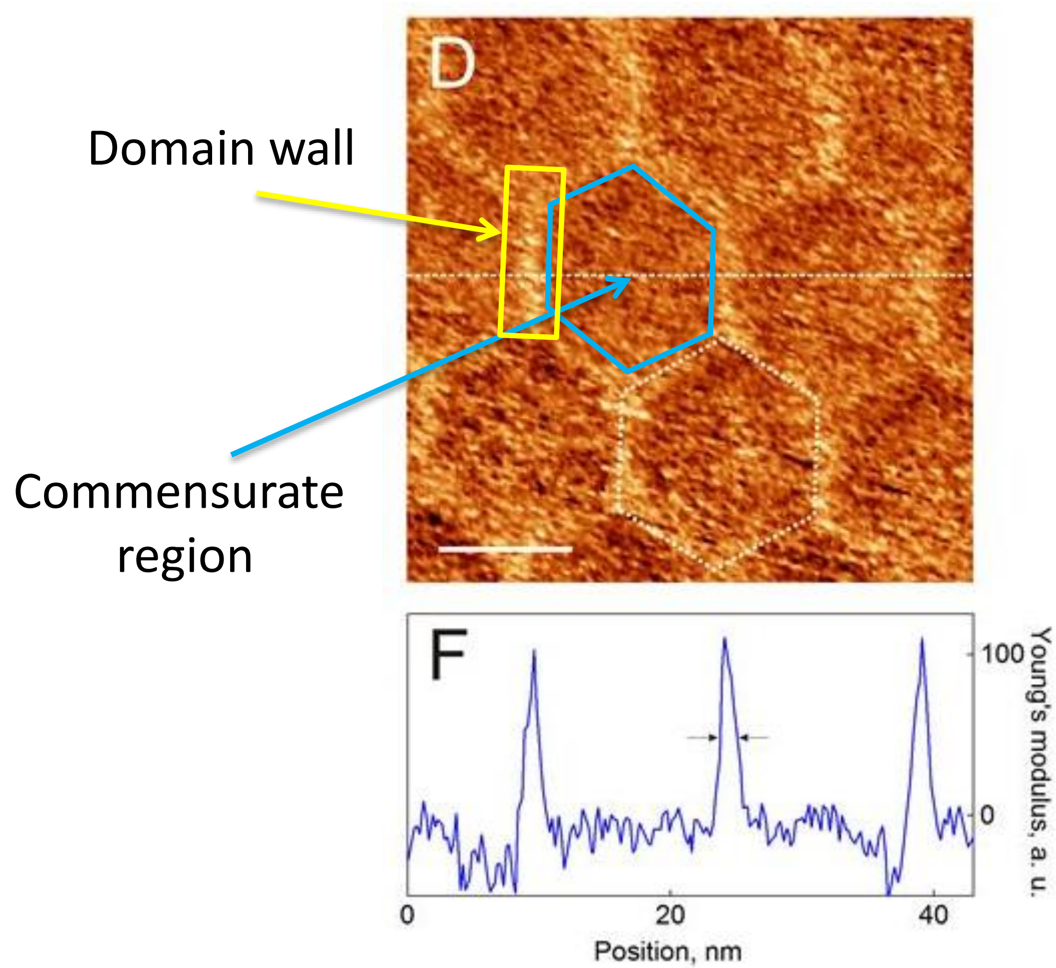

LARGE angular mismatch between the two constituent lattices (φ>1°)

(SMALL (< 10 nm) superlattice period)

For **SMALL** angular mismatch between the two constituent lattices (φ<1°)

(LARGE (> 10 nm) superlattice period)

STM measurements

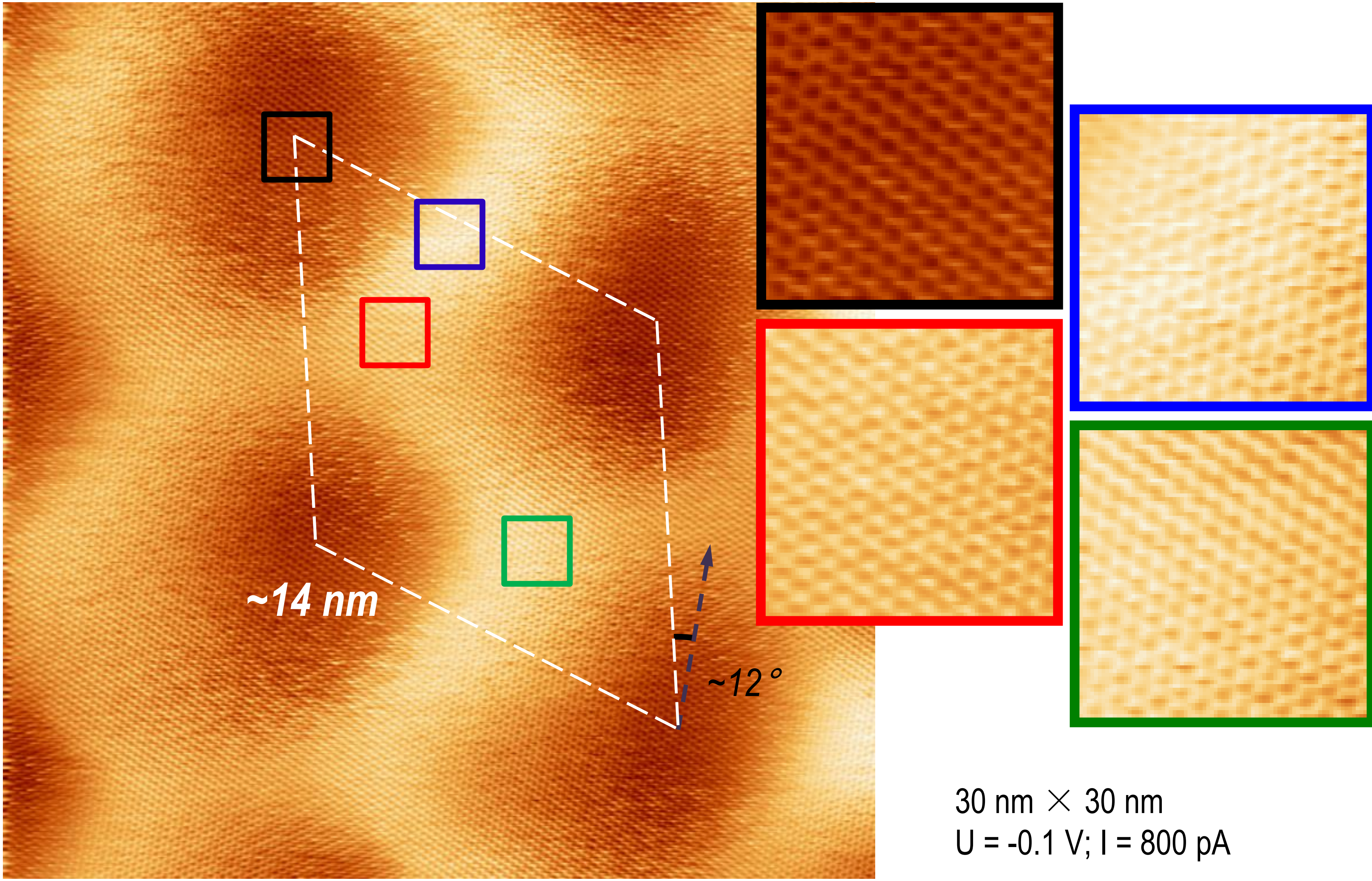

30 nm × 30 nm
U = -0.1 V; I = 800 pA

STM measurements

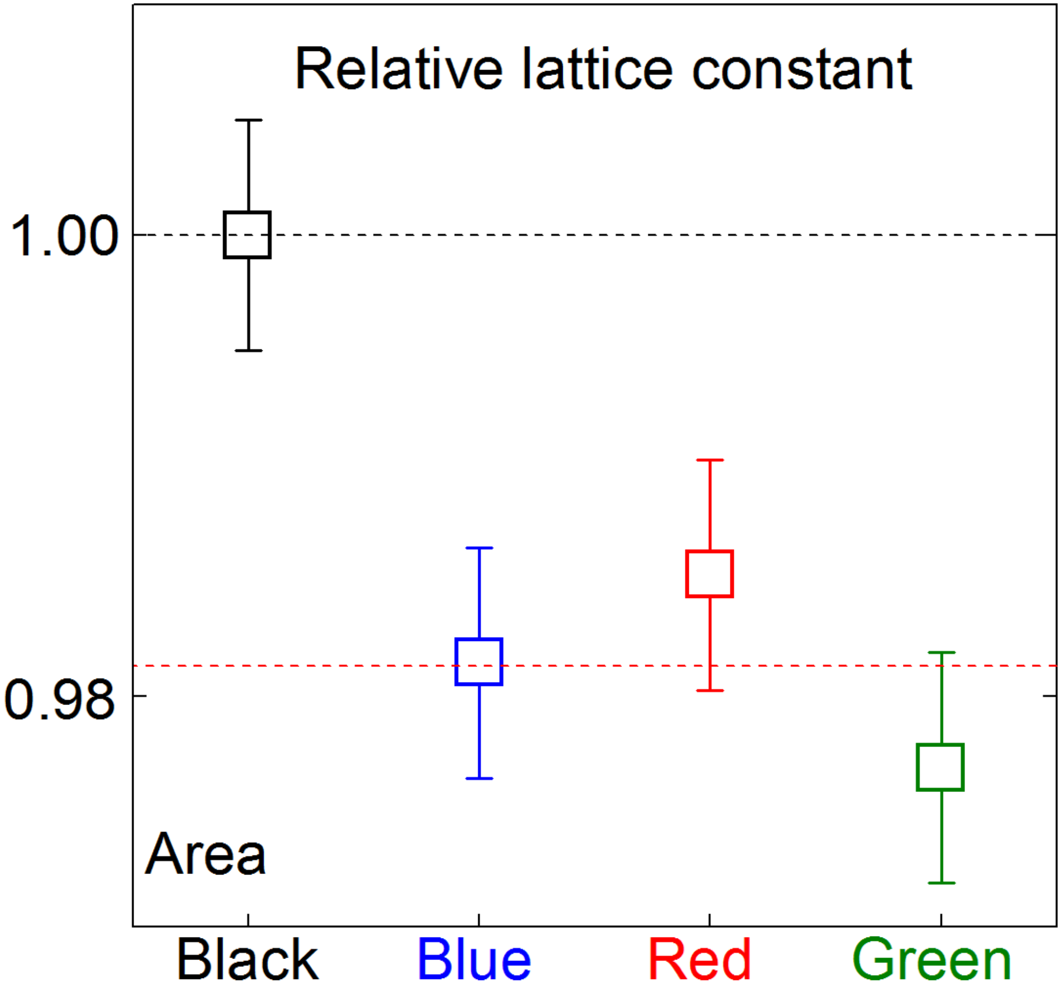

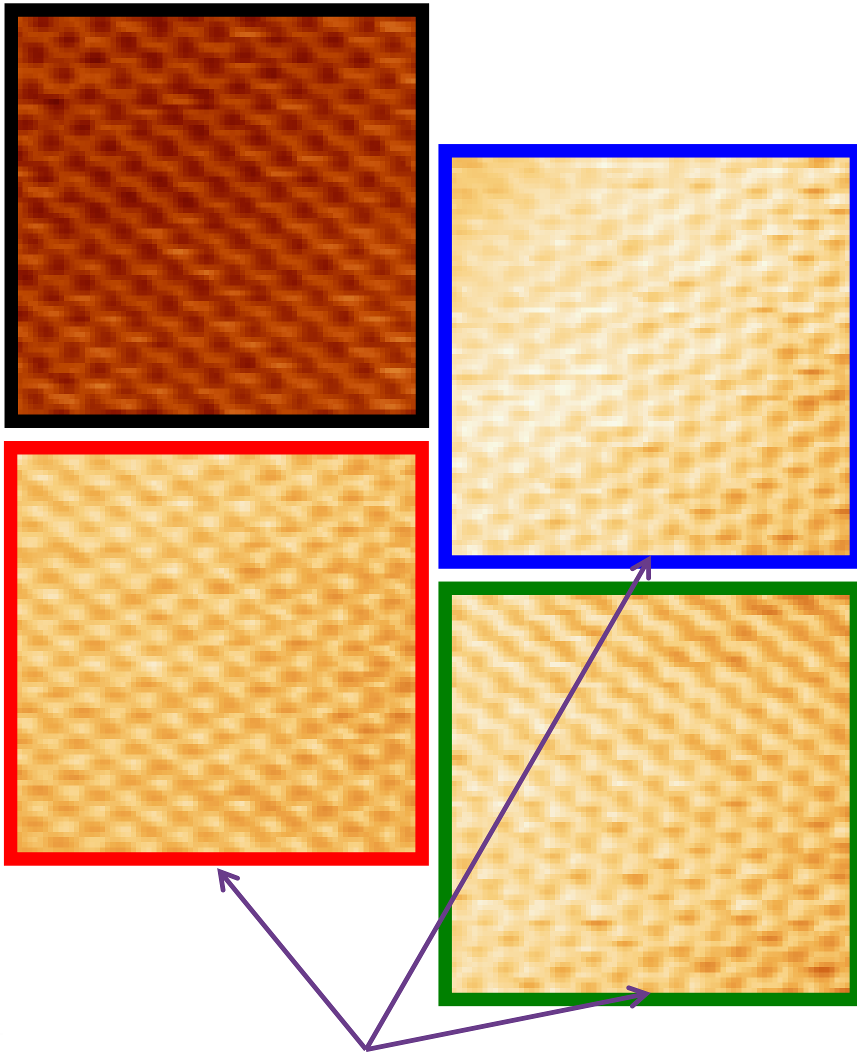

Commensurate state extended by ~2%

No compression observed

Shear strain

Tensile vs Shear

Tensile Soliton

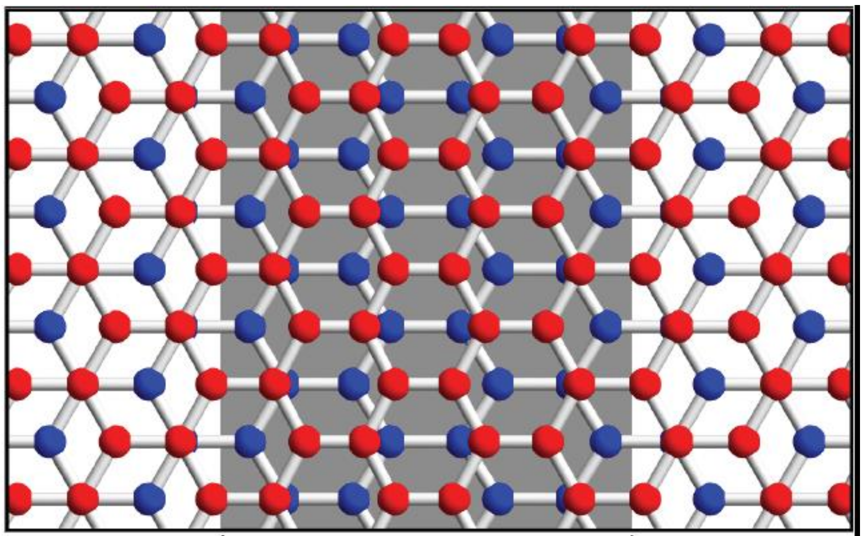

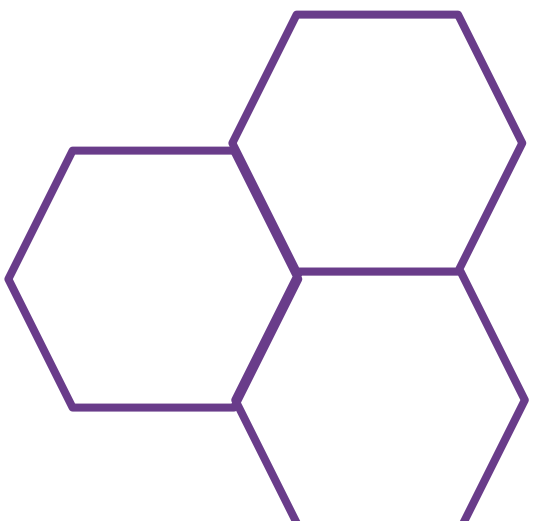

Shear Soliton

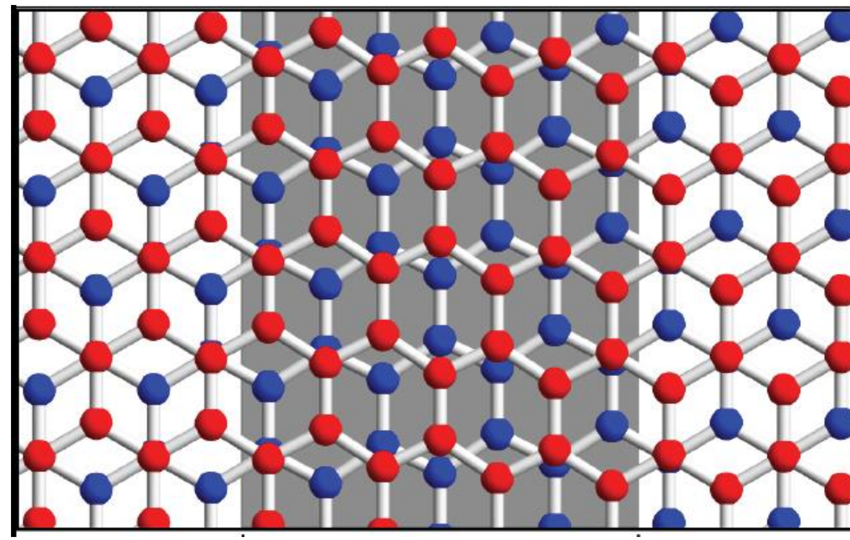

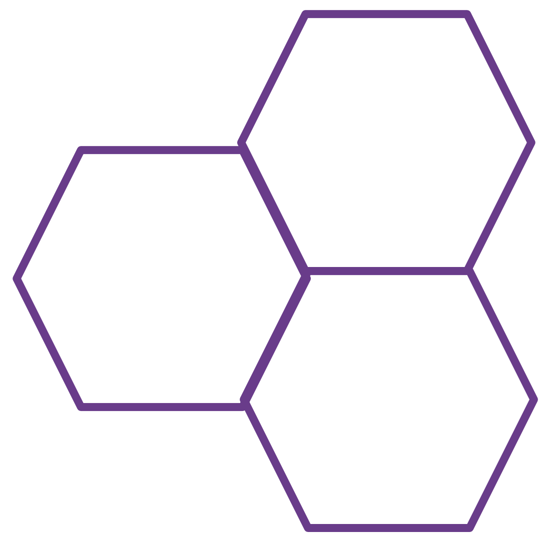

Consequences: Raman

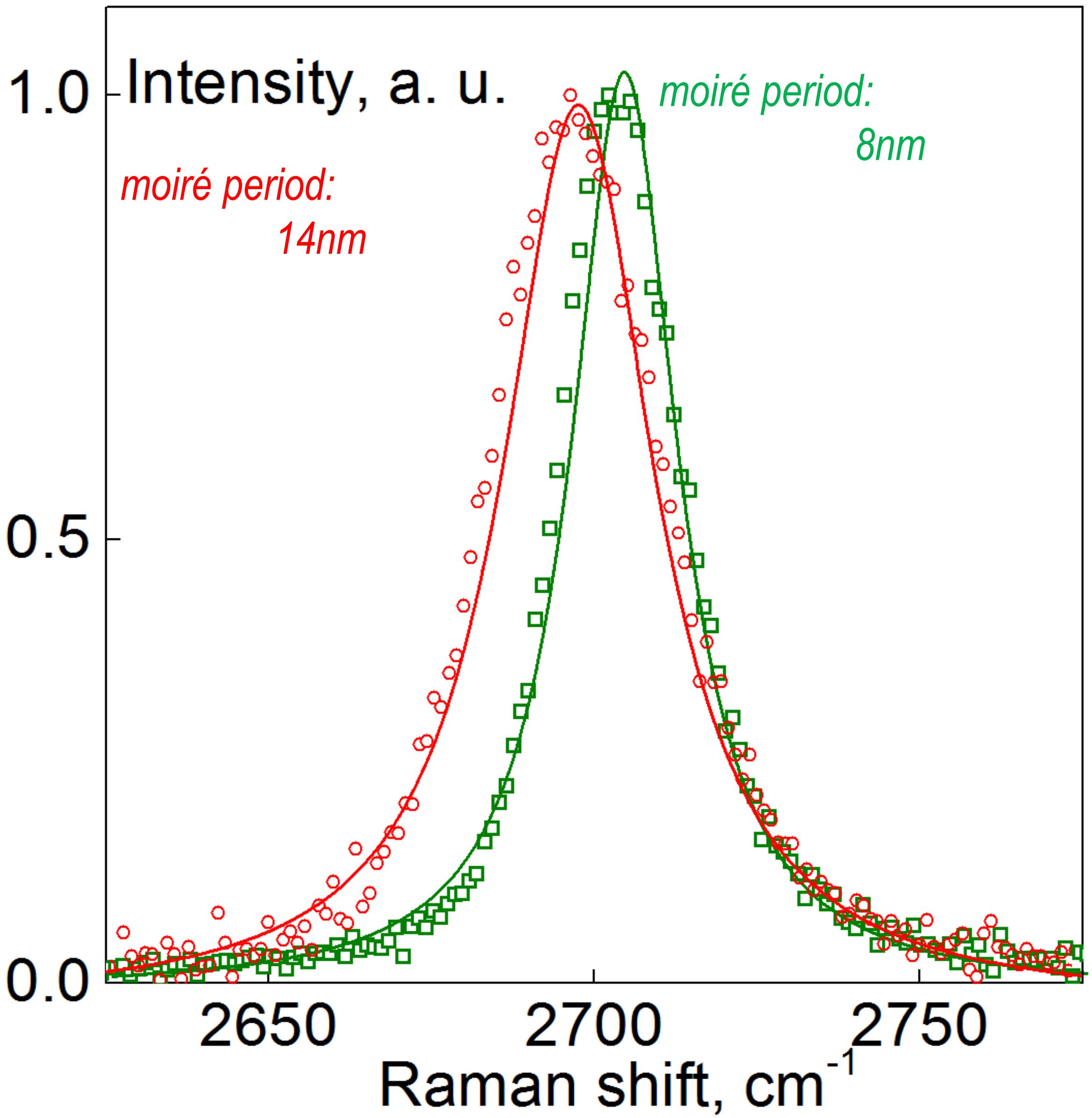

Raman 2D peak: contains information about strain

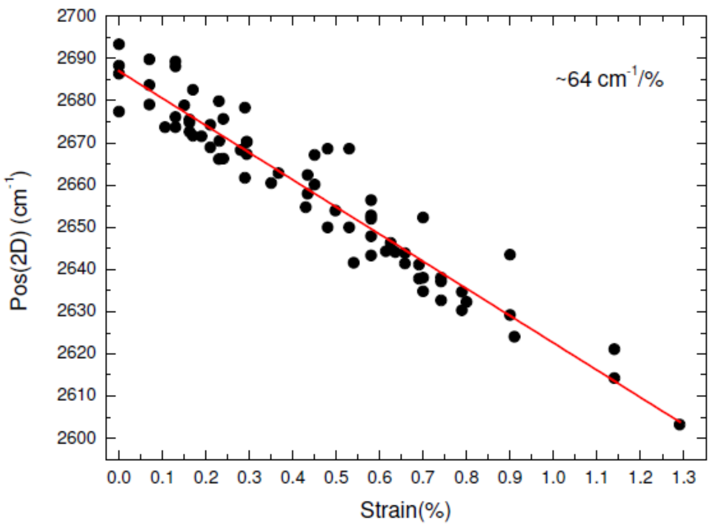

Mohiuddin et al PRB '0

Broadening: distribution of strain

Hard to get a number

Consequences: Raman

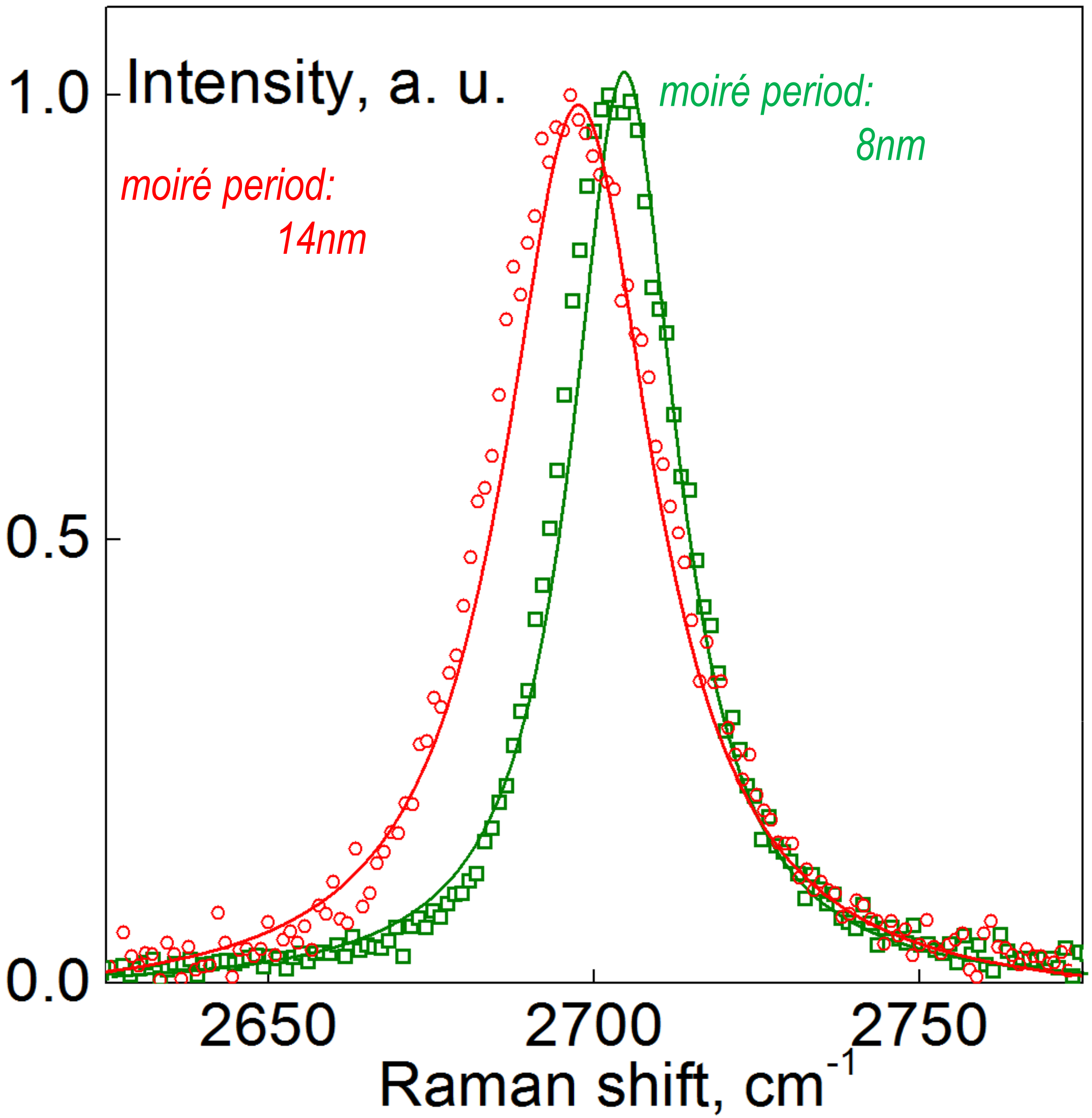

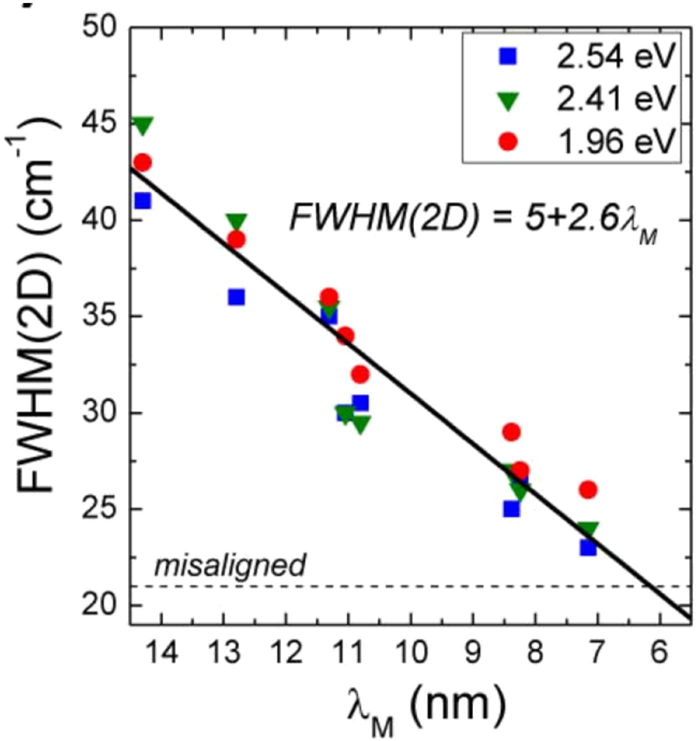

Eckmann et al NanoLetters ‘1

Self-aligning

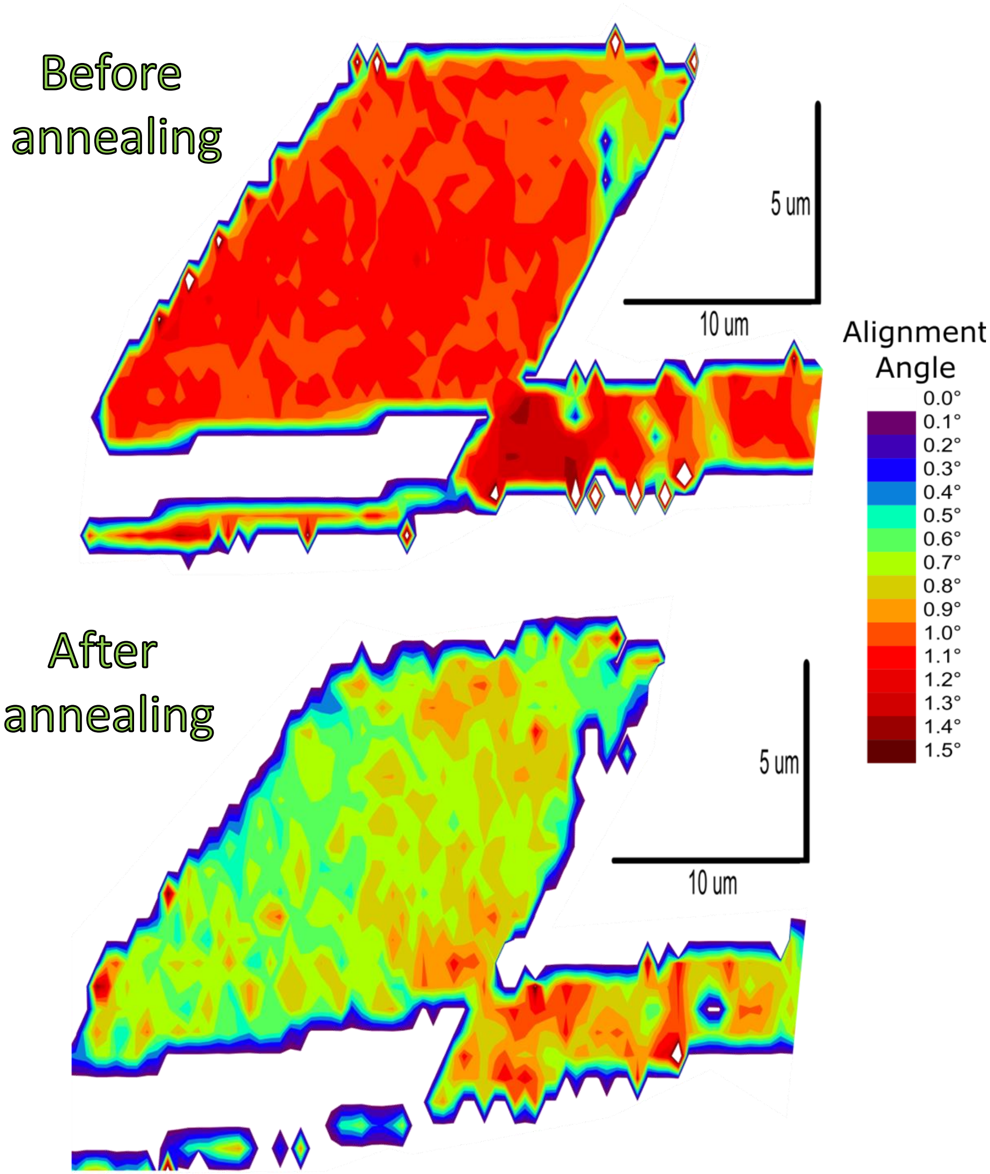

Woods et al Nature Communications ‘16

Raman allows direct measurements of the alignment angle

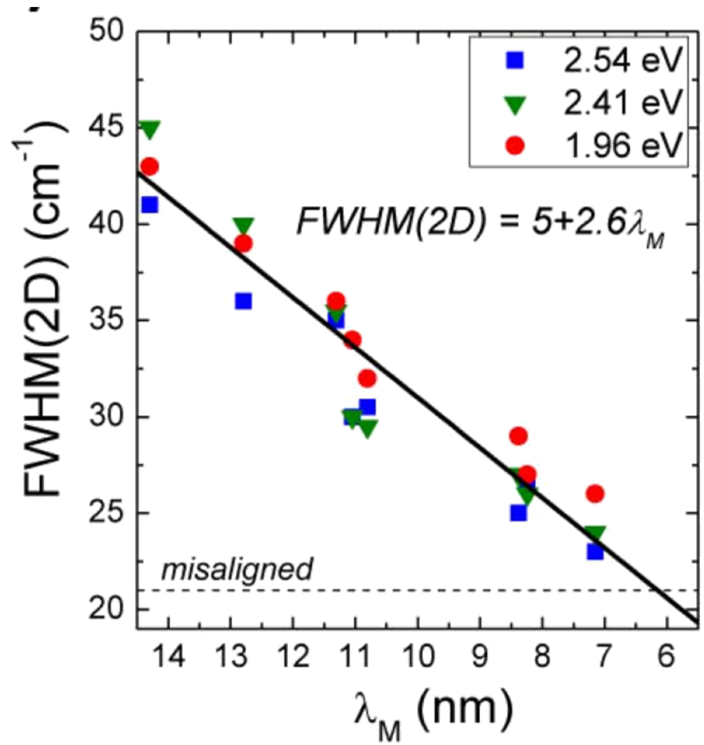

Eckmann et al NanoLetters ‘13

Self-aligning

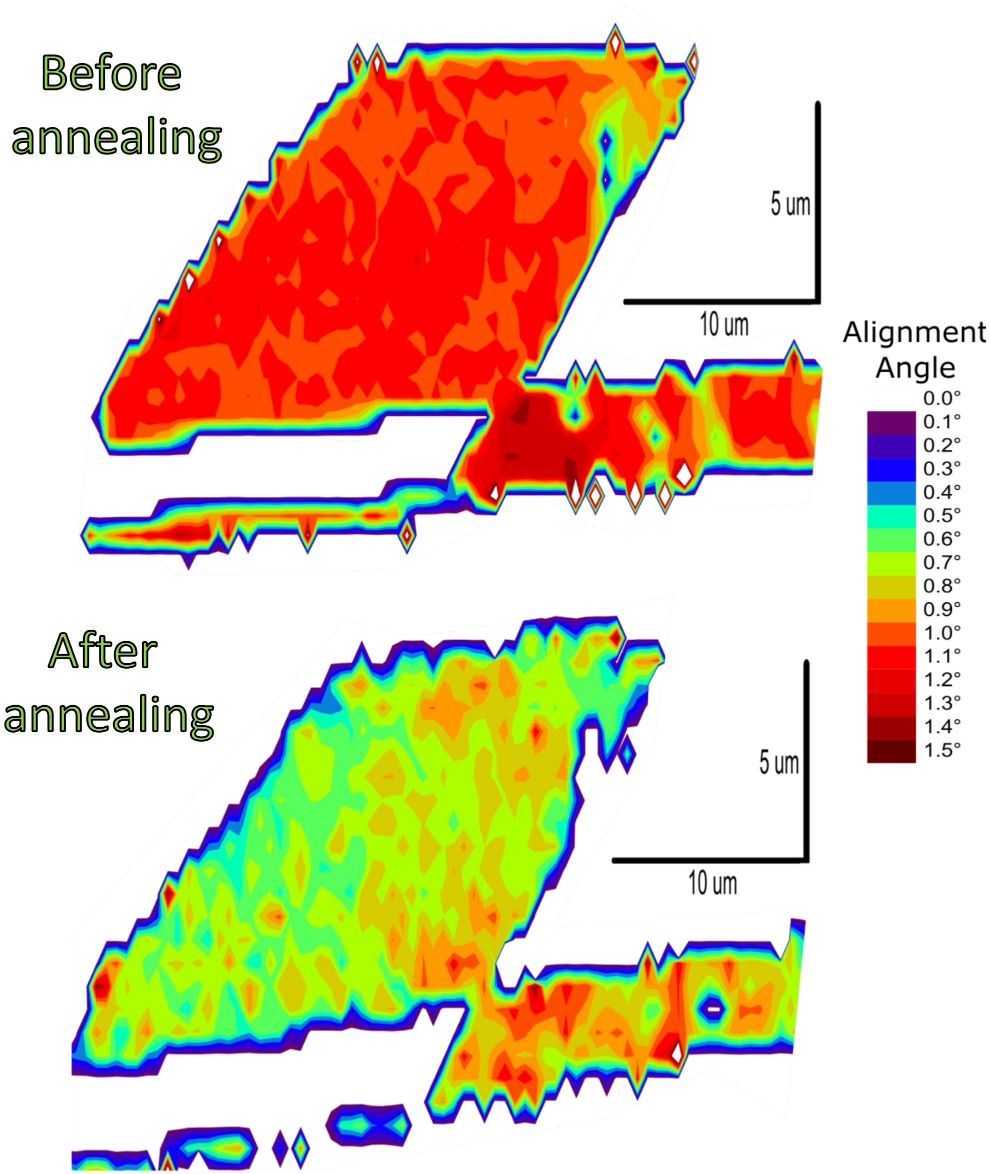

Woods et al Nature Communications '16

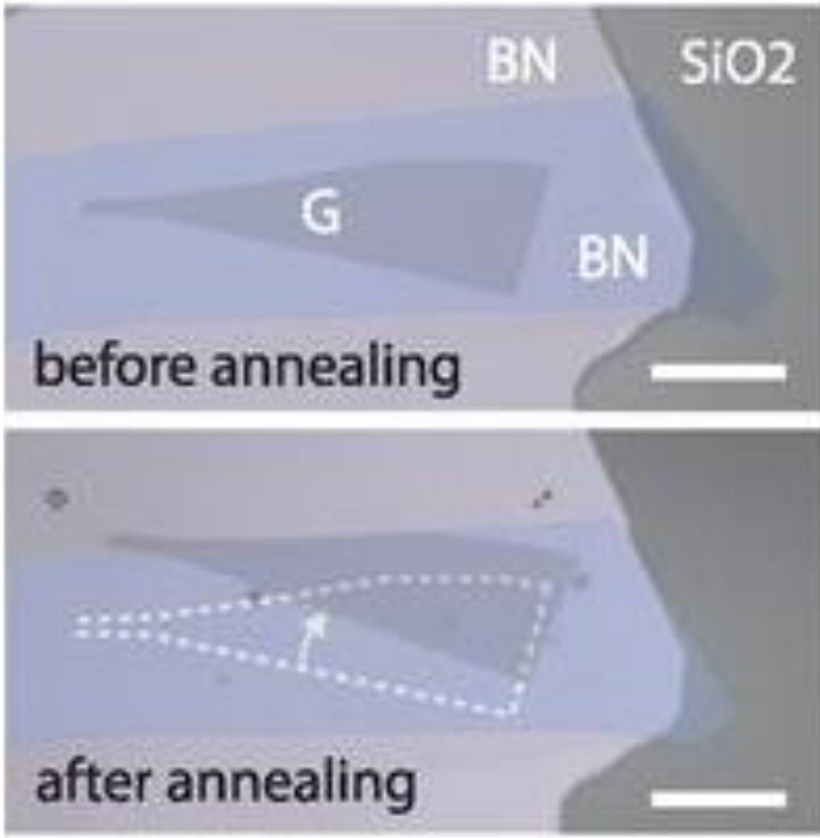

Wang et al Science '15

Self-aligning

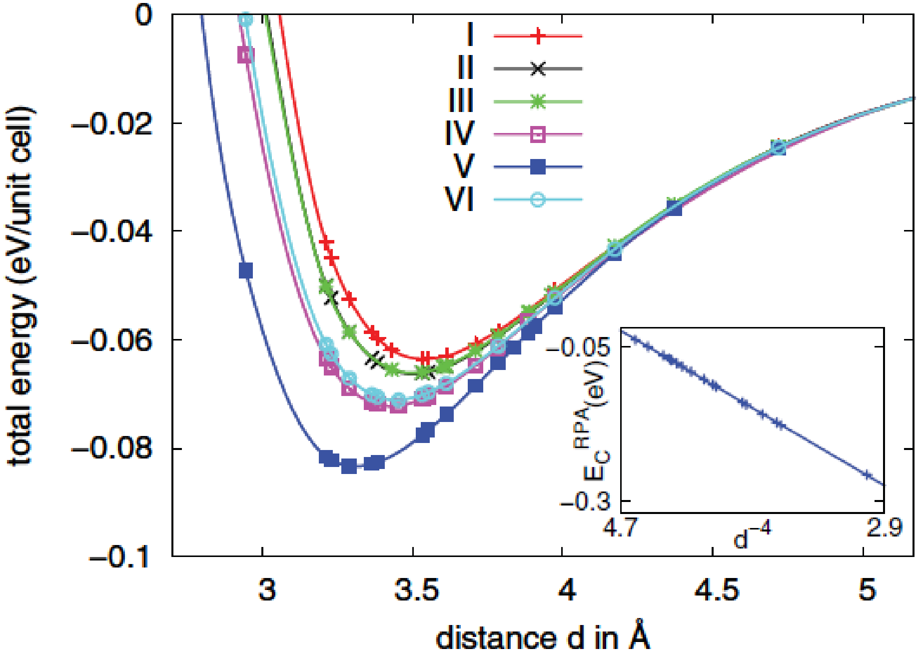

minimisation of van der Waals interaction and strain

PHYSICAL REVIEW B **84**, 195414 (2011)
Adhesion and electronic structure of graphene on hexagonal boron nitride substrates
B. Sachs, T. O. Wehling, M. I. Katsnelson, and A. I. Lichtenstein

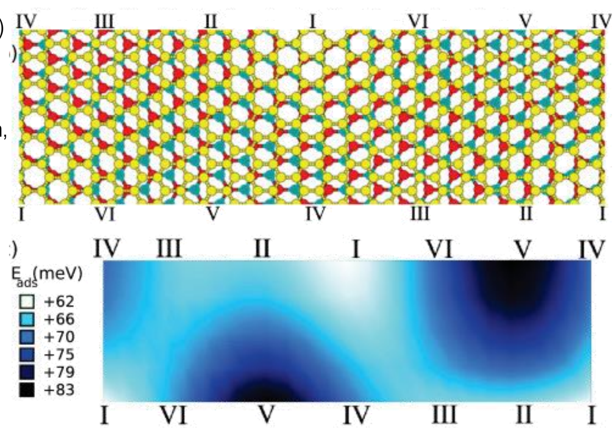

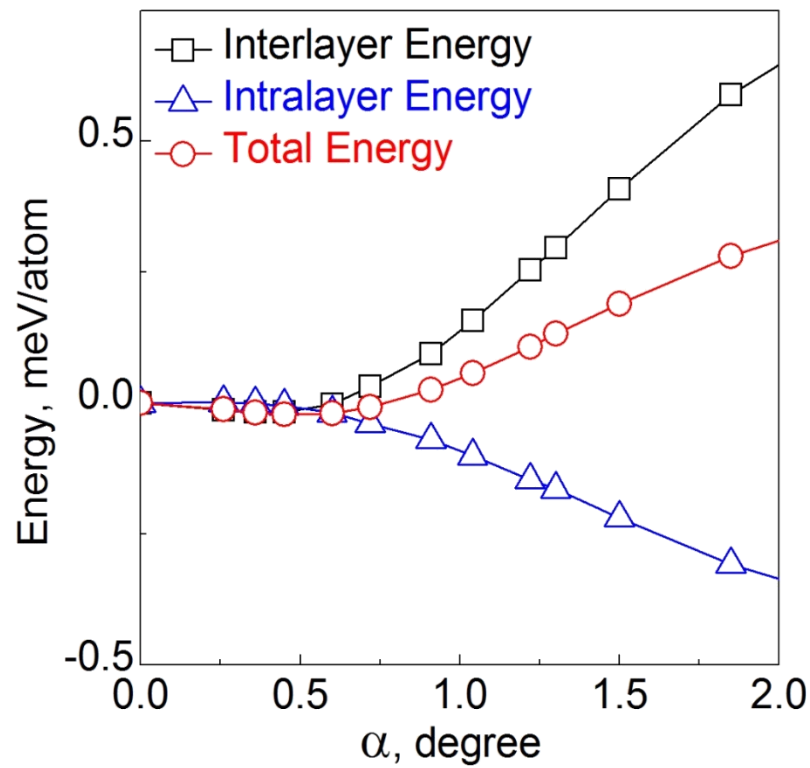

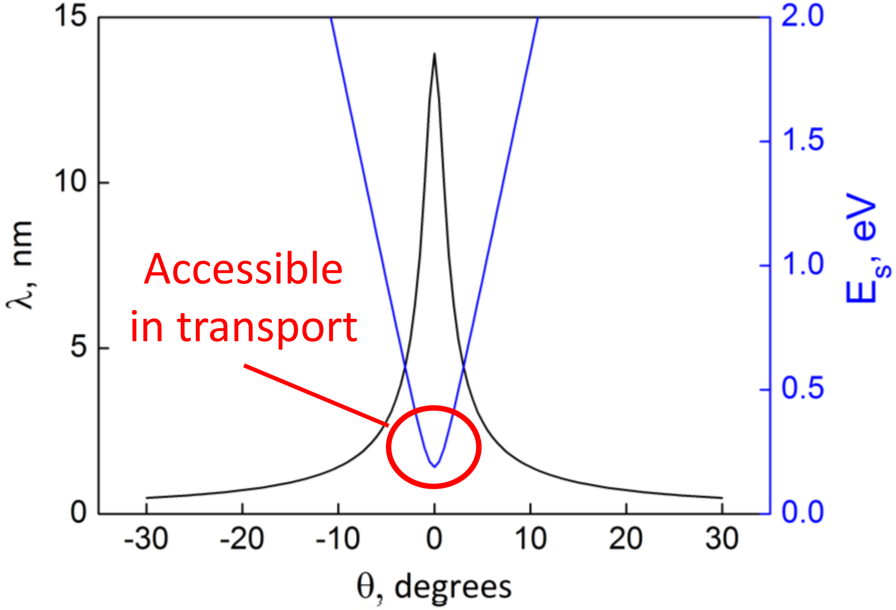

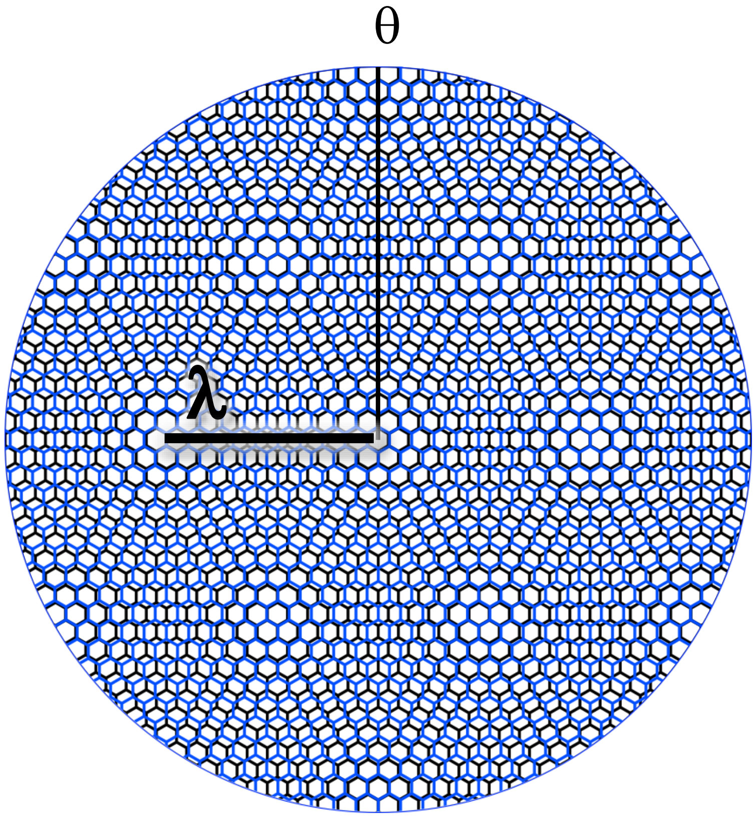

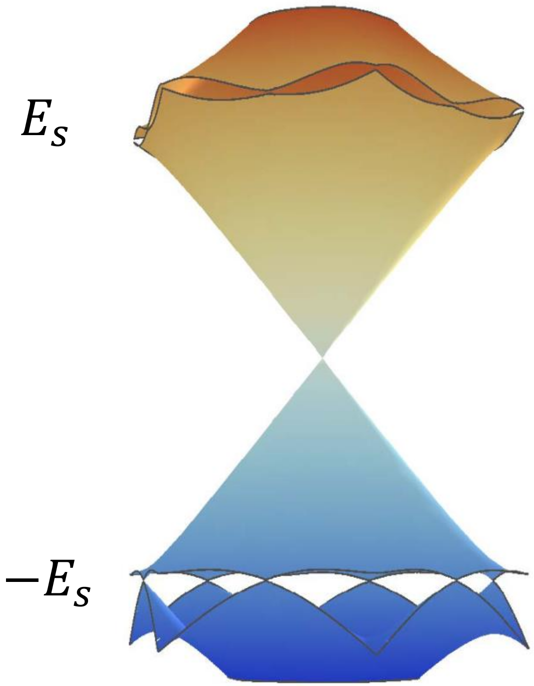

Moire potential strength ~ 50 meV leads to changes in graphene's spectrum around

$$E_s = \frac{2\pi\hbar V_F}{\sqrt{3}\,\lambda}$$

Specially aligned graphene devices

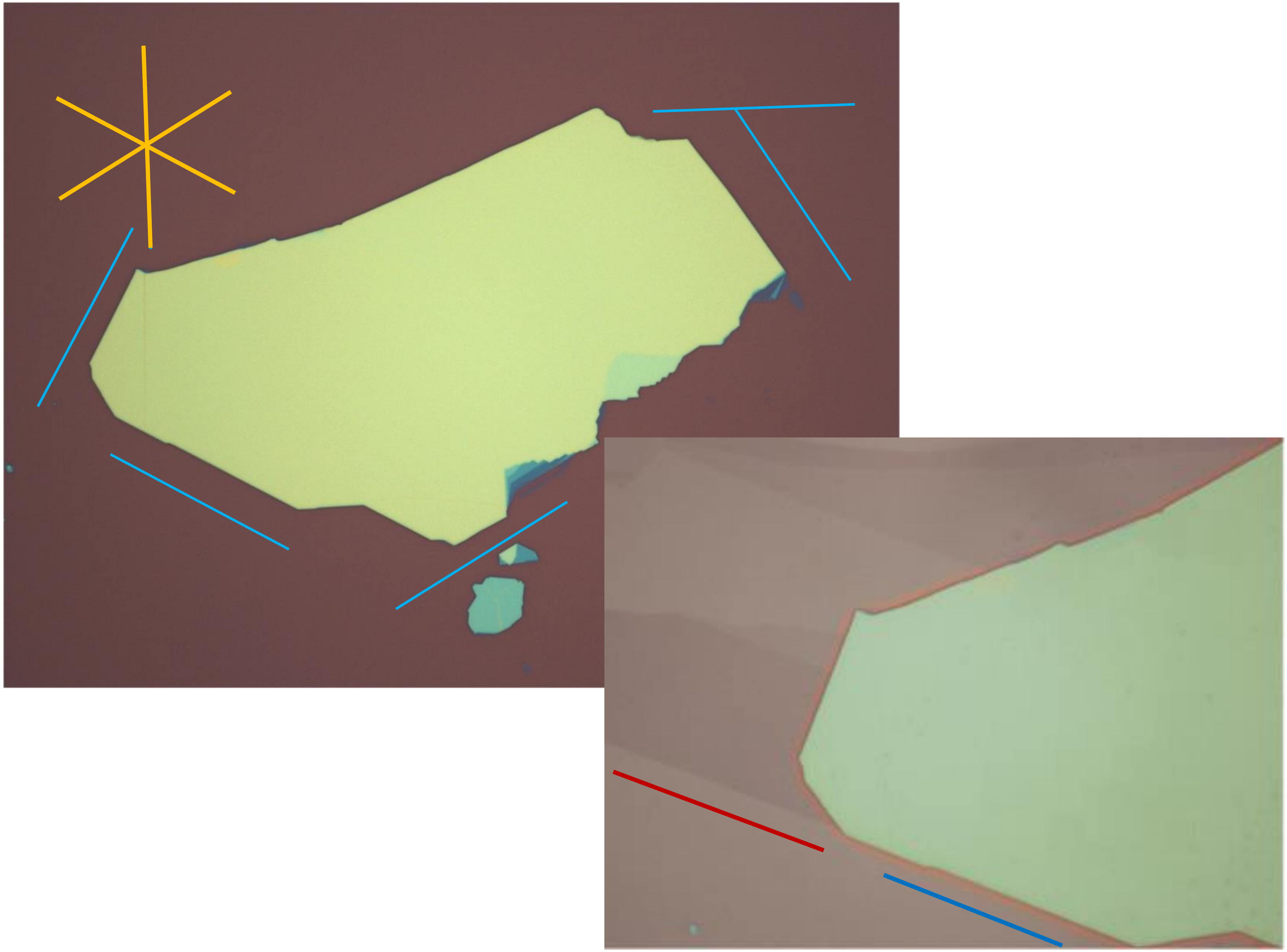

New dirac points

- New Dirac points emerge at ± E_s
- Additional peaks in ρ_{xx} + reversal of the ρ_{xy} Hall sign
- Temperature dependence of the peak shapes consistent with Dirac-like spectrum near ± E_s
- Broken electron-hole symmetry

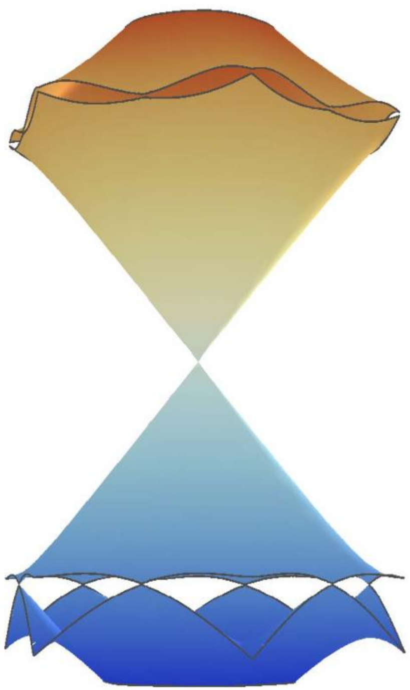

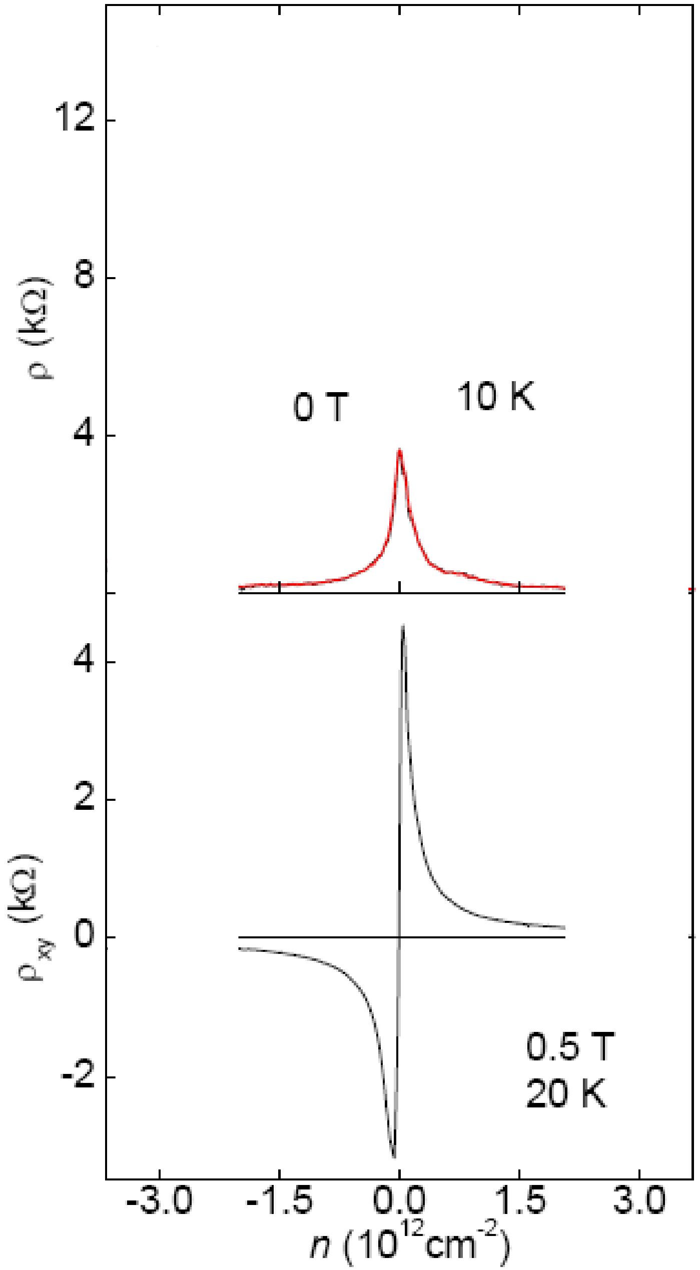

Magnetic field:

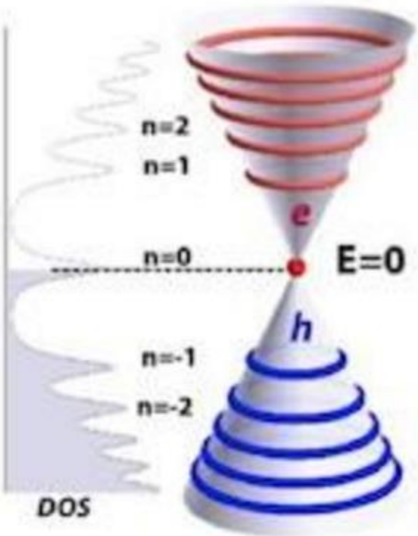

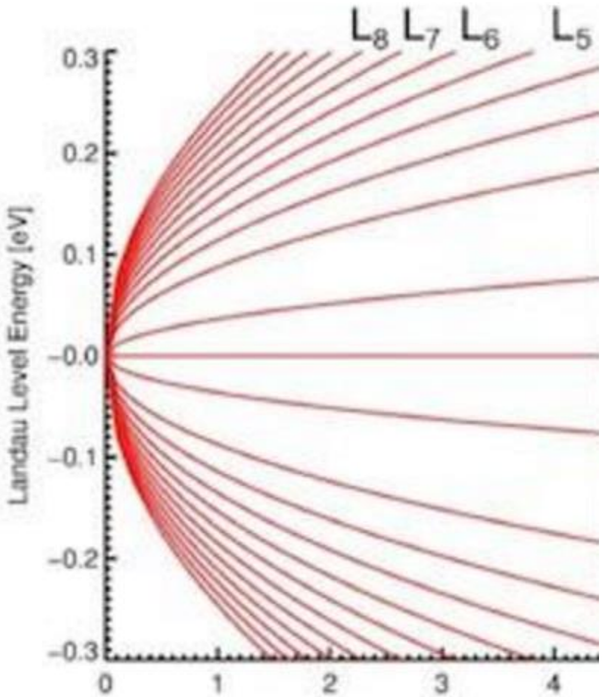

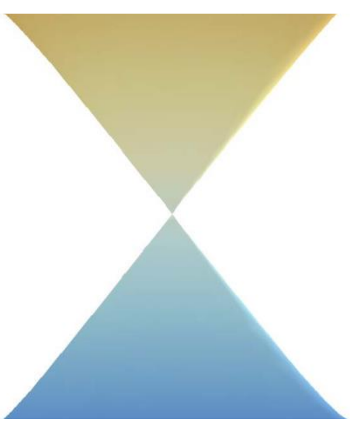

Landau levels
typically observed in graphene

Magnetic field:

standard 4-fold degeneracy observed

distance between LL is greater than the miniband width above 1T

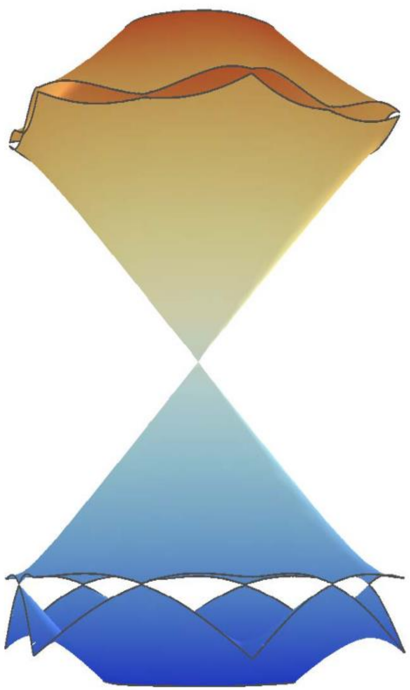

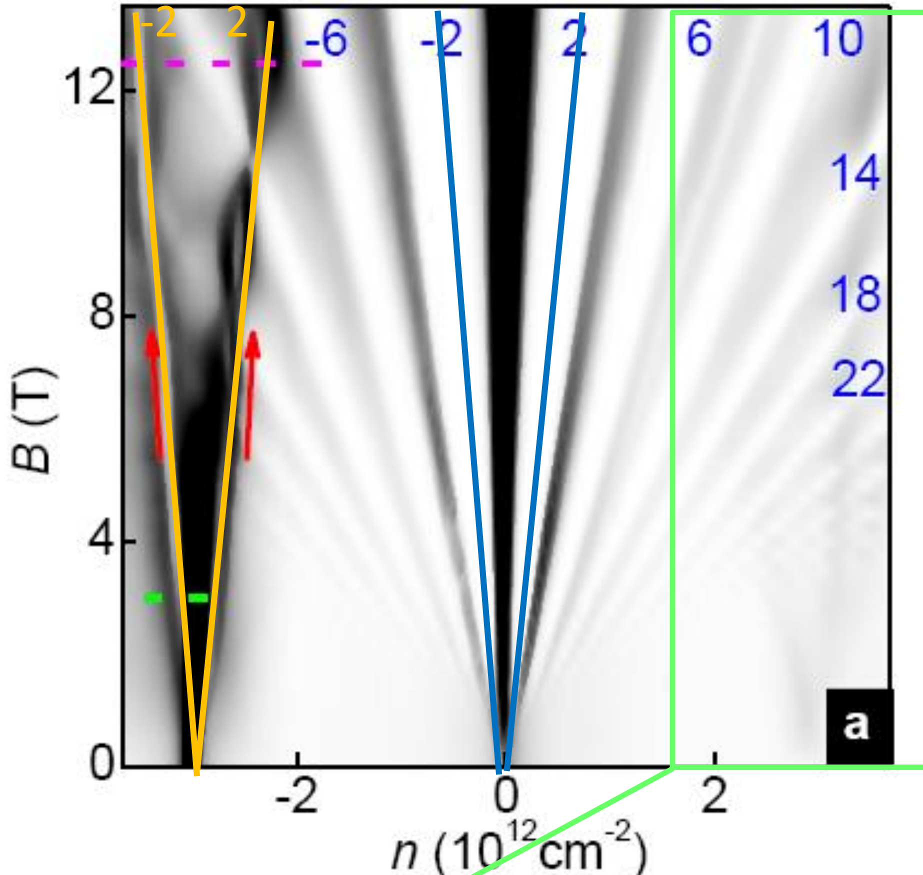

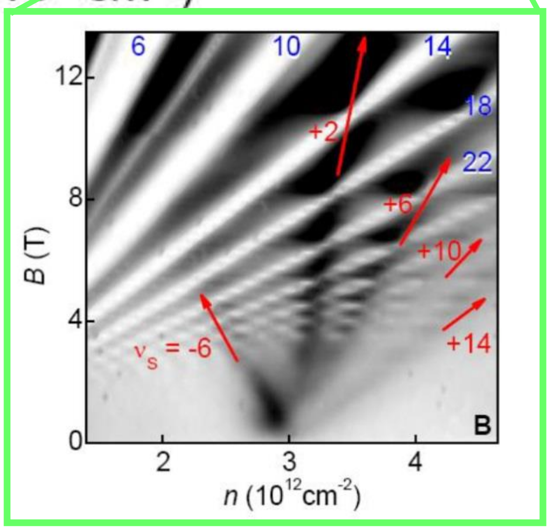

Hofstadter-Like Oscillations

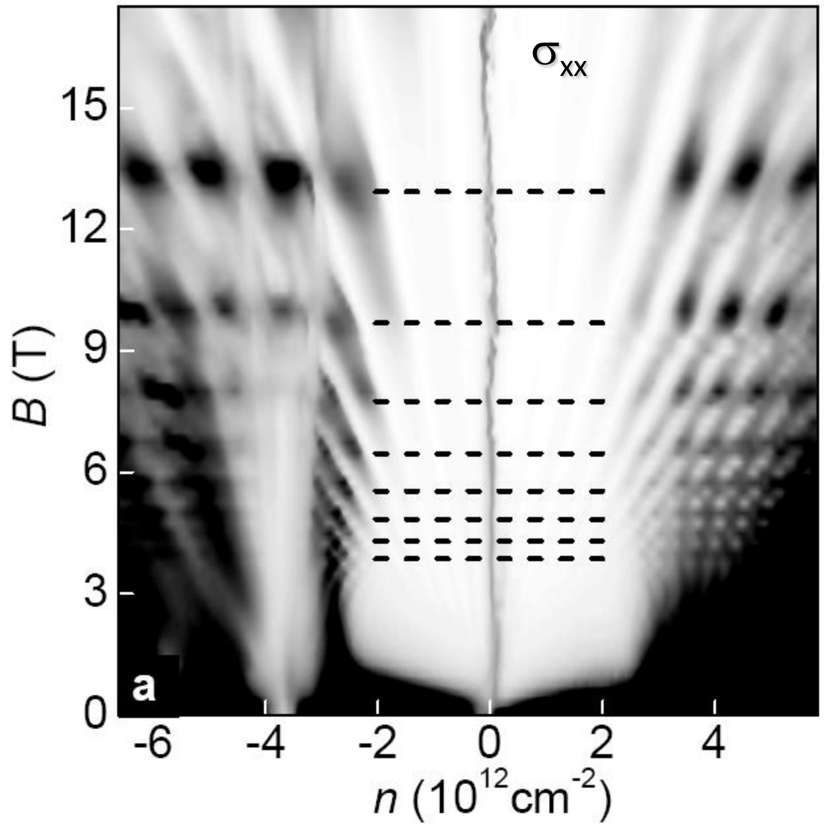

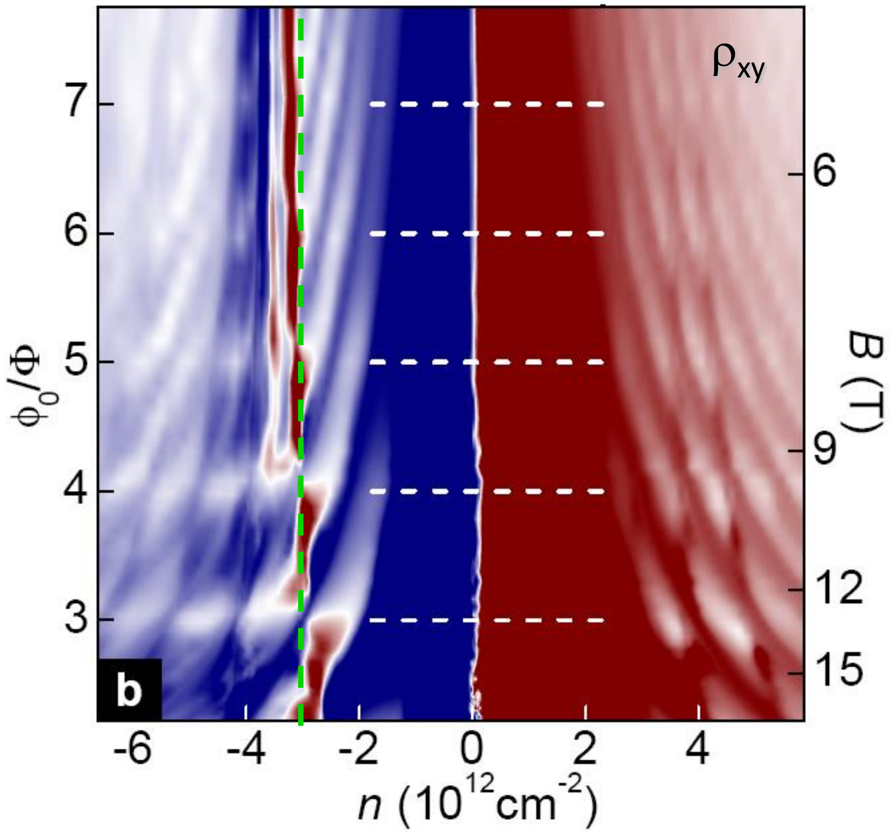

1/*B* oscillations independent of carrier density

neither Landau nor Weiss oscillations

Hall effect repeatedly changes its sign with *B*

cloning of new neutrality points

ϕ_0/N: unit fractions of flux quantum per superlattice unit cell

Hofstadter-Like Oscillations

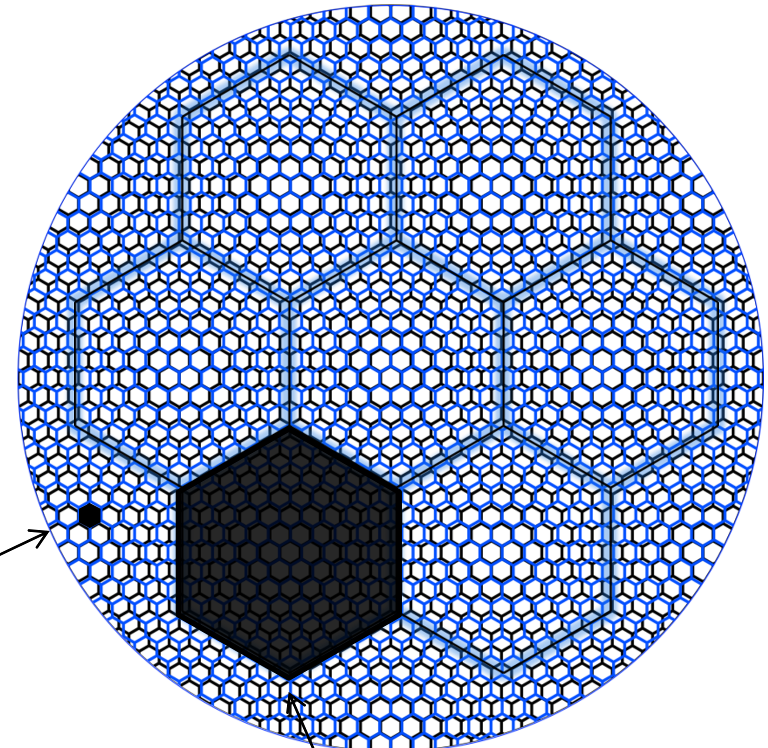

One flux per
one lattice cell $\sim 10^{5}$ T

One flux per $\Phi = B \times S_{\hexagon}$
one superlattice cell, B $\sim$ 40 T

Repeating features are expected when Φ/ϕ_0 = 0,1,2…

Phys. Rev. B **14**, 2239-2249 (1976)
Phys. Rev. **134**, A1602–A1606 (1964)

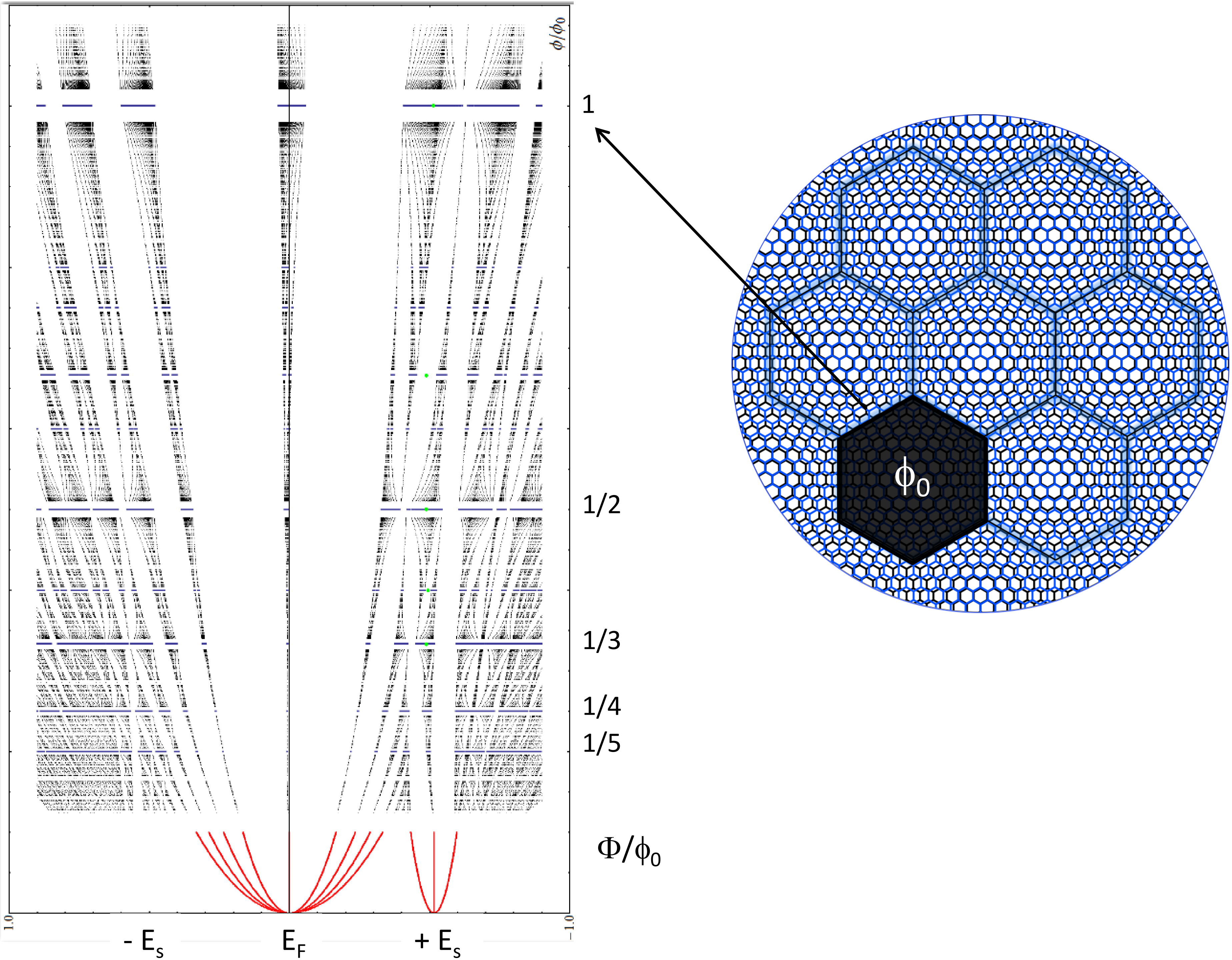

ϕ/ϕ0
1
1/2
1/3
1/4
1/5
Φ/ϕ0
ϕ0
1.0
-1.0
- Es
EF
+ Es

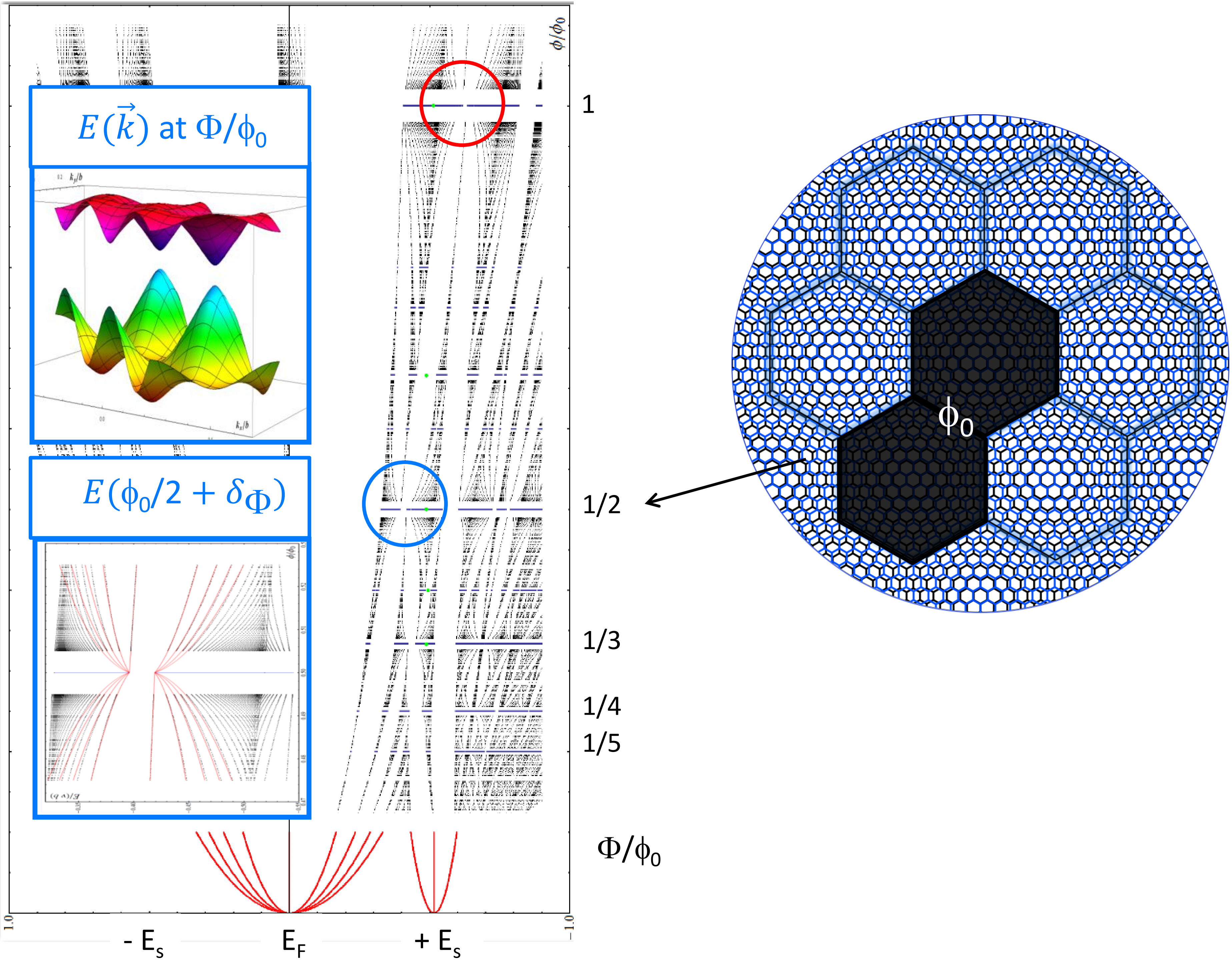

$E(\vec{k})$ at Φ/ϕ_0
$E(\phi_0/2+\delta_\Phi)$
ϕ/ϕ_0
1
1/2
1/3
1/4
1/5
Φ/ϕ_0
ϕ_0
1.0
-1.0
$-E_s$
E_F
$+E_s$

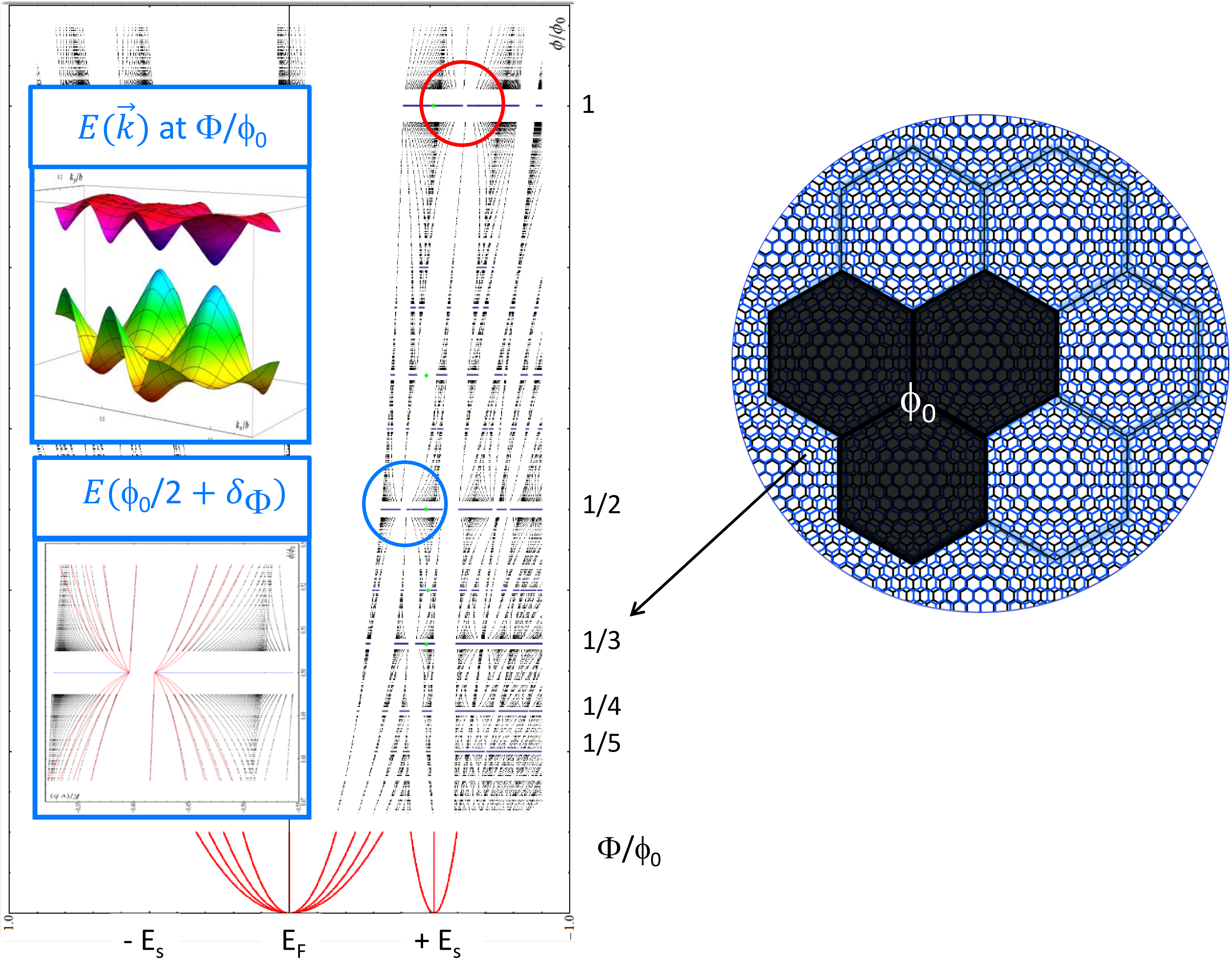

$E(\vec{k})$ at Φ/ϕ_0
$E(\phi_0/2 + \delta_\Phi)$
ϕ/ϕ_0
1
1/2
1/3
1/4
1/5
Φ/ϕ_0
ϕ_0
- E_s
E_F
+ E_s

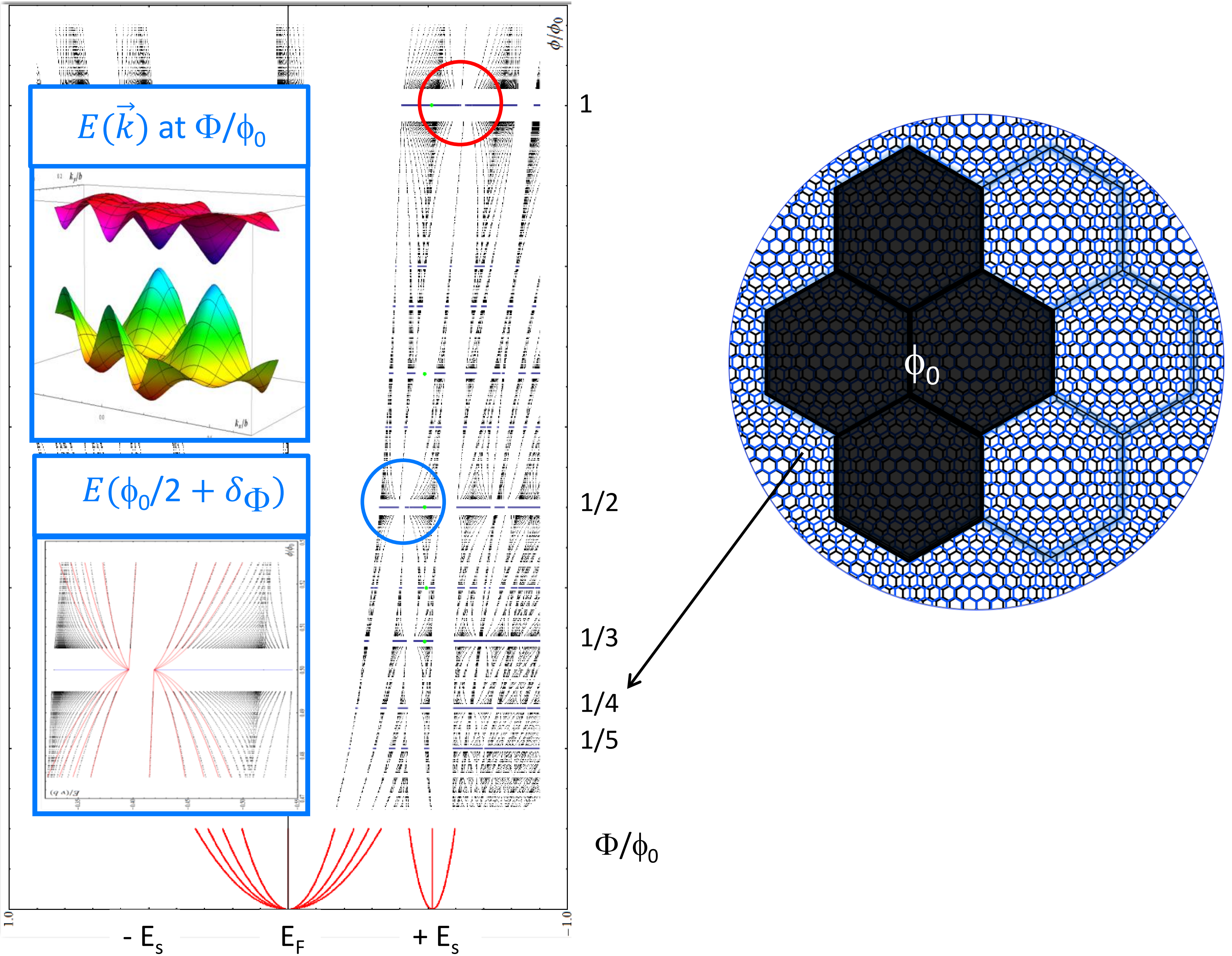

φ/φ0
E(k⃗) at Φ/φ0
E(φ0/2 + δΦ)
1
1/2
1/3
1/4
1/5
Φ/φ0
- Es
EF
+ Es
φ0

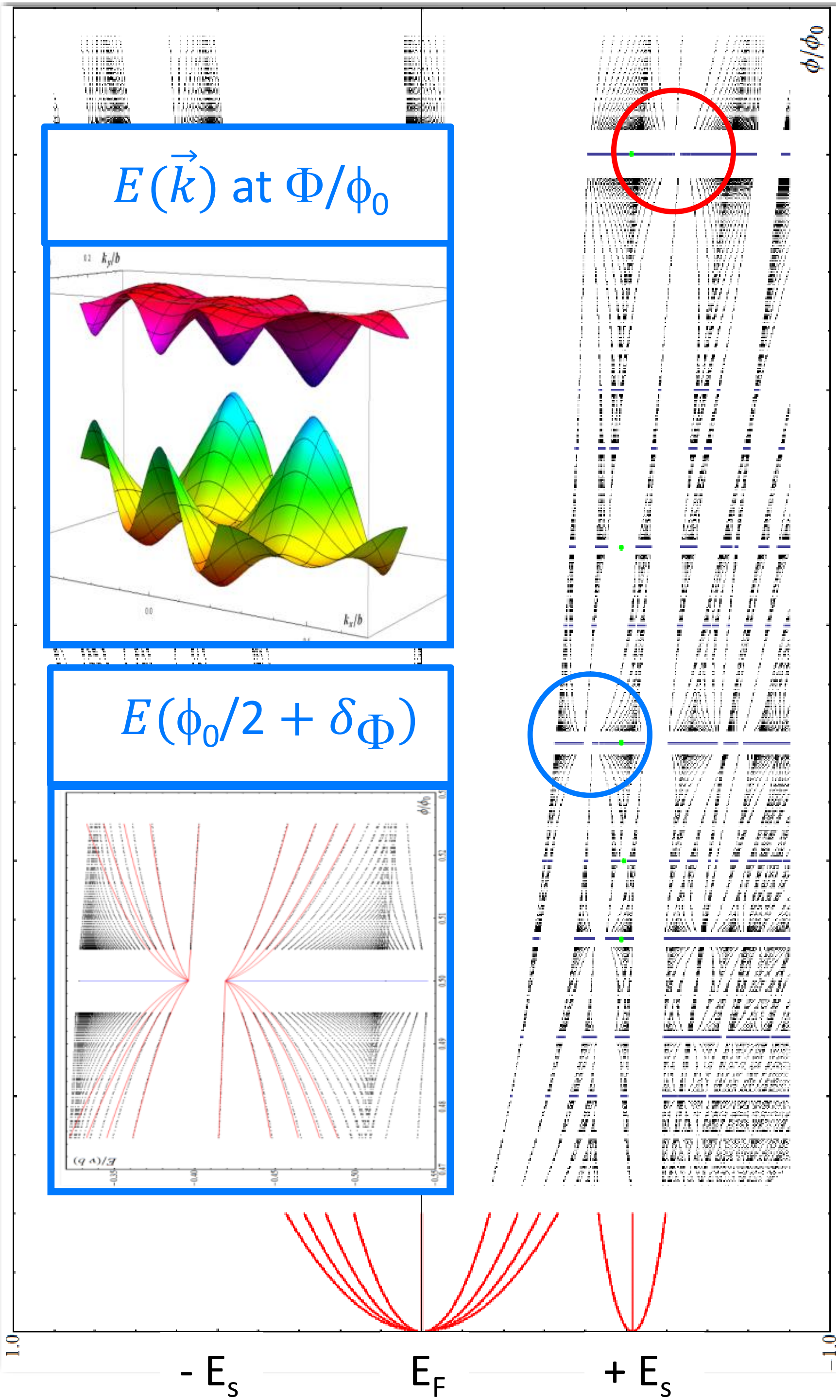

Magnetic microbands at

$$\phi = \frac{p}{q}\phi_0$$

gapped Dirac electrons

$$H_{Dirac} = v_{mDP}(\vec{k} - \tfrac{e}{c}\delta\vec{A})\cdot\vec{\sigma} + \Delta\sigma_z$$

Patel, Wallbank, Mucha-Kruczynski, Fal'ko (2013)

Self-similar cloning of dirac specta

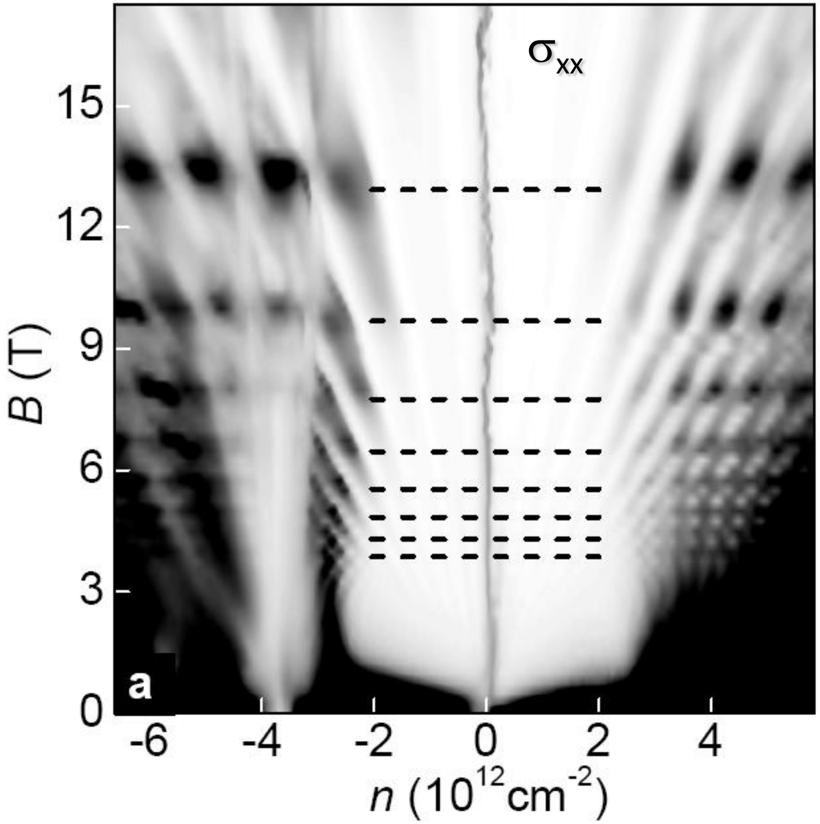

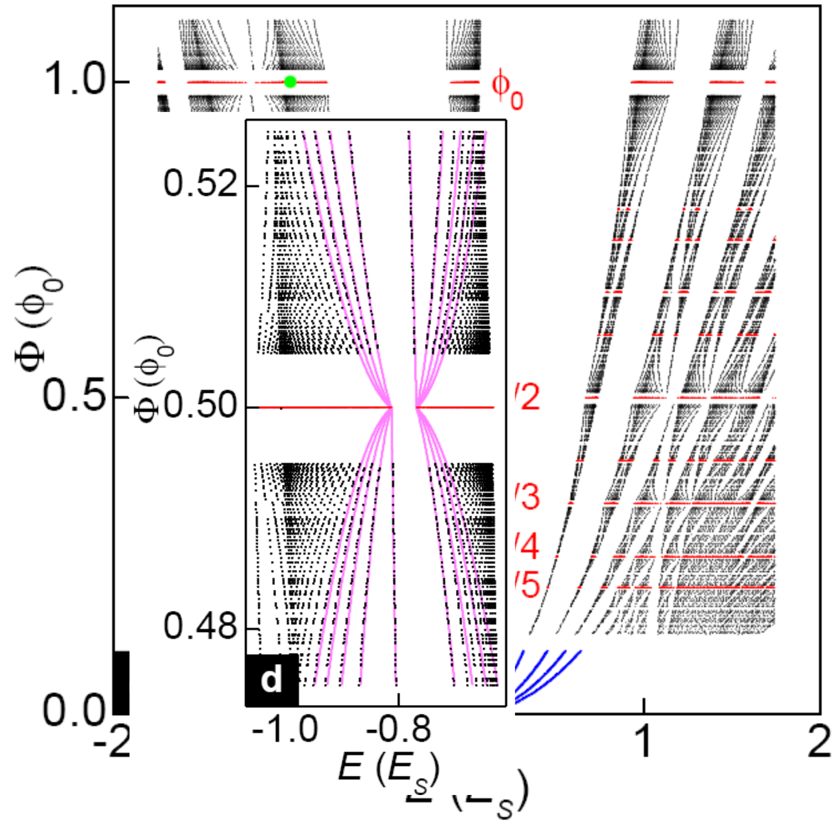

anomalies at unit fractions of ϕ_0

magnetic field clones numerous
Dirac points at fractal flux quanta

Nature. 497: 594–597

Nature. 497: 598–602

G / hBN / G

Vertical FET

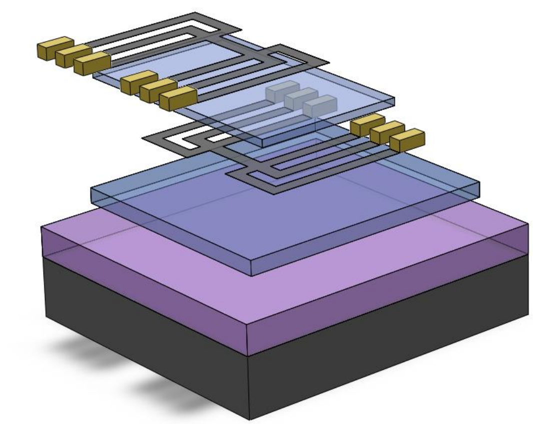

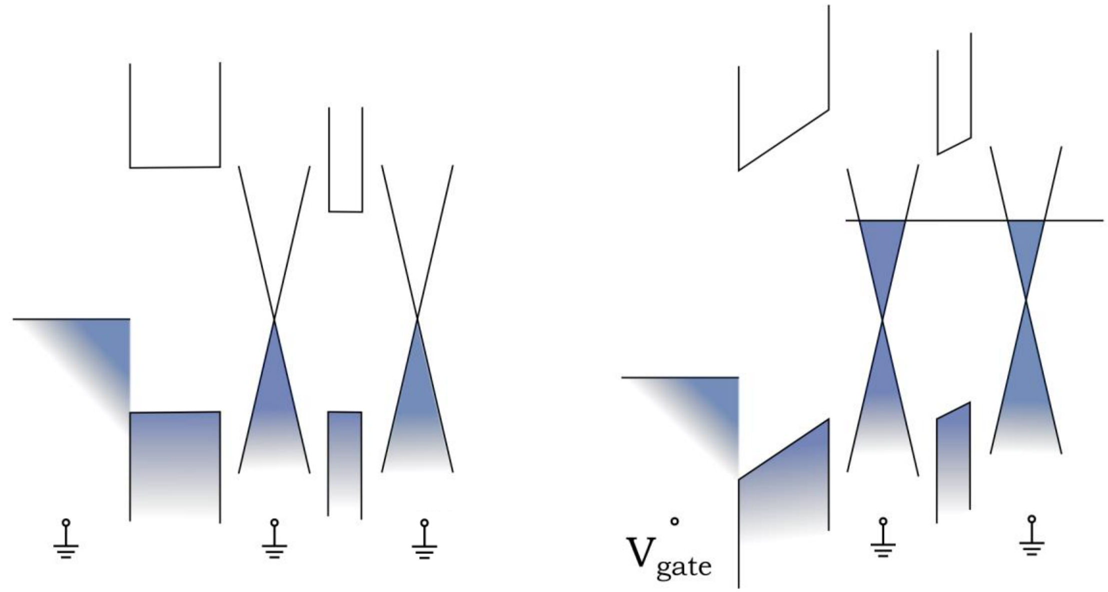

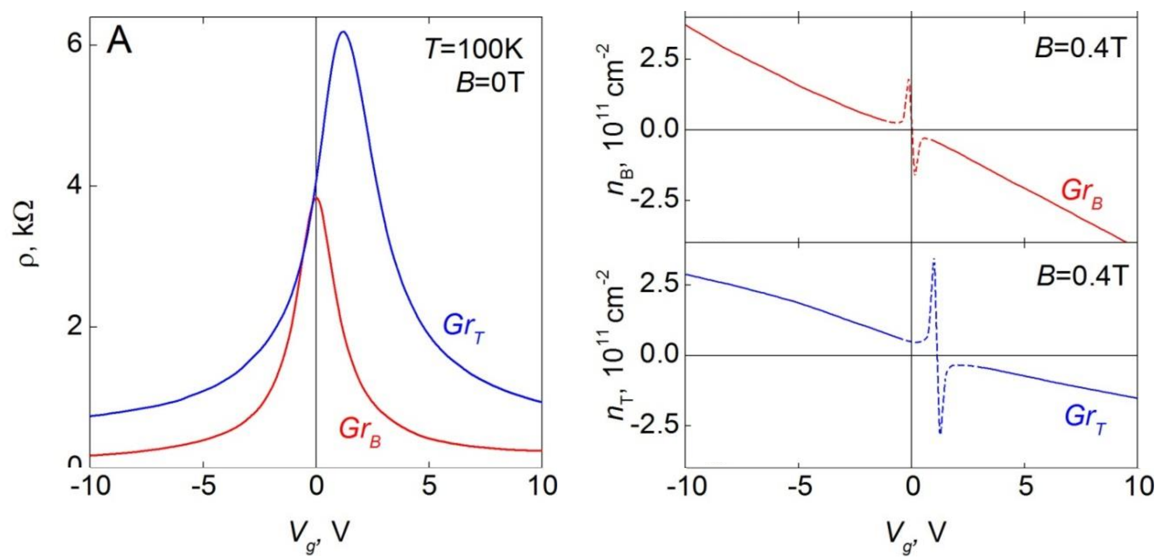

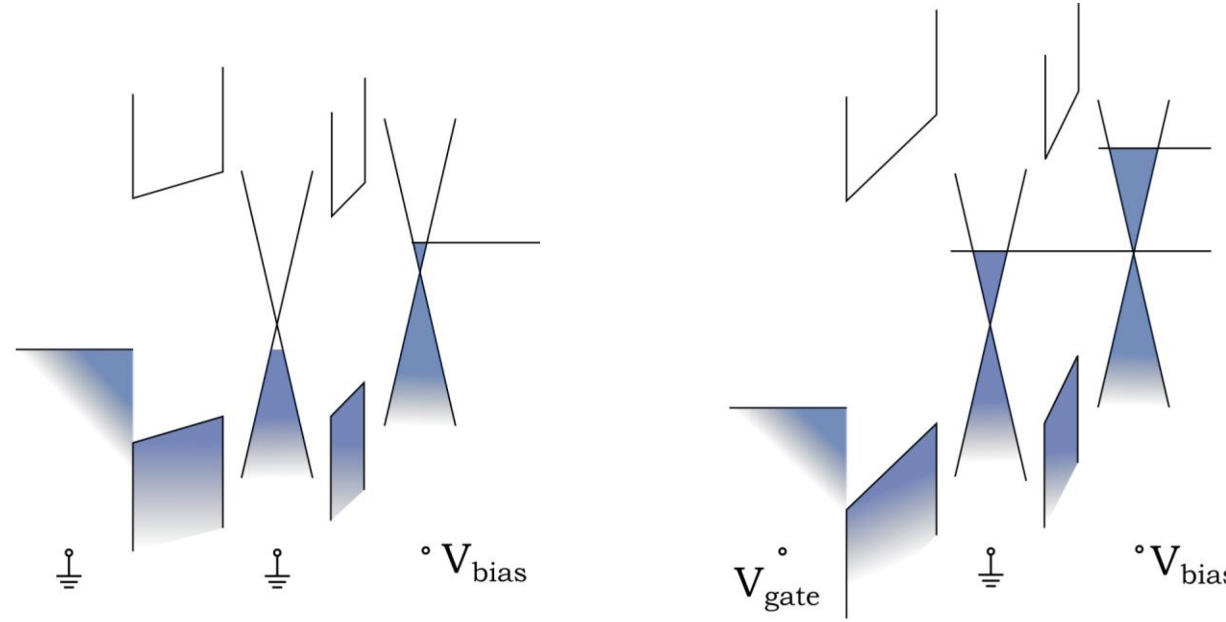
V_bias
V_gate
V_bias

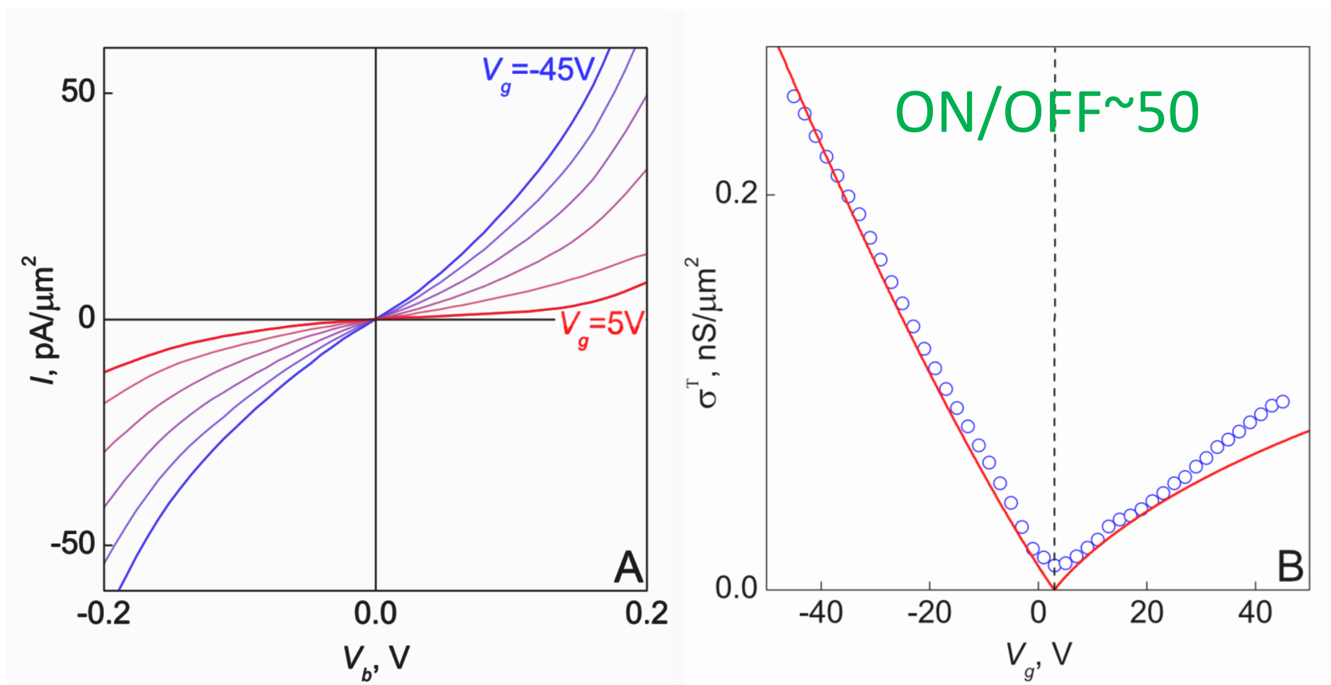
V_g=-45V
V_g=5V
I, pA/μm²
V_b, V
A
ON/OFF~50
σ^T, nS/μm²
V_g, V
B

Increasing ON/OFF

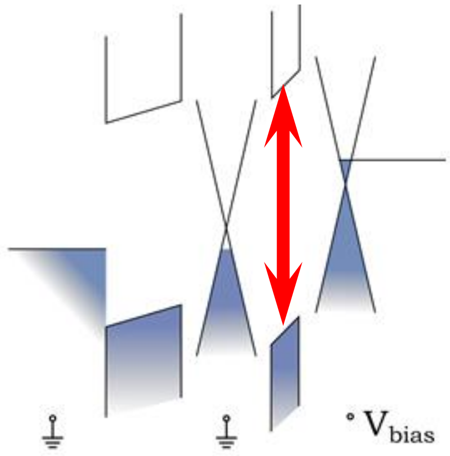

Gap in hBN: 5.9 eV

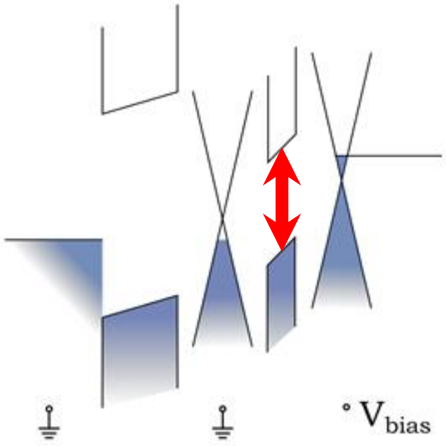

Gap in MoS_2: 1.9eV

for BN barrier:
dominated by the
Density of States in graphene

for MoS_2 barrier:
dominated by the
barrier change

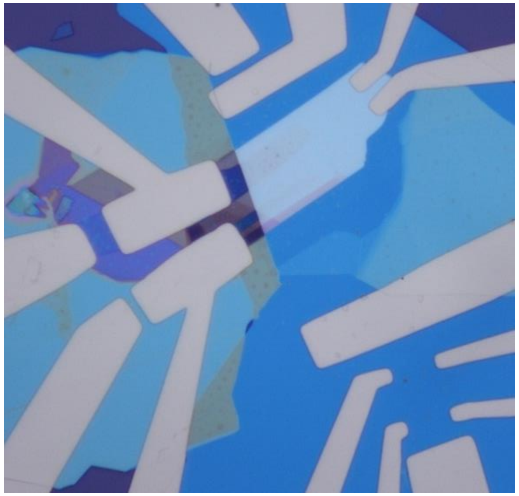

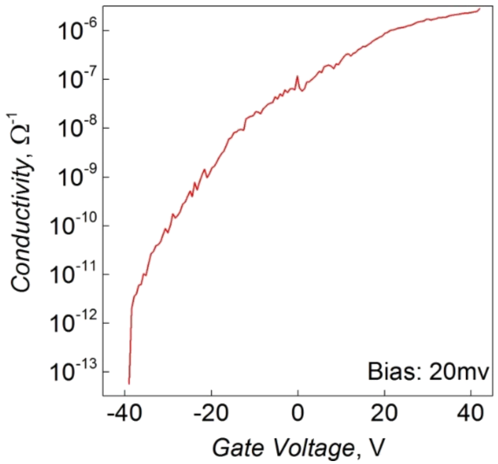

T. Georgiou et al
Nature Nanotechnology ‘13

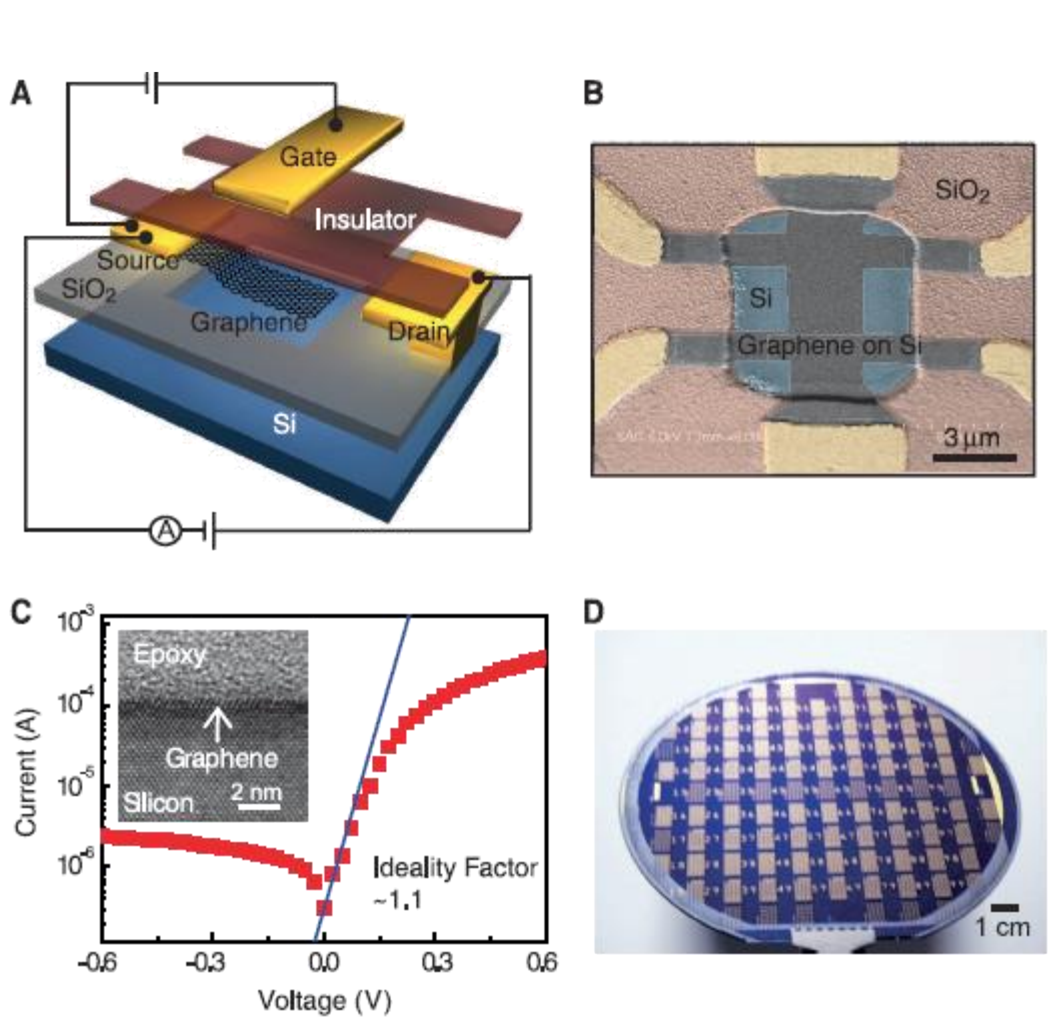

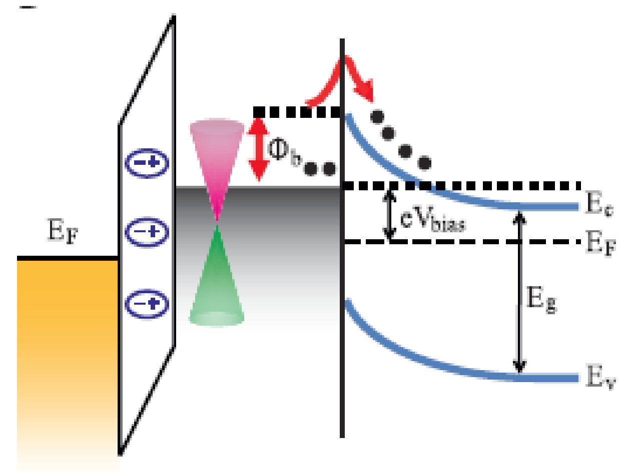

Tunnelling through Schottky barrier

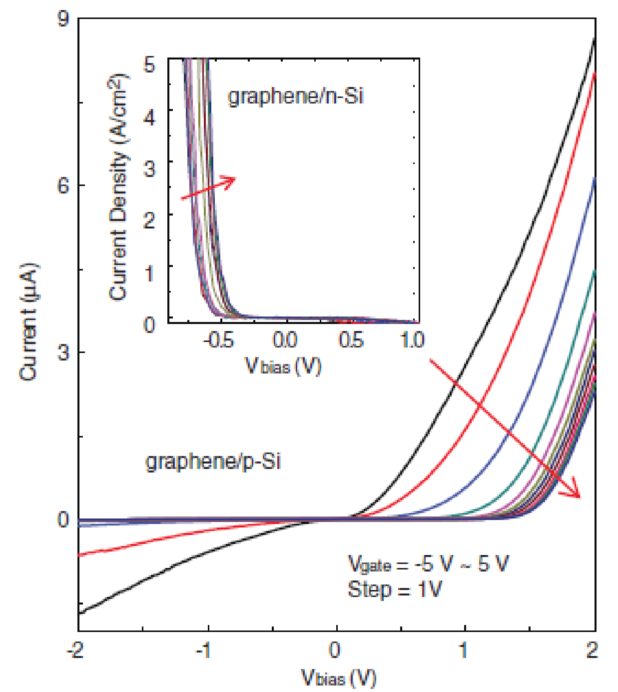

Graphene on Silicon

ON/OFF 10^5

Yang et al Science '12

G / hBN / G
Crystal alignment

Tunnelling Transistor

L. Britnell et al
Science '12

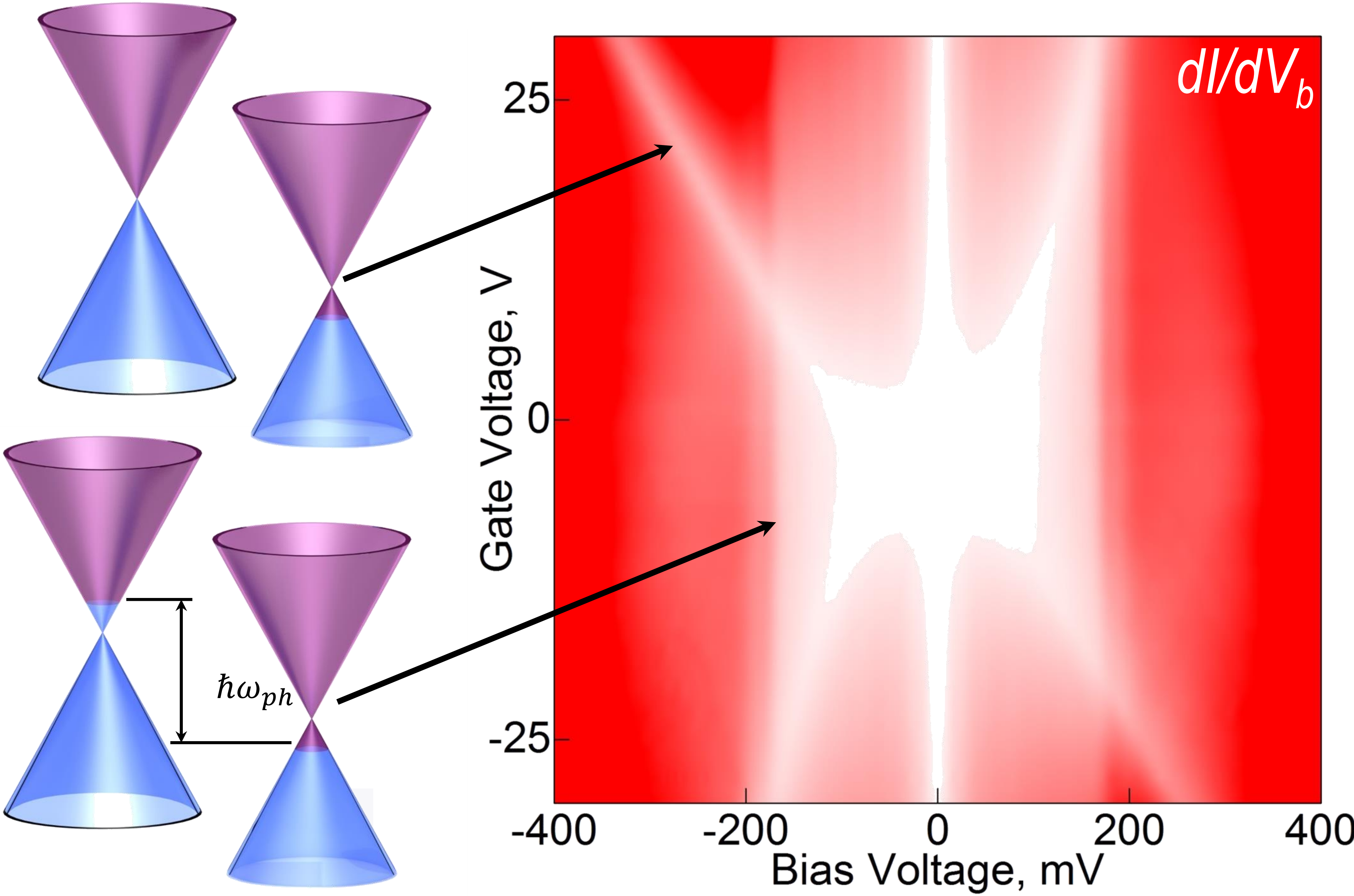

Tunnelling with momentum conservation

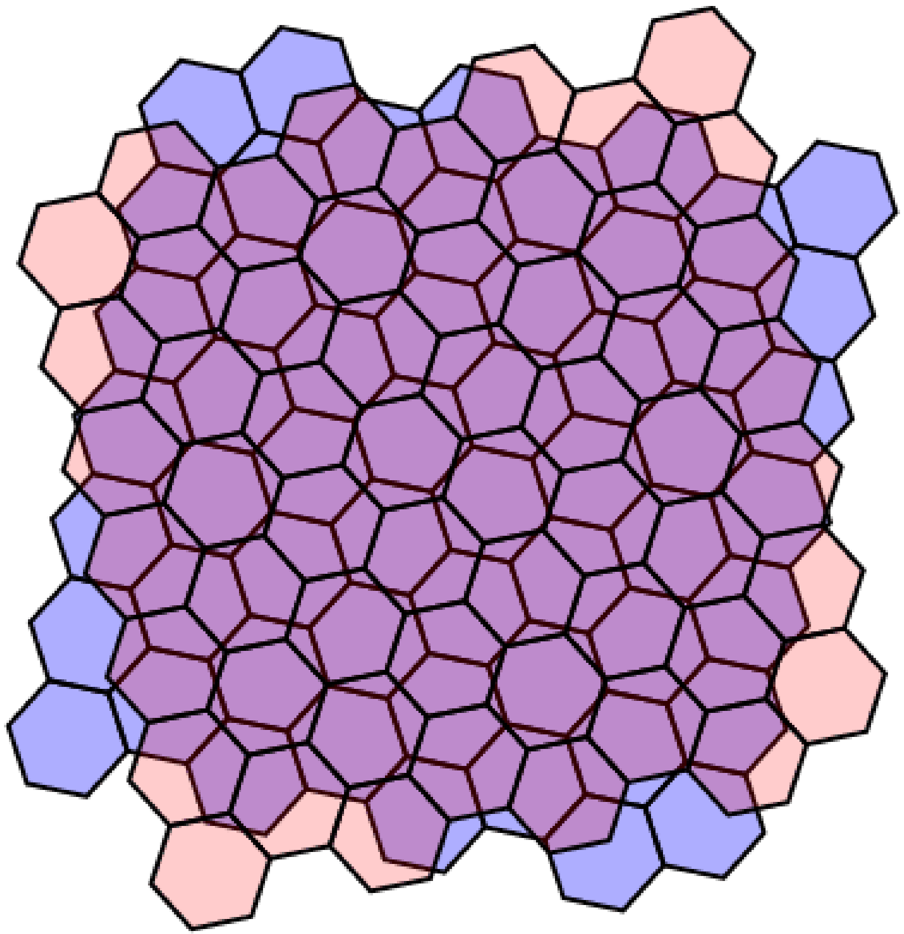

real space

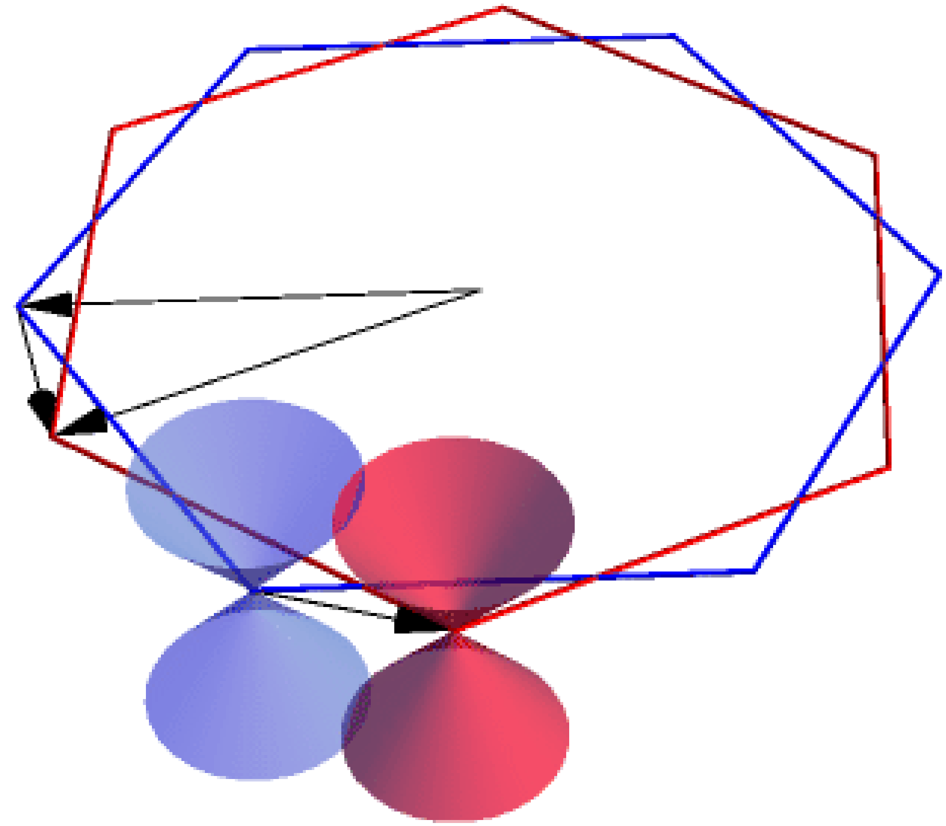

reciprocal space

Align the two graphene layers

Mishchenko et al
Nature Nano. '14

Tunnelling with momentum conservation

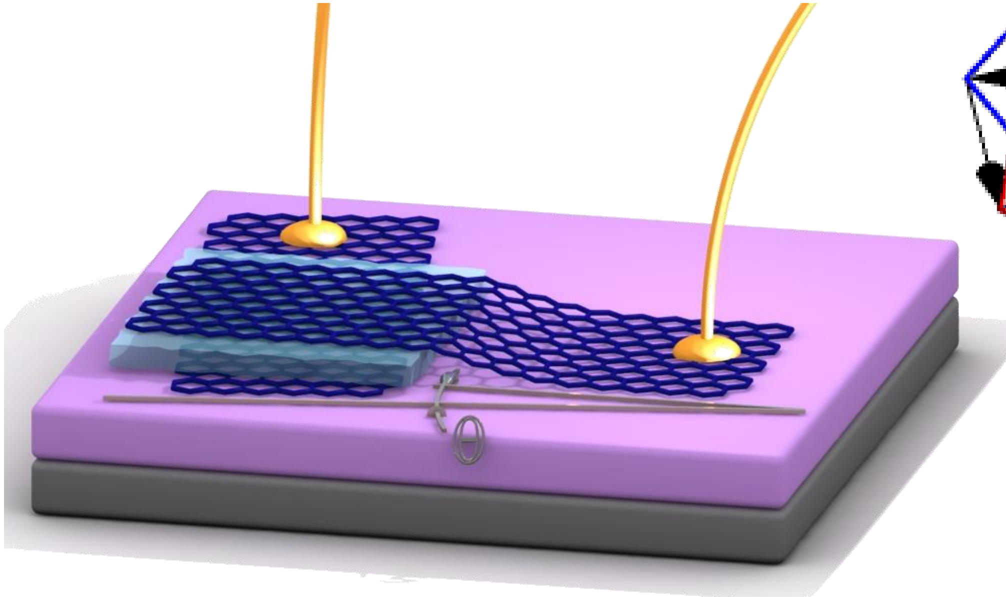

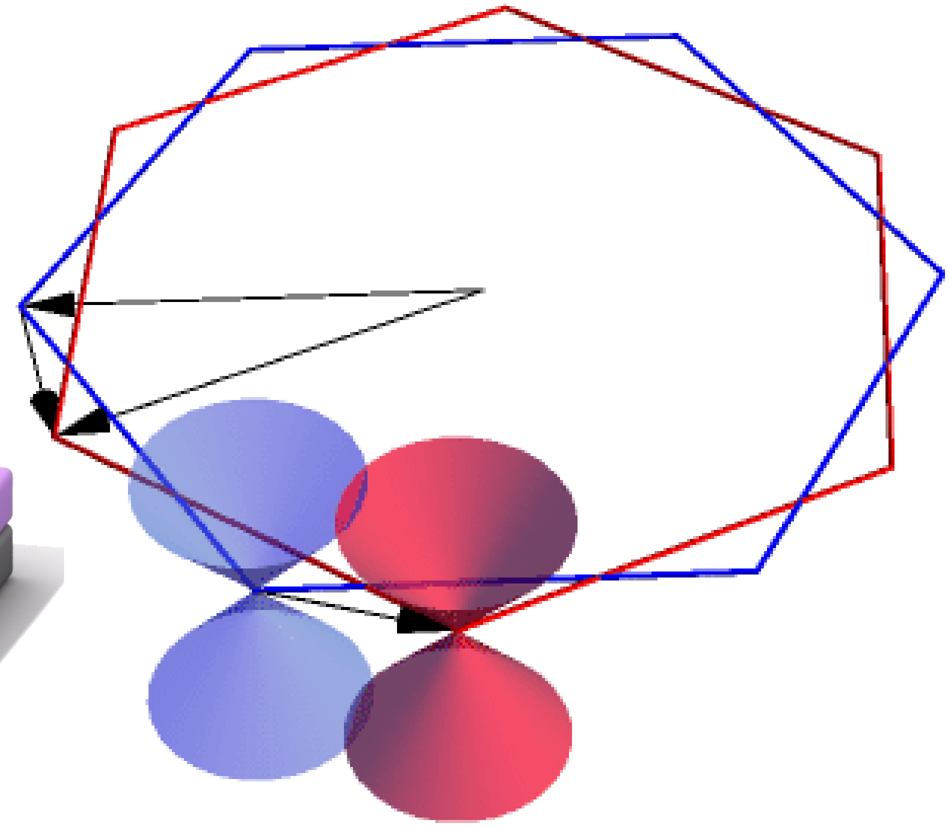

real space

reciprocal space

Align the two graphene layers

Mishchenko et al
Nature Nano. '14

Tunnelling with momentum conservation

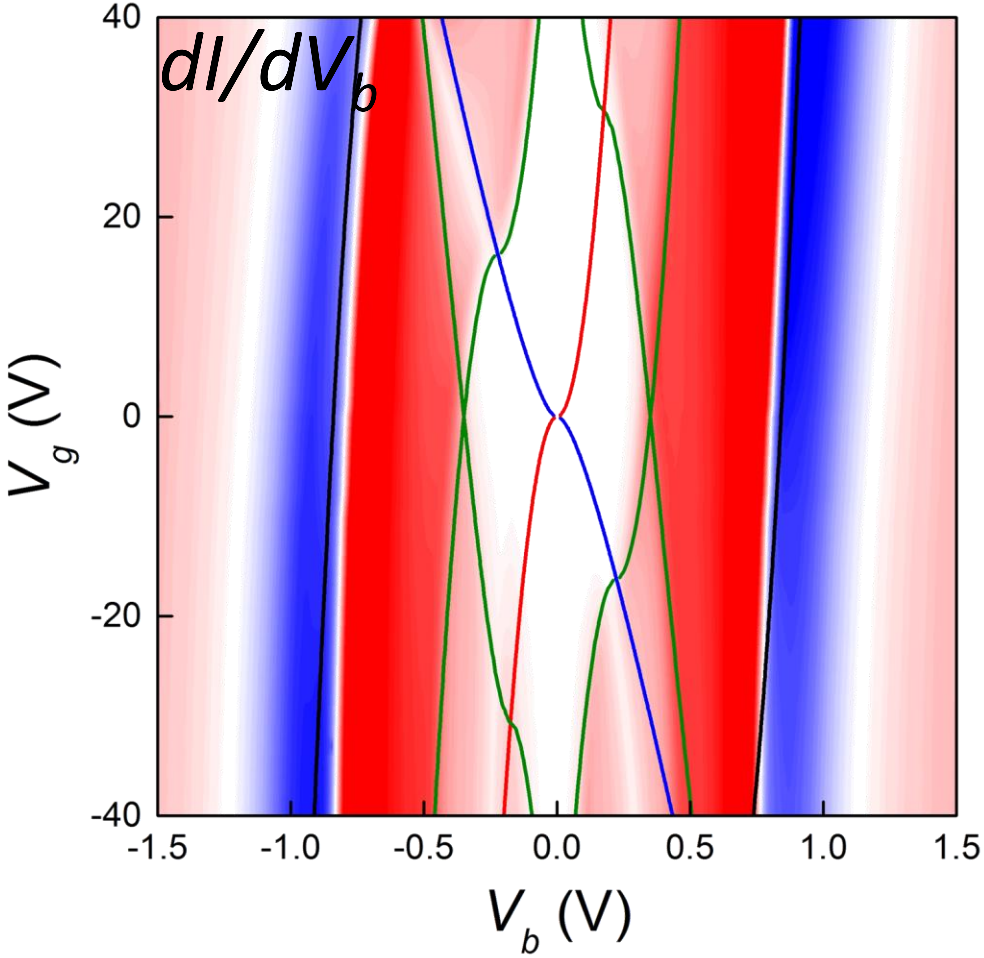

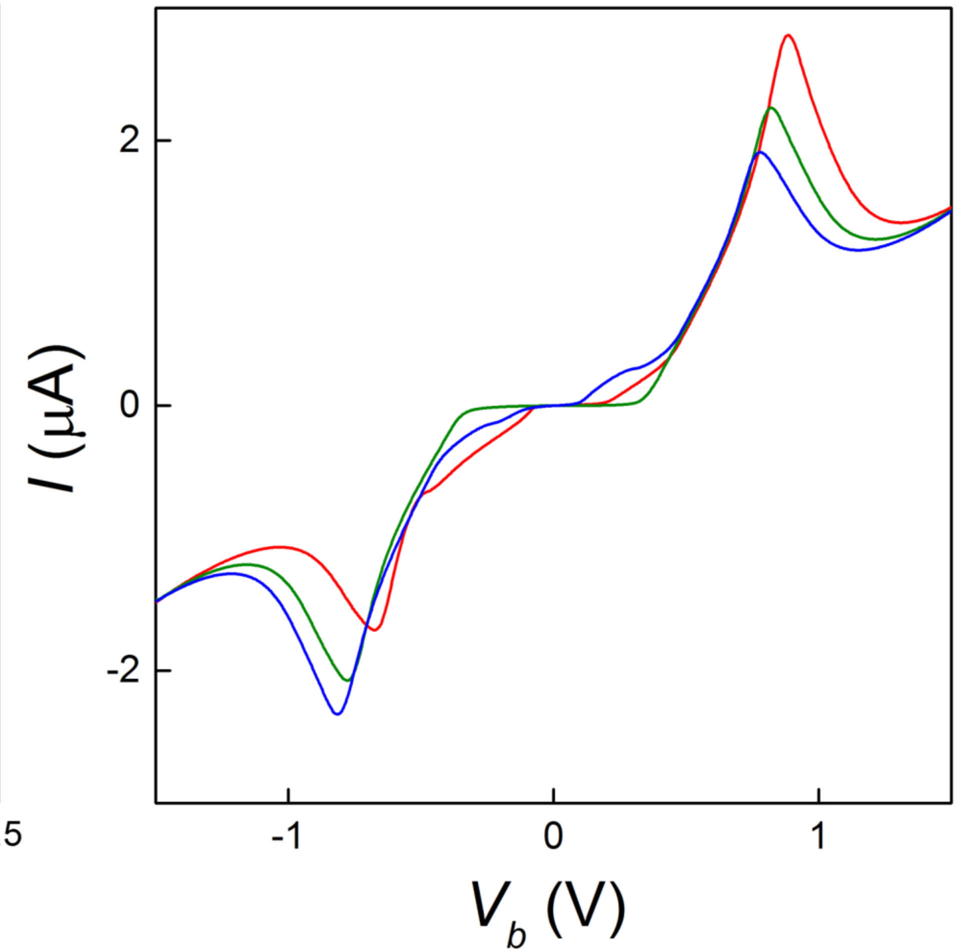

Negative differential conductance:

- large peak to valley current
- tunable by gate

Tunnelling with momentum conservation

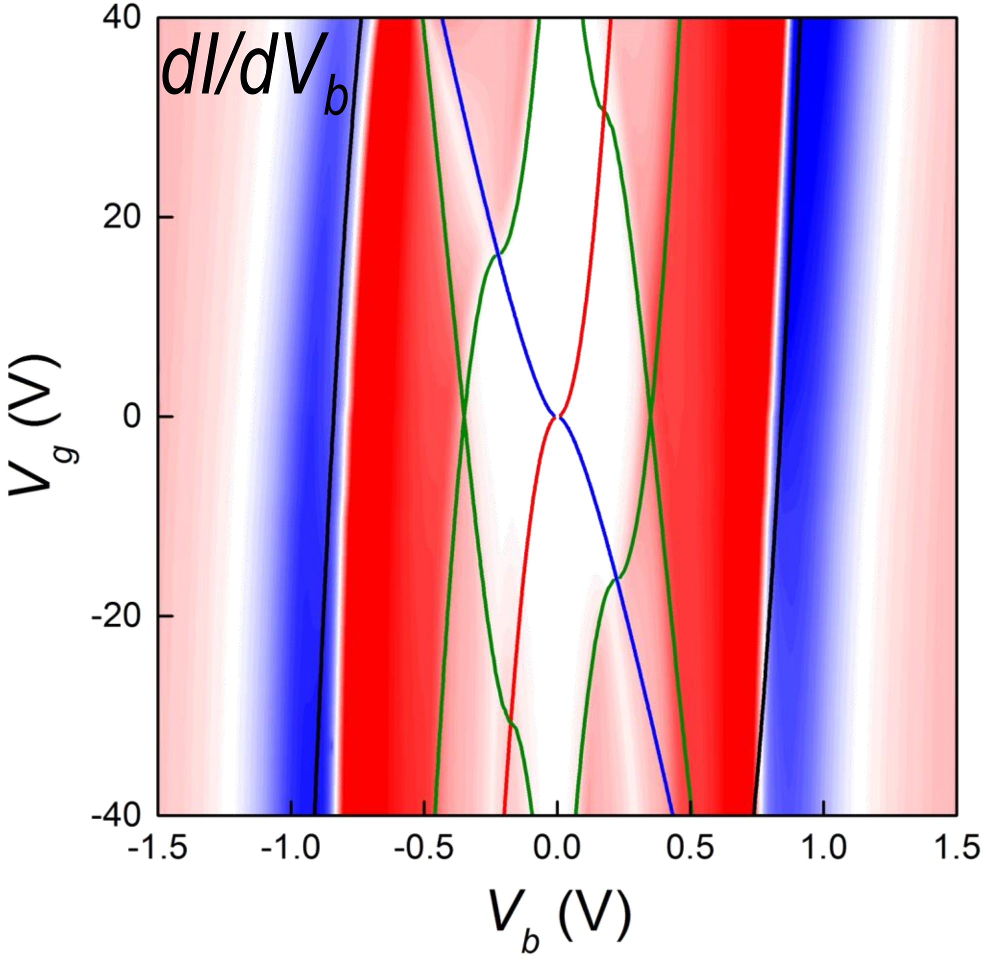

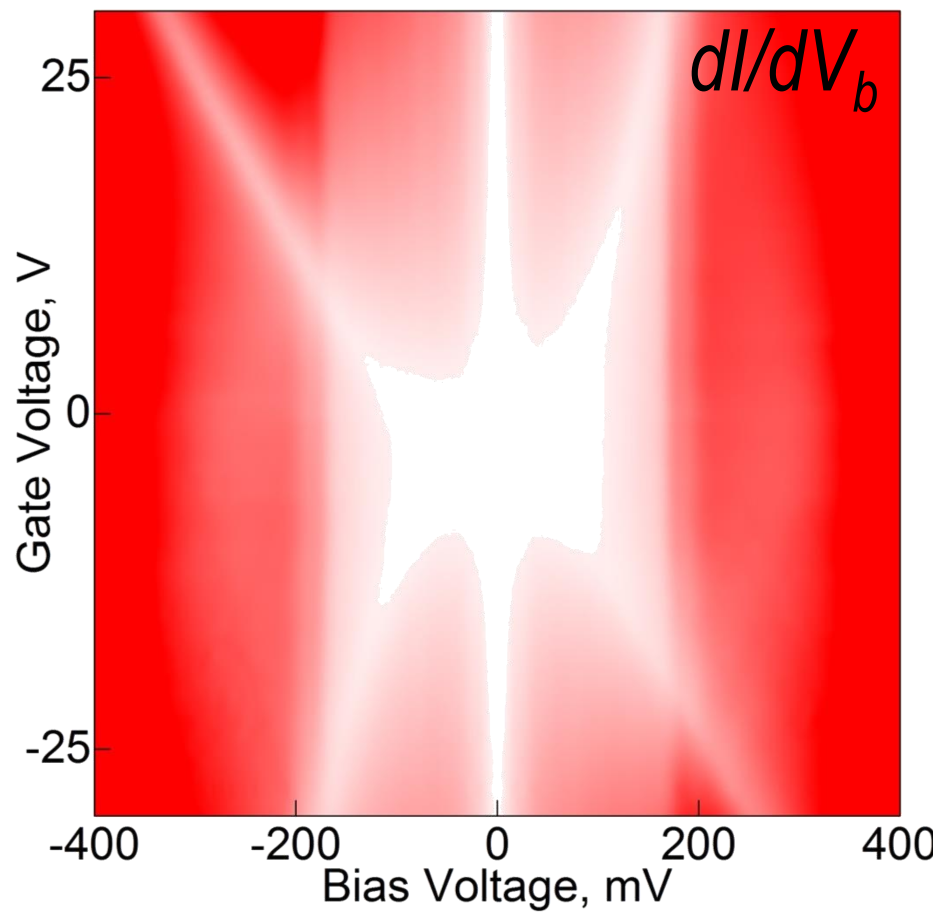

Negative differential conductance:

- large peak to valley current
- tunable by gate

Momentum conservation

Mishchenko et al
Nature Nano. '14

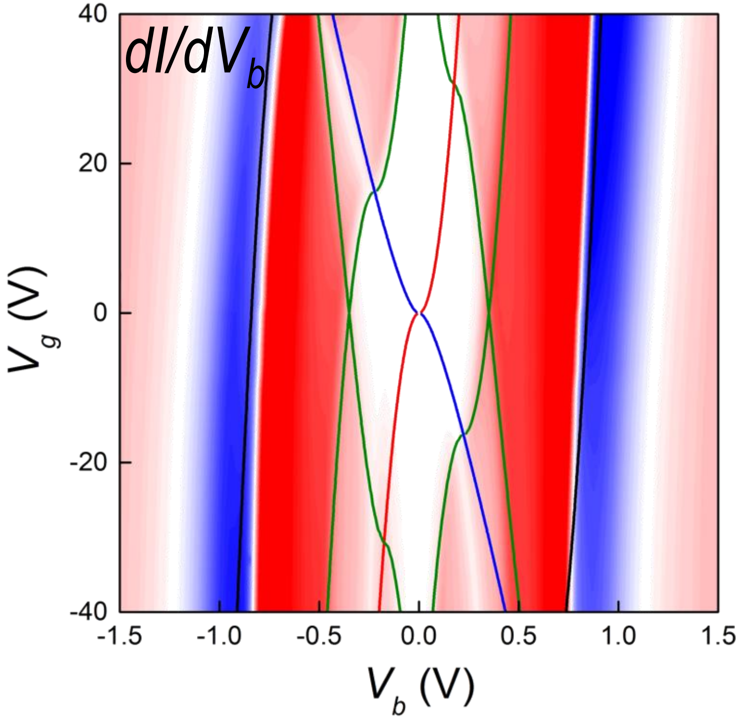

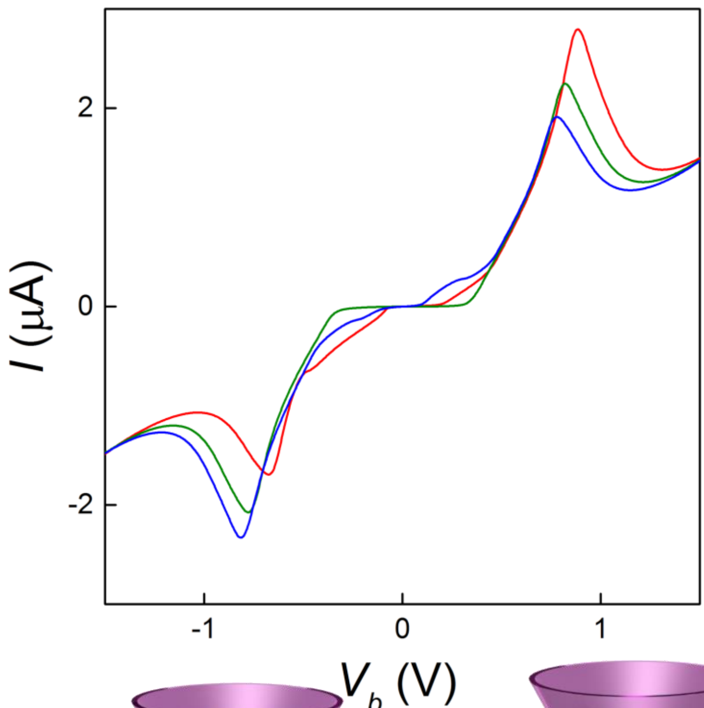

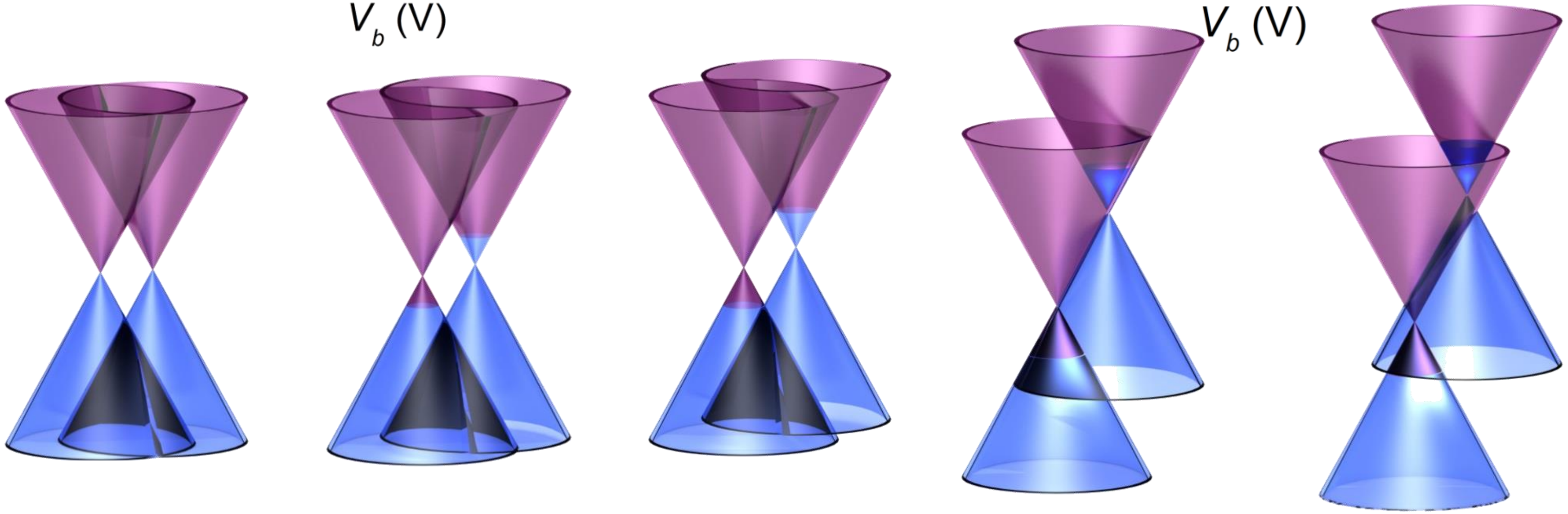

In-plane magnetic field

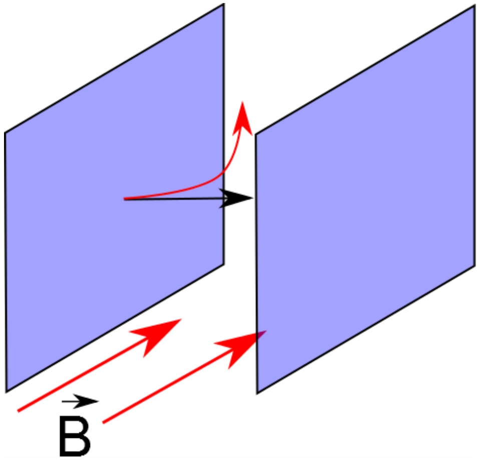

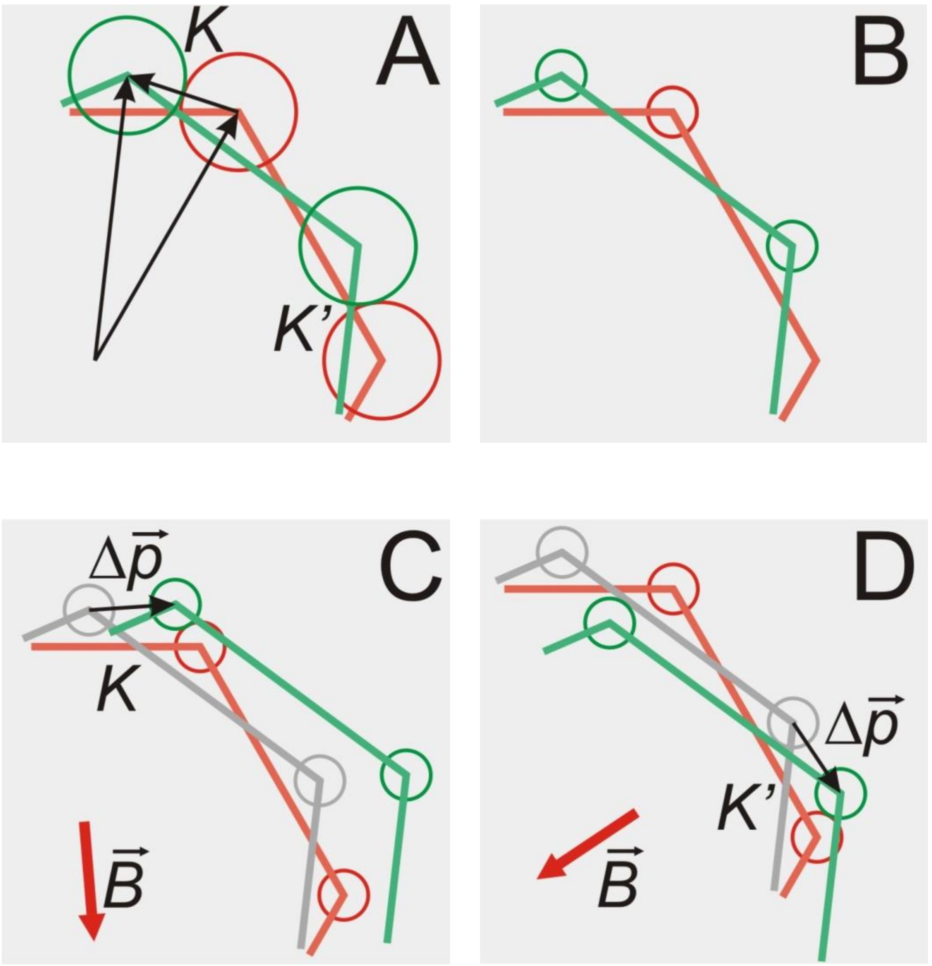

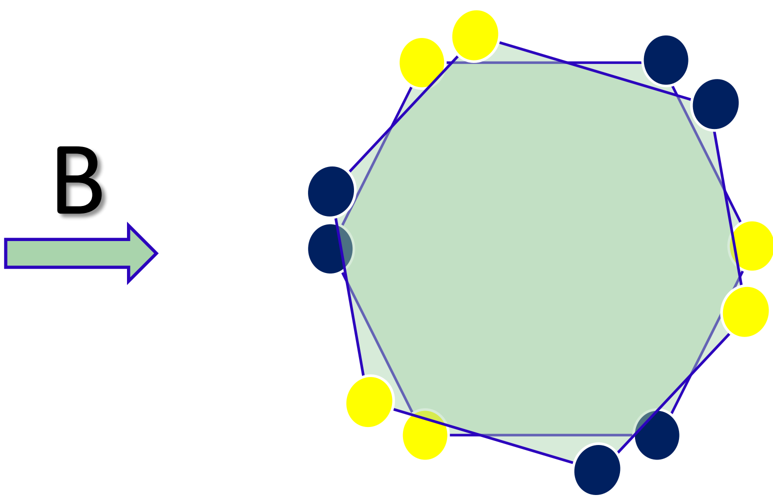

In-plane magnetic field

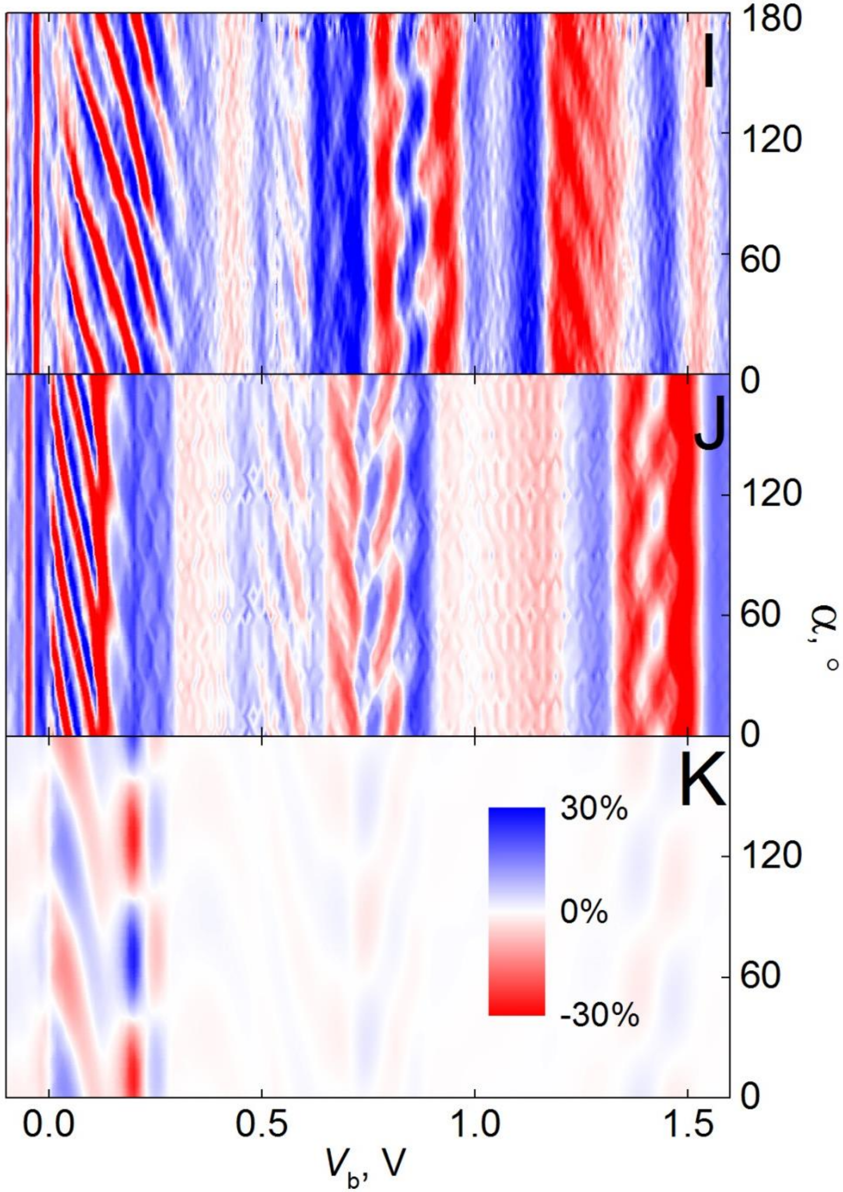

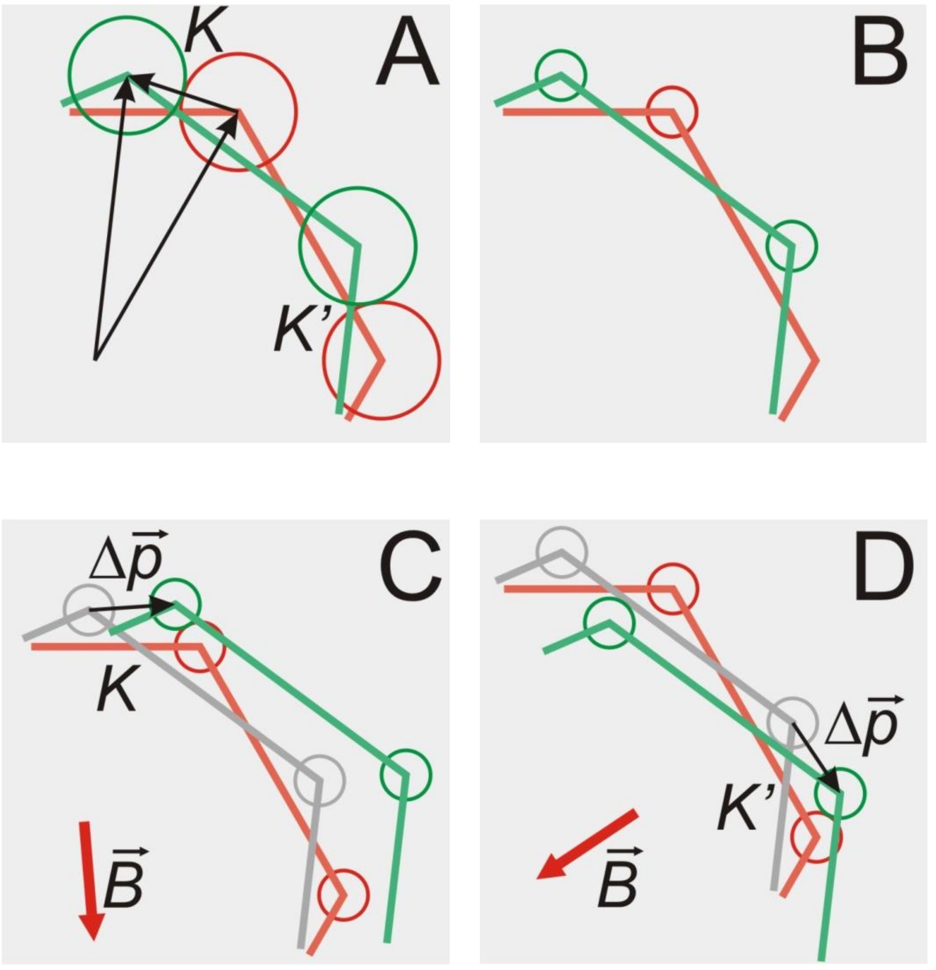

Mishchenko et al
Nature Nano. '14

Conical cross sections with a twist

Chirality introduces additional conservation restrictions

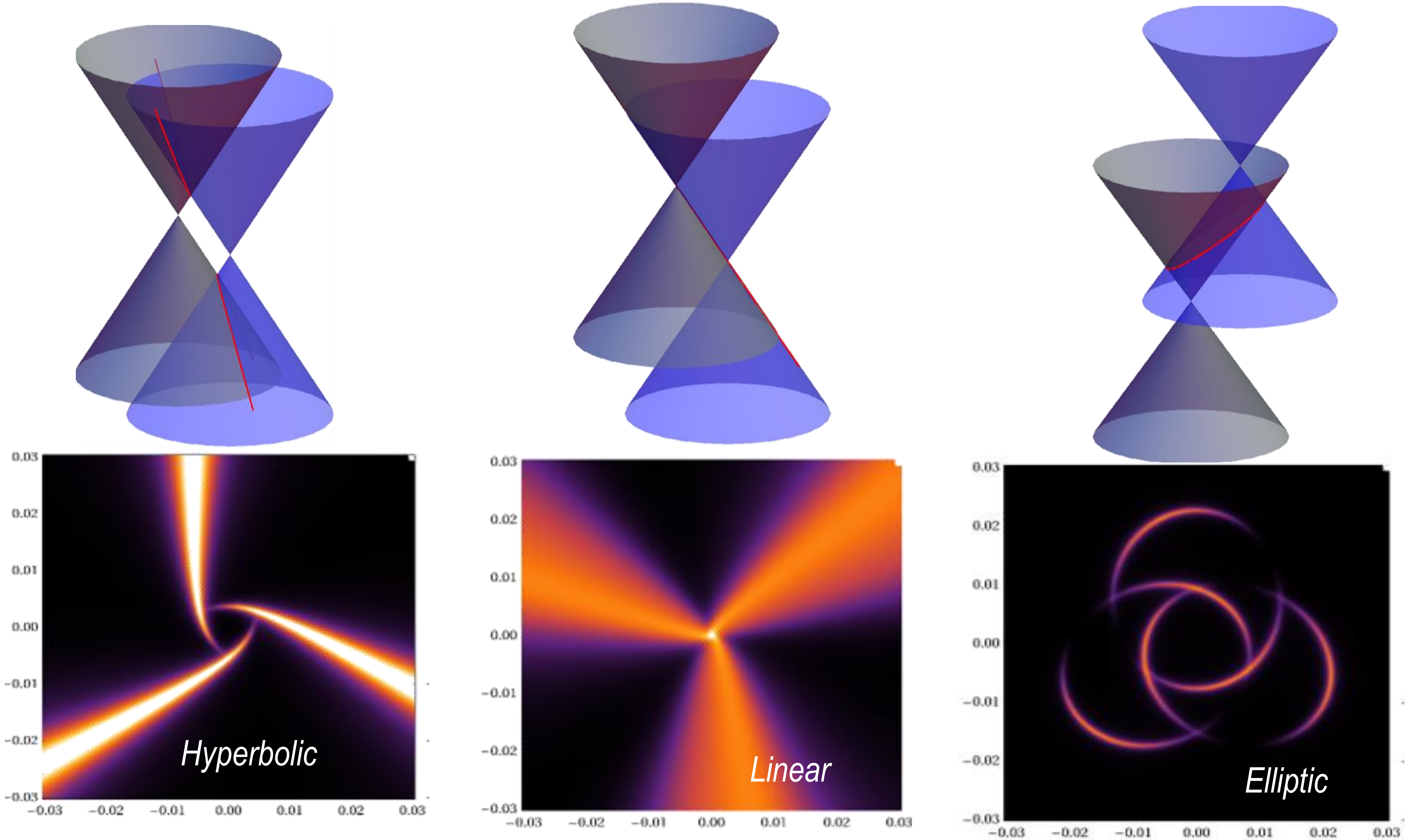

Room-temperature operation

Traditional RTD:

- Hard to make operation at room temperatures
- Trade-off between peak to valley current and total current

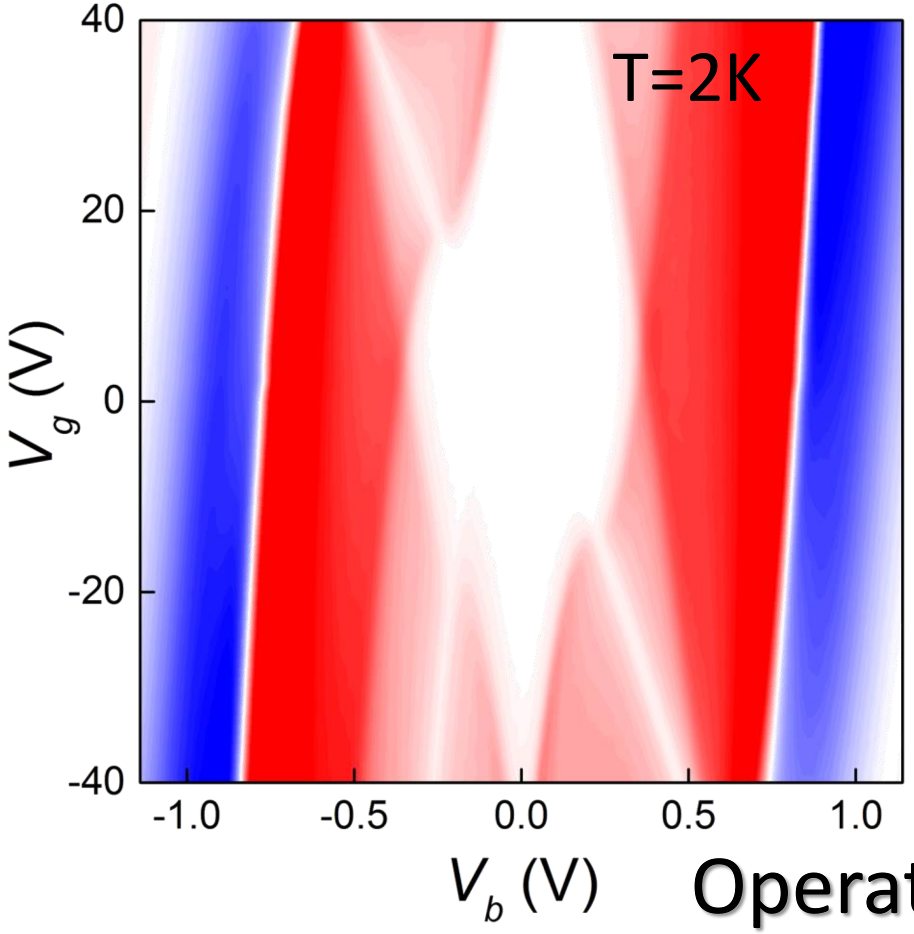

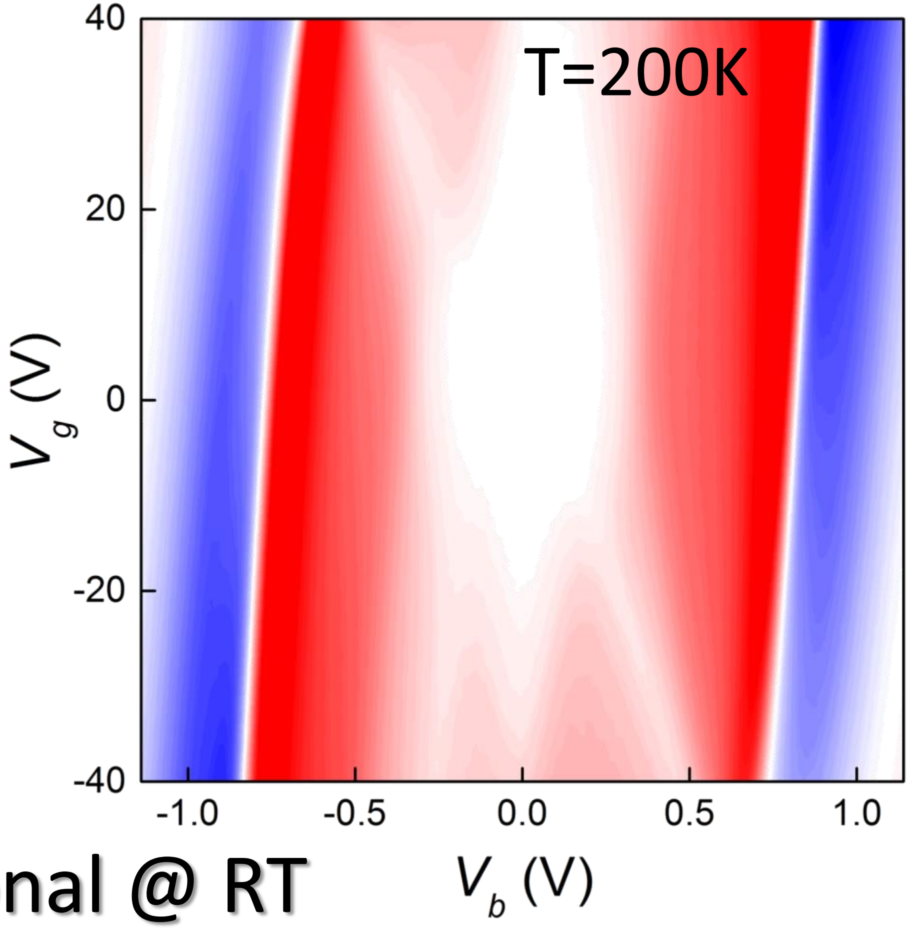

Operational @ RT

hBN / G / hBN / G / hBN

BN / G / BN / G

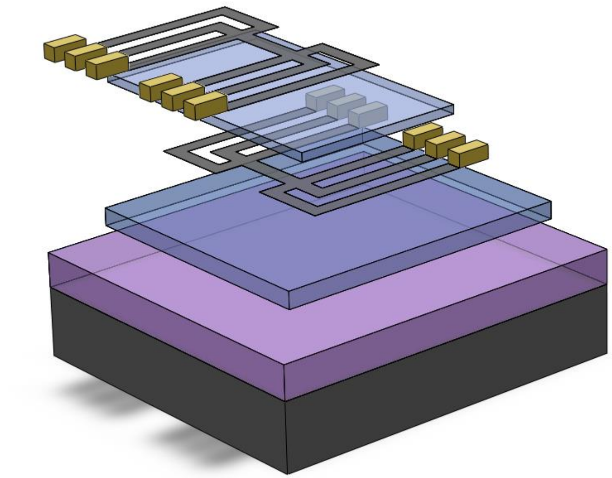

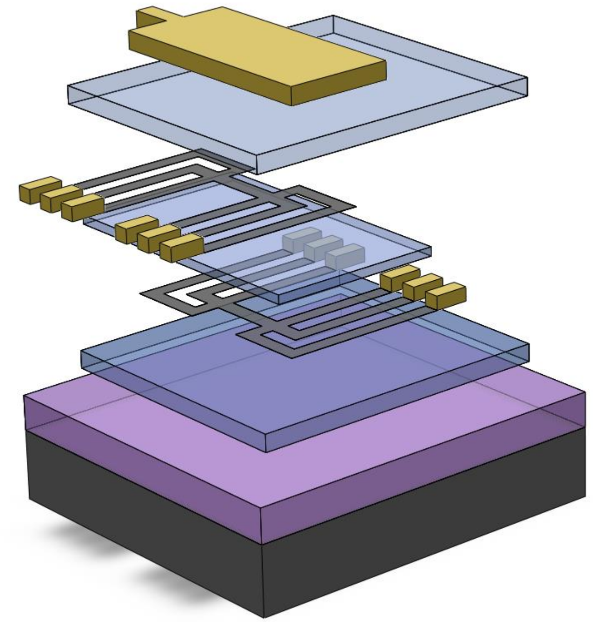

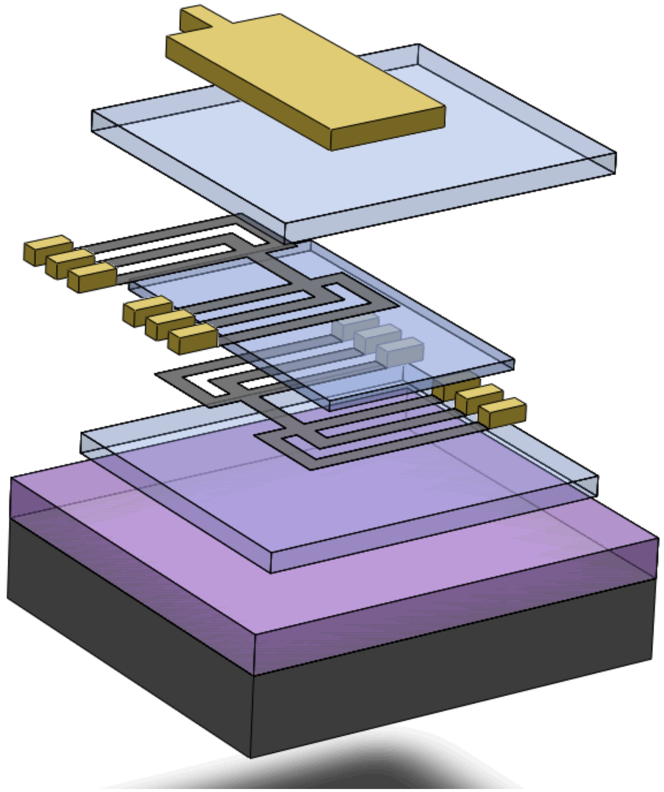

Flake transfer x 4

EBL x 6

Annealing x 4

Plasma etch x 4

Metal evaporation x 3

top gated double layer devices

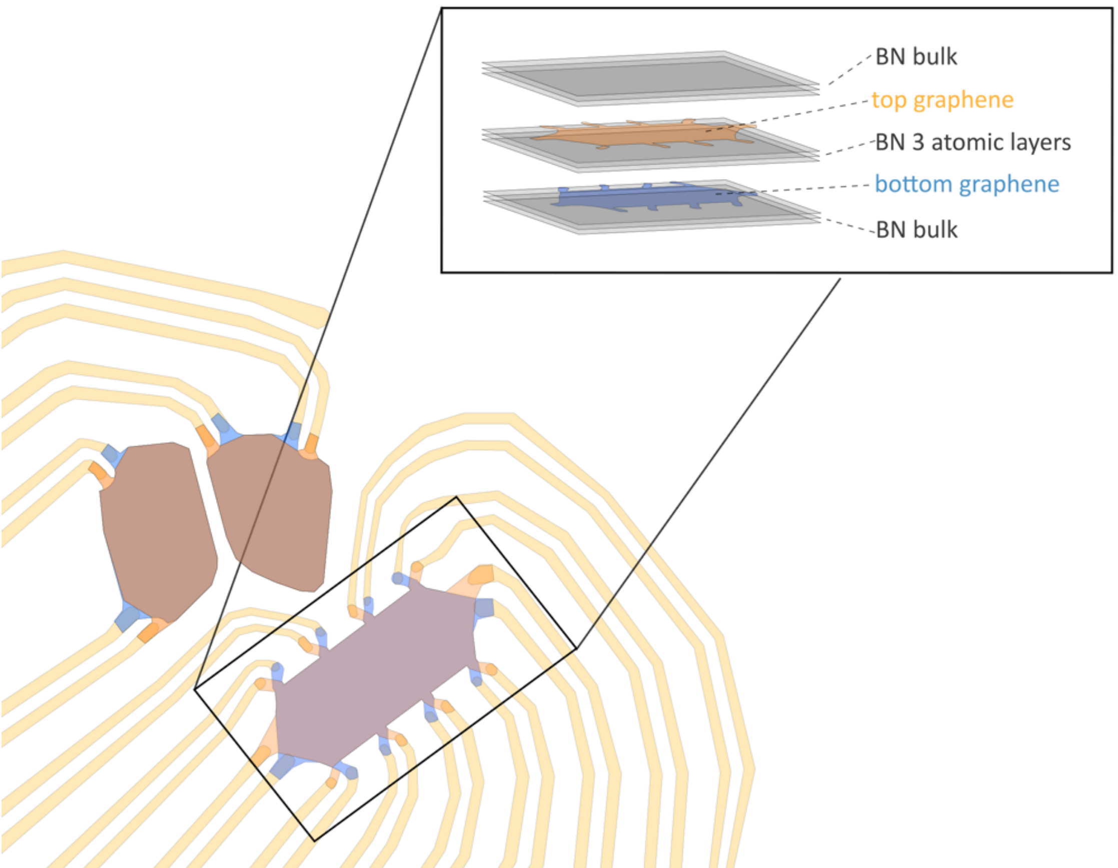
BN bulk
top graphene
BN 3 atomic layers
bottom graphene
BN bulk
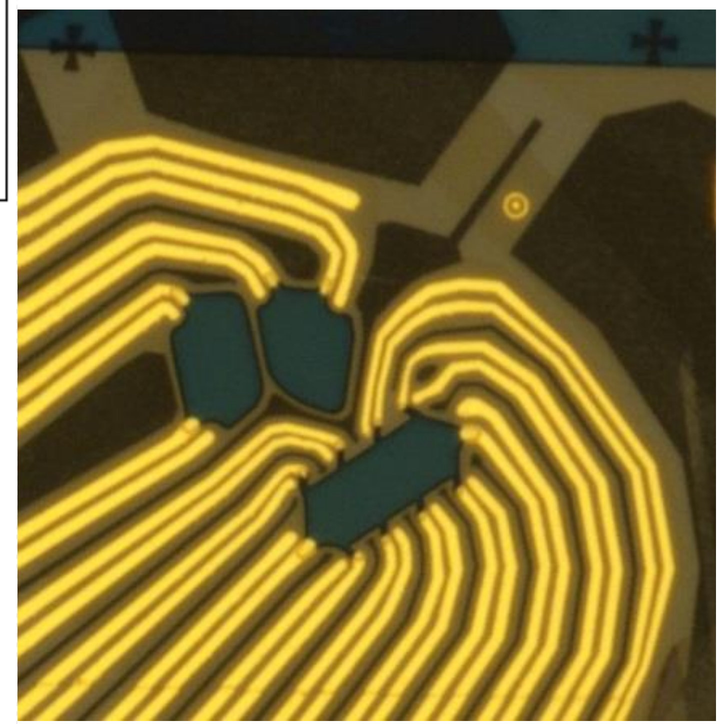

Double layer structures

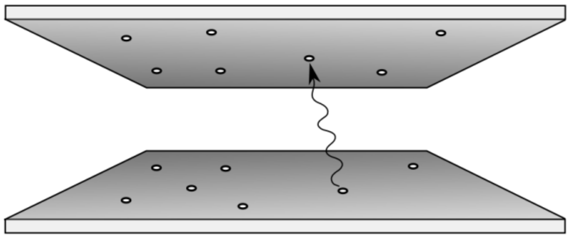

Vertical: tunnelling

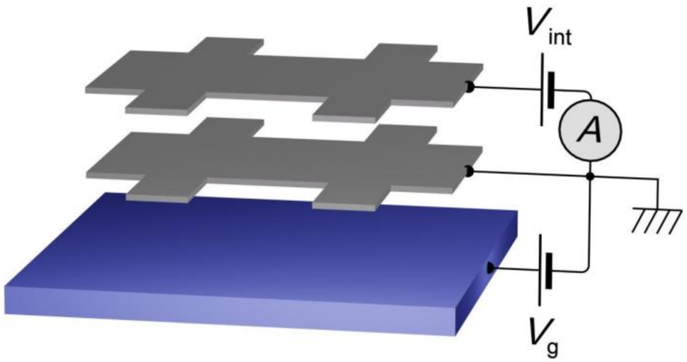

Metal – Insulator transition

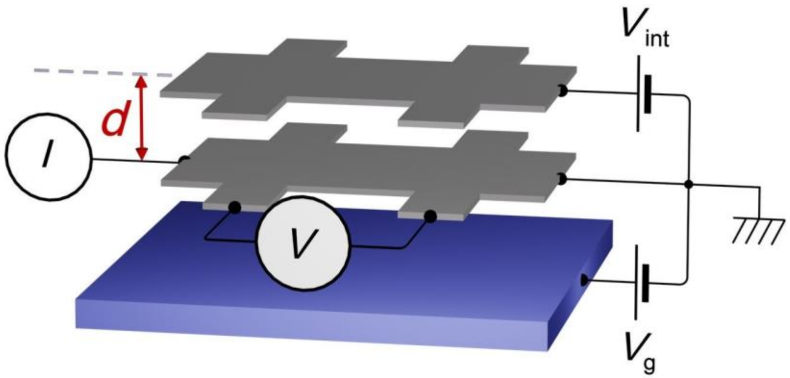

Nature Physics 7, 958-961 (2011)

Coulomb drag & Excitons

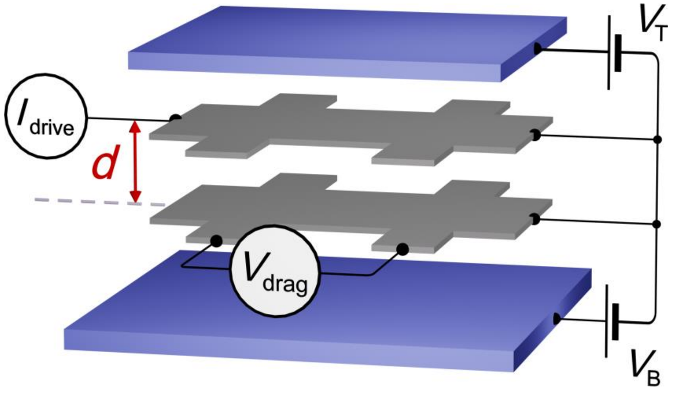

Nature Phys 8, 896-901 (2012)

End of part 1